Yale University

EliScholar – A Digital Platform for Scholarly Publishing at Yale

Yale Medicine Thesis Digital Library School of Medicine

January 2020

Cerebral Autoregulation-Based Blood Pressure Management In The Neuroscience Intensive Care Unit: Towards Individualizing Care In Ischemic Stroke And Subarachnoid Hemorrhage

Andrew Silverman

Follow this and additional works at: https://elischolar.library.yale.edu/ymtdl

Recommended Citation

Silverman, Andrew, "Cerebral Autoregulation-Based Blood Pressure Management In The Neuroscience Intensive Care Unit: Towards Individualizing Care In Ischemic Stroke And Subarachnoid Hemorrhage" (2020). *Yale Medicine Thesis Digital Library*. 3951.
https://elischolar.library.yale.edu/ymtdl/3951

This Open Access Thesis is brought to you for free and open access by the School of Medicine at EliScholar – A Digital Platform for Scholarly Publishing at Yale. It has been accepted for inclusion in Yale Medicine Thesis Digital Library by an authorized administrator of EliScholar – A Digital Platform for Scholarly Publishing at Yale. For more information, please contact elischolar@yale.edu.

Cerebral autoregulation-based blood pressure management in the neuroscience intensive care unit

Towards individualizing care in ischemic stroke and subarachnoid hemorrhage

A Thesis Submitted to the
Yale University School of Medicine
in Partial Fulfillment of the Requirements for the
Degree of Doctor of Medicine

by

Andrew Silverman

Class of 2020

ABSTRACT

The purpose of this thesis is to review the concept of cerebral autoregulation, to establish the feasibility of continuous bedside monitoring of autoregulation, and to examine the impact of impaired autoregulation on functional and clinical outcomes following subarachnoid hemorrhage and ischemic stroke. Autoregulation plays a key role in the regulation of brain blood flow and has been shown to fail in acute brain injury. Disturbed autoregulation may lead to secondary brain injury as well as worse outcomes. Furthermore, there exist several methodologies, both invasive and non-invasive, for the continuous assessment of autoregulation in individual patients. Resultant autoregulatory parameters of brain blood flow can be harnessed to derive optimal cerebral perfusion pressures, which may be targeted to achieve better outcomes. Multiple studies in adults and several in children have highlighted the feasibility of individualizing mean arterial pressure in this fashion.

The thesis herein argues for the high degree of translatability of this personalized approach within the neuroscience intensive care unit, while underscoring the clinical import of autoregulation monitoring in critical care patients. In particular, this document recapitulates findings from two separate, prospectively enrolled patient groups with subarachnoid hemorrhage and ischemic stroke, elucidating how deviation from dynamic and personalized blood pressure targets associates with worse outcome in each cohort. While definitive clinical benefits remain elusive (pending randomized controlled trials), autoregulation-guided blood pressure parameters wield great potential for constructing an ideal physiologic environment for the injured brain.

The first portion of this thesis discusses basic autoregulatory physiology as well as various tools to interrogate the brain's pressure reactivity at the bedside. It then reviews the development of the optimal cerebral perfusion pressure as a biological hemodynamic construct. The second chapter pertains to the clinical applications of bedside neuromonitoring in patients with aneurysmal subarachnoid hemorrhage. In this section, the personalized approach to blood pressure monitoring is discussed in greater detail. Finally, in the third chapter, a similar autoregulation-oriented blood pressure algorithm is applied to a larger cohort of patients with ischemic stroke. This section contends that our novel, individualized strategy to hemodynamic management in stroke patients represents a better alternative to the currently endorsed practice of maintaining systolic blood pressures below fixed and static thresholds.

ACKNOWLEDGMENTS

This work would not have been possible without the leadership and encouragement of Dr. Nils Petersen. I could not have asked for a more insightful, creative, and patient mentor. It has been an extraordinary opportunity learn about physiology, critical care, and balancing research and clinical work from such a dedicated and kind role model.

Many thanks also to our larger research team, which includes Sumita Strander, Sreeja Kodali, Alex Kimmel, Cindy Nguyen, Krithika Peshwe, and Anson Wang. Sumita and Sreeja, now first-year medial students at Harvard and Yale, respectively, were incredible teammates throughout my research year. They helped enroll patients, problem solve, and run new scripts. Their energy and friendship sustained me during some of the longer days (and nights) of neuromonitoring and abstract construction before midnight deadlines.

More gratitude to my thesis committee and mentors in the Neurology Department, including Dr. Emily Gilmore, Dr. Kevin Sheth, Dr. Charles Wira, and Dr. Charles Matouk. In particular, Dr. Gilmore volunteered her time to adjudicate clinical and radiologic scores for over 30 patients with subarachnoid hemorrhage. Many thanks overall to the Divisions of Vascular Neurology and Neurocritical Care for hosting me and providing me with a suitable workspace for an entire year.

Thank you to Yale's amazing Office of Student Research: Donna Carranzo, Kelly Jo Carlson, Reagin Carney, and Dr. John Forrest. Without their coordination efforts and sponsorship, I would not have been able to obtain funding from the American Heart Association, practice presenting my work at research in progress meetings, or learn about my peers' awesome project developments – not to mention all the coffee and snacks they provided.

Much gratitude, as always, to my grandma, my mom, my older brother, and to Lauren. Although they are not in the medical field and will probably never read this thesis, they have continually been enthusiastic and unconditionally supportive.

Finally, I would like to thank the patients and families who volunteered to participate in our studies. Research reported in this publication was supported by the American Heart Association (AHA) Founders Affiliate training award for medical students as well as the Richard A. Moggio Student Research Fellowship from Yale.

TABLE OF CONTENTS

PART I **1**
A. Introduction: a brief history of autoregulation research 1
B. Cerebral blood flow regulation and physiology 8
C. Methods to measure cerebral autoregulation 17
D. Autoregulation indices and signal processing 22
E. Comparisons between autoregulatory indices 28
F. Optimal cerebral perfusion pressure 29
PART II **37**
A. Subarachnoid hemorrhage 37
B. Clinical relevance of autoregulation following subarachnoid hemorrhage 45
C. Pilot study on autoregulation monitoring in subarachnoid hemorrhage 51
D. Results of the subarachnoid hemorrhage pilot study 65
E. Discussion 89
PART III **95**
A. Large-vessel occlusion (LVO) ischemic stroke 95
B. Clinical relevance of autoregulation following ischemic stroke 99
C. Pilot study on autoregulation monitoring in ischemic stroke 103
D. Results of the ischemic stroke pilot study 111
E. Discussion 122
PART IV **131**
A. Concluding remarks and future studies 131
References **138**

LIST OF PUBLICATIONS AND ABSTRACTS

Peer-reviewed original investigations

1. **Silverman A**, Kodali S, Strander S, Gilmore E, Kimmel A, Wang A, Cord B, Falcone G, Hebert R, Matouk C, Sheth KN, Petersen NH. **Deviation from personalized blood pressure targets is associated with worse outcome after subarachnoid hemorrhage**. Stroke 2019 Oct;50(10):2729-37.

2. **Silverman A***, Petersen NH*, Wang A, Strander S, Kodali S, Matouk C, Sheth KN. **Exceeding Association of Personalized Blood Pressure Targets With Hemorrhagic Transformation and Functional Outcome After Endovascular Stroke Therapy**. JAMA Neurology. 2019 Jul 29. doi: 10.1001/jamaneurol.2019.2120. [Epub ahead of print] (*equally contributed)

3. **Silverman A***, Petersen NH*, Wang A, Strander S, Kodali S, et al. **Fixed Compared to Autoregulation-Oriented Blood Pressure Thresholds after Mechanical Thrombectomy for Ischemic Stroke**. Stroke 2020, Mar;51(3):914-921. (*equally contributed)

Abstracts and presentations

1. **Silverman A**, Kodali S, Strander S, Gilmore E, Kimmel A, Cord B, Hebert R, Sheth K, Matouk C, Petersen NH. **Deviation from Dynamic Blood Pressure Targets Is Associated with Worse Functional Outcome After Subarachnoid Hemorrhage**. Platform Presentation, Congress of Neurological Surgeons Annual Meeting, San Francisco 2019.

2. **Silverman A**, Wang A, Strander S, Kodali S, Sansing L, Schindler J, Hebert R, Gilmore E, Sheth K, Petersen NH. **Blood Pressure Management Outside Individualized Limits of Autoregulation is Associated with Neurologic Deterioration and Worse Functional Outcomes in Patients with Large-Vessel Occlusion (LVO) Ischemic Stroke**. Platform Presentation, American Academy of Neurology Annual Meeting, Philadelphia 2019.

3. **Silverman A**, Wang A, Kodali S, Strander S, Cord B, Hebert R, Matouk C, Sheth K, Gilmore E, Petersen NH. **Dynamic Cerebral Autoregulation and Personalized Blood Pressure Monitoring in Patients with Aneurysmal Subarachnoid Hemorrhage (aSAH)**. Poster Presentation, American Academy of Neurology Annual Meeting, Philadelphia 2019.

4. **Silverman A**, Wang A, Kodali S, Strander S, Cord B, Hebert R, Matouk C, Gilmore E, Sheth K, Petersen NH**. Individualized blood pressure management after subarachnoid hemorrhage using real-time autoregulation monitoring: a pilot study using NIRS and ICP-derived limits of autoregulation**. Platform Presentation, International Stroke Conference, Honolulu 2019.

Acronyms			
aSAH	Aneurysmal subarachnoid hemorrhage	**MAP_{OPT}**	Optimal mean arterial pressure
BP	Blood pressure	**PRx**	Pressure reactivity index
ICP	Intracranial pressure	**TOx**	Tissue oxygenation index
NIRS	Near-infrared spectroscopy	**%time outside LA**	Percent time outside limits of autoregulation
DCI	Delayed cerebral ischemia	**OR**	Odds ratio
MAP	Mean arterial pressure	**CI**	Confidence interval
IQR	Interquartile range	**aOR**	Adjusted odds ratio
CBF	Cerebral blood flow	**CVR**	Cerebrovascular resistance
CPP	Cerebral perfusion pressure	**TCD**	Transcranial Doppler
CPP_{OPT}	Optimal cerebral perfusion pressure	**LA**	Limits of autoregulation
ULA	Upper limit of autoregulation	**LLA**	Lower limit of autoregulation
mRS	Modified Rankin scale	**HH**	Hunt and Hess classification
mF	Modified Fisher score	**WFNS**	World Federation of Neurological Surgeons score
LoC	Loss of consciousness	**ROC**	Receiver operating characteristic
TBI	Traumatic brain injury	**LVO**	Large-vessel occlusion
tPA	Tissue plasminogen activator	**EVT**	Endovascular thrombectomy
HT	Hemorrhagic transformation	**HI**	Hemorrhagic infarction
PH	Parenchymal hematoma	**sICH**	Symptomatic intracranial hemorrhage
NIHSS	National Institute of Health Stroke Scale	**ASPECTS**	Alberta Stroke Program Early CT Score
ESCAPE trial	Endovascular Treatment for Small Core and Anterior Circulation Proximal Occlusion with Emphasis on Minimizing CT to Recanalization Times	**DAWN trial**	DWI or CTP Assessment with Clinical Mismatch in the Triage of Wake-Up and Late Presenting Strokes Undergoing Neurointervention with Trevo

PART I

A. Introduction: a brief history of autoregulation research

In 1959, Dr. Niels Lassen published a pivotal review on cerebral blow flow and popularized the concept of cerebral autoregulation. [1] He writes, "Until about 1930 the cerebral circulation was generally believed to vary passively with changes in the perfusion pressure. This concept was based mainly on the Monro-Kellie doctrine of a constant volume of the intracranial contents, from which it was deduced that no significant changes in intracranial blood volume or vascular diameter were likely to occur." In fact, Monro promoted this conceit regarding the skull's non-compliance in 1783, and it wasn't until 1890 that Roy and Sherrington submitted that cerebral blood flow might be dependent on both arterial pressure in conjunction with intrinsic cerebrovascular properties capable of autonomously regulating flow. [2, 3] In their letter to the *Journal of Physiology*, the authors speculate on the origins of these properties:

> *"Presumably, when the activity of the brain is not great, its blood-supply is regulated mainly by the intrinsic mechanism and without notable interference with the blood-supply of other organs and tissues. When, on the other hand, the cerebral activity is great, or when the circulation of the brain is interfered with, the vasomotor nerves are called into action, the supply of blood to other organs of the body being thereby trenched upon."*

Then, in 1902, Sir W.M. Bayliss performed a series of experiments on anesthetized cats, dogs, and rabbits, observing peripheral vasoconstriction during increased blood pressure inductions. [4] In a sample of his meticulous tracings below, one can appreciate that after excitation of the splanchnic nerve, arterial pressure rises and causes passive distention of hindleg volume (Figure 1). Bayliss points out that instead of merely returning to its original

volume when the blood pressure returns to baseline, the volume of the limb constricts considerably below its previous level before returning to normal. This phenomenon was later dubbed the Bayliss effect, referring to a pressure-reactive, myogenic vascular system.

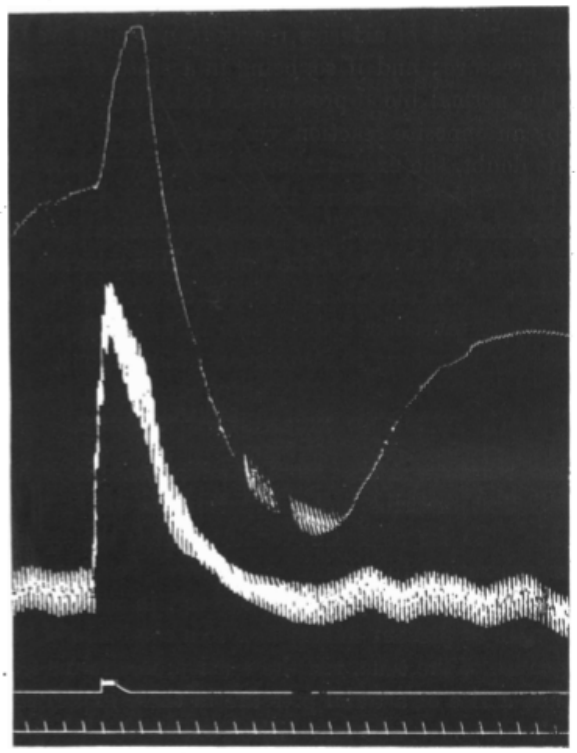

Fig. 2. *Effect of splanchnic excitation on enervated limb of dog.* Upper curve—volume of limb. Lower curve—blood-pressure, zero being 45 mm. below excitation marker, which is the upper of the two bottom lines. Time in 10″.

Figure 1. Exemplary myogenic reactivity as demonstrated by W.M. Bayliss at the turn of the 20th century. [4]

In the ensuing decades leading up to Lassen's review, quantitative studies in both animal models and humans confirmed observations of autoregulation as an objective homeostatic phenomenon, first described by Forbes in 1928 and later by Fog in 1938. [5-8] Through direct observation of feline pial vessels through a pioneering cranial window (a so-called *lucite calvarium*), they noticed that systemic blood pressure increases resulted in surface vessel vasoconstriction, while pressure decrements yielded local vasodilation, thus

sustaining the Bayliss effect. In summarizing these studies, Lassen found that optimal and constant cerebral blood flow tended to occur within a cerebral perfusion pressure range of roughly 50 to 150 mmHg. This autoregulatory doctrine has now made its way to first-year medical school classrooms and can be heard on neurocritical care rounds on a virtually daily basis (Figure 2).

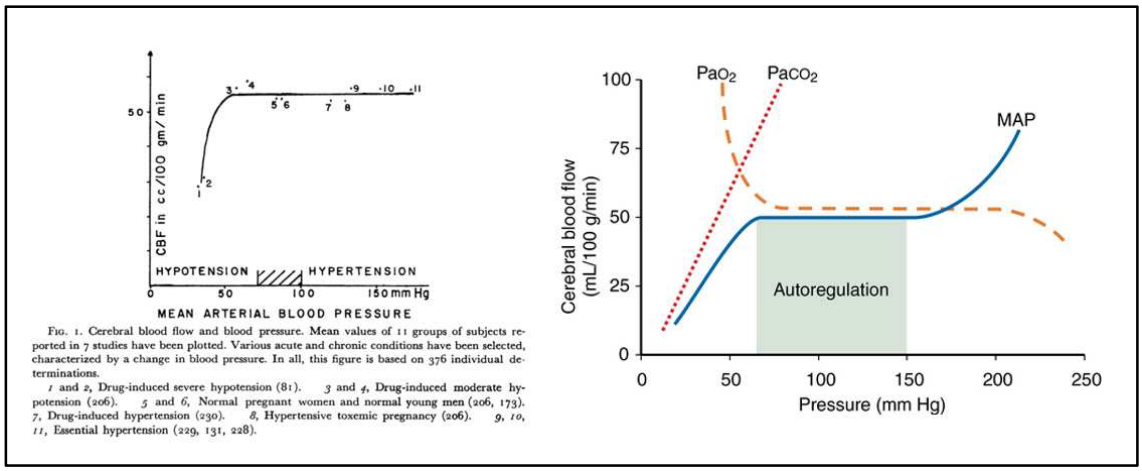

Figure 2. The evolution of the autoregulatory curve from Lassen's original 1959 publication (left) to the instructive illustration that can be found in First Aid for the USMLE Step 1 (right). [1]

Furthermore, in 2019, animal model researchers in Belgium have effectively cast the *lucite calvarium* into the realm of modern translation medicine. Using a porcine cranial window, Klein *et al*. used laser Doppler flow to measure pial arteriole diameter and erythrocyte velocity, allowing the team to quantify cerebrovascular autoregulation and its limits (Figure 3). [9] The development of such models has the potential to help close the translational gap between experimental and clinical work on autoregulation.

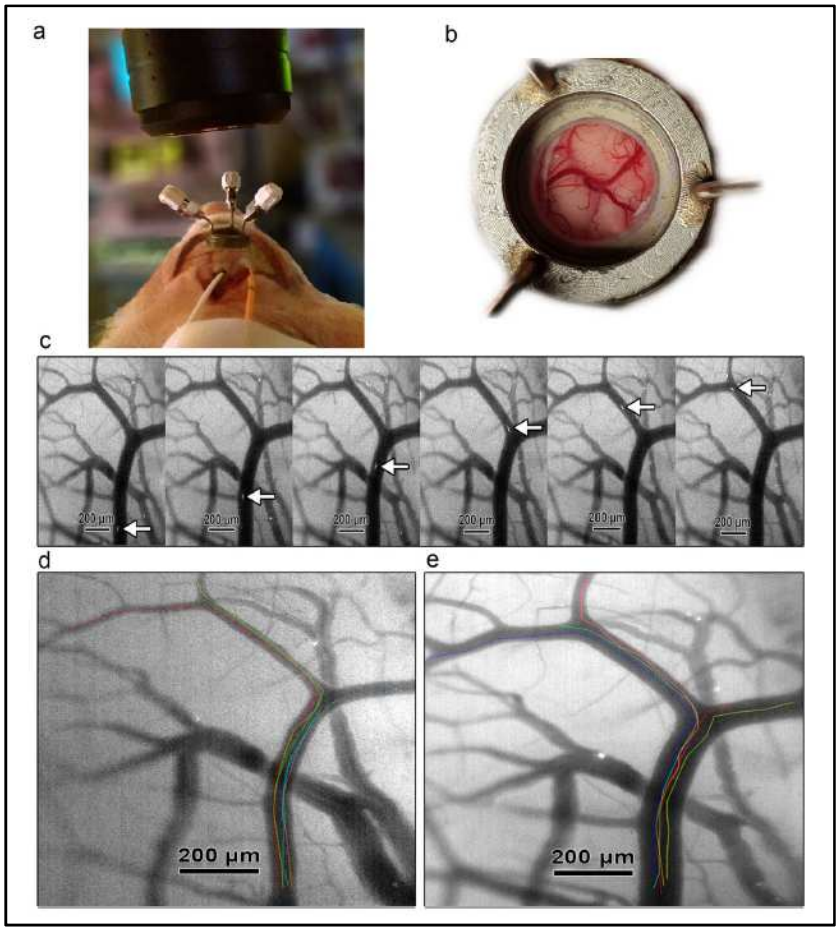

Figure 3. Adapted from *Klein et al*., this figure illustrates *in vivo* measurements of pial arteriole red blood cell flux. (a) Microscope positioned over the porcine cranial window with cortical laser Doppler probe (white) and intraparenchymal ICP-PbtO2 probe (orange) placed ipsilaterally behind the cranial window. (c) Fluorescent-labeled erythrocyte moving through a pial arteriole at 200 frames/second. (d) Baseline visualization of pial arterioles and individual red cell tracks. Individual red blood cell tracks are superimposed on the original frame in different colors. (e) Vasodilation of pial arterioles and individual red blood cell tracks during induced hypotension, thereby demonstrative of cerebrovascular autoregulation. [9]

Clearly, science has evolved, but the definition of autoregulation has remained constant (much like the plateau of Lassen's curve). Cerebral autoregulation is the cerebrovascular tree's intrinsic capacity to maintain a stable blood flow despite changes in blood pressure or – more accurately – cerebral perfusion pressure. [10] In his report, Lassen observes that

cerebral perfusion pressures vary to a modest extent in a normal person and that "the most important regulating factor probably [is] the tissue carbon dioxide tensions and the direct reaction of the muscular cells of the cerebral arteries in response to variations of the distending blood pressure." [1] Indeed, under normal circumstances, cerebral blood flow is regulated through changes in arteriolar diameter, which, in turn, drive changes in cerebrovascular resistance in accordance with the Hagen-Poiseuille equation. [11] Although decades of subsequent research have illuminated some underpinning mechanisms, the exact molecular means underlying autoregulation remain elusive. Various processes, including myogenic, neurogenic, endothelial, and metabolic responses, have been implicated in the mediation of cerebral vasomotor reactions, but it is important to differentiate carbon dioxide reactivity and flow-metabolism coupling from cerebral autoregulation. [12] Carbon dioxide reactivity describes vascular reactions in response to changes in the partial pressure of arterial carbon dioxide (P_aCO_2) but does not take into consideration reactions to pressure changes. Flow-metabolism coupling, in comparison, involves regulation of cerebral blood flow with regard to local cellular demand, for example, as a consequence of neural activation during cognitive tasks. Similar to P_aCO_2 reactivity, flow-metabolism coupling and the neurovascular unit function irrespective of fluctuations in cerebral perfusion pressure. [11]

With a working definition of autoregulation and an understanding of what it is not, researchers have built technology that now boasts the ability to collect autoregulation-derived data in real-time, which may lead to the fine-tuning of decades-old guidelines. [13, 14] By individualizing cerebral perfusion pressure in the neurocritical care unit, updated guidelines may potentially ameliorate clinical and functional outcomes. [15]

Autoregulation can now efficaciously be assessed by examining changes in cerebral blood flow, or its surrogates, in response to changes in cerebral perfusion pressure, or mean arterial pressure (MAP) as its surrogate. [11] Individualization of autoregulatory pressure ranges, together with the developing concept of an optimum mean arterial pressure landscape for the injured brain, represent a novel and innovate application of autoregulation neuromonitoring.

Numerous studies in recent years have demonstrated that large differences between actual MAP and an optimal, calculated MAP (based on autoregulatory status) associate with poor outcome across several disease states. These papers encompass traumatic brain injury, intracerebral hemorrhage, subarachnoid hemorrhage, ischemic stroke, adults undergoing cardiac bypass surgery, children with moyamoya vasculopathy, and neonates with hypoxic-ischemic encephalopathy. [13, 16-22] The cumulative strength of these findings triggered the Brain Trauma Foundation to recommend autoregulation monitoring in an effort to optimize brain perfusion in patients with traumatic brain injury. [23]

Nevertheless, guidelines for blood pressure management persistently recommend a single, fixed target value for many critically ill patients. For example, the American Heart Association and American Stroke Association endorse a systolic blood pressure of less than 140 mmHg after intracerebral hemorrhage; they also suggest systolic pressures under 160 mmHg before aneurysm obliteration, and less than 140 mmHg after clipping or coiling of the aneurysm following a subarachnoid hemorrhage. [24, 25] The same societies recommend systolic readings of less than 180 mmHg after intravenous recombinant tissue

plasminogen activator for ischemic stroke. [26] In contrast, the European Society of Intensive Care Medicine acknowledges that septic patients with a history of hypertension may have autoregulation curves shifted to the right, thus requiring a higher MAP for adequate cerebral perfusion. [27] These guidelines, however, do not currently consider autoregulation-guided hemodynamic management of critically ill patients. In this omission, many questions in the field of neuromonitoring are left unanswered. [15] First and foremost, with respect to this thesis, is it feasible to effectively personalize MAP targets based on an individual's dynamic autoregulatory composition? Might this method be clinically beneficial? How can it be tailored across various monitoring techniques and disease states?

Notwithstanding such unanswered questions, the science of autoregulation has come a long way since 1959. [1] Speaking perhaps to the incremental, and yet potentially groundbreaking nature of scientific investigation, Dr. Lassen concludes his 56-page review with the following remarks:

> *"These major findings and the wealth of additional observations have very substantially increased our understanding of this important area of human physiology. Undoubtedly our knowledge is still incomplete at various points. However, a solid foundation for relevant physiological thinking and for future studies has been established."*

It is now 60 years down the line, and autoregulation research is at the precipice of tangibly translatable use at the bedside, as clinical trials of autoregulation-guided therapy are underway across Europe (NCT02982122). [28] Moreover, this thesis will discuss two prospective, observational studies at Yale-New Haven Hospital, each investigating the feasibility of using an innovative algorithm to determine personalized, autoregulation-

based blood pressure targets at the bedside. To our knowledge, these studies are the first to examine the impact of deviation from personalized, autoregulation-based blood pressure limits in patients with subarachnoid hemorrhage and large-vessel occlusion ischemic stroke. [13, 14] Thus, these studies arguably set the stage for imminent interventional trials within Yale's Divisions of Vascular Neurology as well as Neurocritical Care and Emergency Neurology. [29] Before delving into the details of these studies, it is important to more meticulously review autoregulation physiology, monitoring techniques, and the development of the optimal cerebral perfusion pressure. In doing so, perhaps Lassen's solid foundation will grow, and future studies will be all the more within reach.

B. Cerebral blood flow regulation and physiology

Cerebral oxygen delivery is a function of brain blood flow and blood oxygen content, whereby cerebral blood flow (CBF) is gradient between cerebral perfusion pressure (CPP) and cerebrovascular resistance (CVR). Another way to conceptualize blood flow to the brain is via the gradient between the brain's arteries and veins, the latter being approximately equivalent to intracranial pressure (ICP).

$$\mathbf{CBF = CPP/CVR = (MAP - ICP)/CVR}$$

The brain's vascular resistance reflects the smooth muscle tone of the vessels, partially influenced by mean arterial pressure (MAP). If CPP increases or decreases, the myogenic reflex will result in vasoconstriction or vasodilation, respectively. This dictum is the classical view of pressure-flow autoregulation. If intracranial pressure is stable, CPP can

be replaced by MAP. In this manner, changes in brain blood flow can be measured for a range of blood pressures to determine autoregulation.

In general, however, four mechanisms regulate cerebral blood flow, including myogenic, neurogenic, endothelial, and metabolic processes, illustrated in Figure 4 (ChemDraw Professional, Version 17.1.0.105). [10] Each of these classical mechanisms will be reviewed in this section, with an important caveat that the interplay and relative contributions of each of these mechanisms is highly complex and poorly understood. [30] Additionally, an imprecise border zone between conductive and resistive facets in the cerebrovascular tree suggests that autoregulation may involve both large and small arteries and arterioles. For instance, large extracranial arteries and intracranial pial vessels comprise roughly half of the brain's vascular resistance, with the remainder stemming from penetrating parenchymal arteries and arterioles. [31, 32] These parenchymal arteries possess distinctive, resistive properties compared to pial vessels; ensuing segmental and spatiotemporal heterogeneity in autoregulation, as well as pathophysiologic correlates of this heterogeneity, will be reviewed in this section.

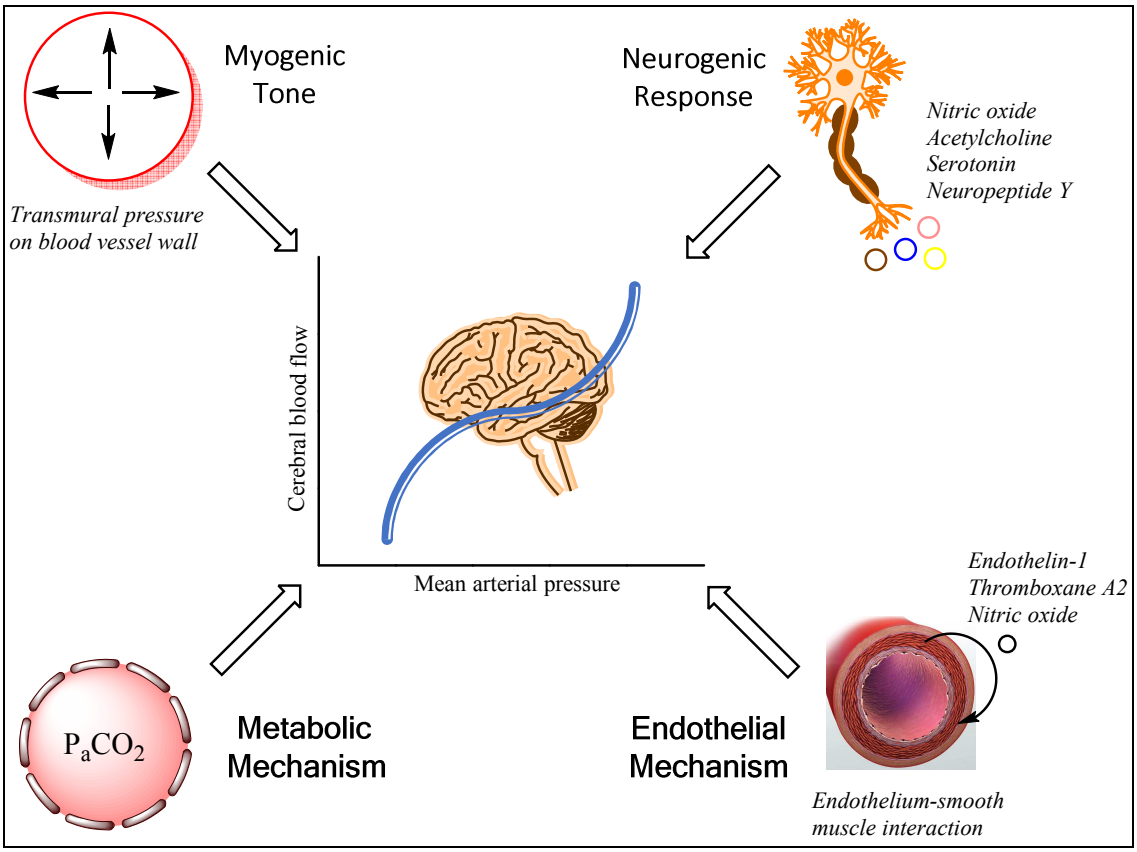

Figure 4. Physiology of cerebral autoregulation. This illustration shows the four classical mechanisms contributing to cerebral autoregulation. Through myogenic tone, transmural pressure influences arterial diameter through direct smooth muscle contraction or relaxation. In the metabolic mechanism, fluctuations in the partial pressure of carbon dioxide lead to vasoconstriction or dilatation. The endothelium secretes paracrine substances that may act directly on smooth muscle cells. Lastly, in the neurogenic response, neurons and glia mediate smooth muscle physiology by releasing various neurotransmitters with vasoactive properties. This figure was created using ChemDraw software.

1) Myogenic Tone

Myogenic tone is produced when arteriole and small artery smooth muscle cells contract in response to increased pressure. [33, 34] In contrast, myogenic tone relaxes in response to decreased pressure. This phenomenon is manifest in the aforementioned Bayliss effect (see Figure 1 in the introduction). More recent work

has unearthed some details about the effect. For example, a rapid change of pressure (ΔP = 10 to 25 mmHg/sec) induces rapid changes in the diameter of the vessel, and the latency of such transmural stimulation typically occurs in under 250 msec. [35]

Transmural pressure changes, in turn, activate mechanically sensitive ion channels and proteins in the vessel wall, triggering various downstream cascades. For instance, membrane depolarization opens voltage-gated calcium channels, leading to an influx of calcium cations into the smooth muscle cell. [36] Calcium activates myosin light chain kinase (MLCK), which goes on to activate myosin by phosphorylation. Phosphorylated MLCK increases actin-myosin interaction, causing muscle cell contraction and vasoconstriction. Furthermore, activation of RhoA, a small GTPase, stimulates Rho-associated kinase (ROCK), which inhibits myosin light chain phosphatase. [37] Inhibiting the dephosphorylating inhibitor in this way potentiates vasoconstriction. Other parallel pathways involve protein kinase C activation, which stabilizes the actin-myosin interaction. [38] More recent hypotheses implicate arachidonic acid metabolites like 20-hydroxyeicosatetraenoic acid (20-HETE), a known vasoconstrictor, and epoxyeicosatrienoic acids (EETs) in the mediation of vessel wall stretch and basal tone. [39]

The importance of smooth muscle cell myogenic regulation can be seen in cerebral autosomal dominant arteriopathy with subcortical infarcts and leukoencephalopathy (CADASIL). [40, 41] Patients with CADASIL show a degree of smooth muscle cell degeneration in small cerebral arteries, and studies have

demonstrated impaired myogenic autoregulatory functioning in both animal models and individuals with the genetic condition. [42, 43] This disease is caused by a mutation in the *NOTCH3* gene and marked by recurrent ischemic strokes, cognitive impairment, subcortical dementia, mood disturbances like depression and apathy, as well as premature death. Lacombe *et al*. provided evidence that transgenic mice expressing a mutant *NOTCH3* in vascular smooth muscle cells exhibited impaired cerebral vasoreactivity, including reduced responses to vasodilatory challenges and a shift of the lower limit of autoregulation toward higher pressures. [44] Interestingly, parenchymal arteries exhibit greater basal tone than pial arteries. This difference may buffer effects of upstream rapid changes in blood pressure on cerebral perfusion and thus attenuate transmission of pulsatile mechanical stress into the brain's microcirculation. Disturbance of this basal tone may exacerbate stroke burden in CADASIL patients. [41, 45]

Increased transmural pressure translates to increased flow, and there is evidence that flow may induce vessel diameter changes independent of pressure changes. In 2011, for example, Toth *et al.* showed that both human and rodent cerebral arteries constrict in response to increased flow when pressure was held constant, possibly due to an increase in reactive oxygen species and cyclooxygenase activity. [46]

2) Neurogenic Response

Neurogenic mediation of cerebral vasoreactivity involves control of small- and medium-sized vessel diameters. Neurons and other cell types like astrocytes and microglia secrete a variety of neurotransmitters with vasoactive properties. For

instance, acetylcholine and nitric oxide are relatively potent vasodilators, while serotonin and neuropeptide Y stimulate vasoconstriction. [47]

Through the creative use of infrared video-microscopy of interneurons and adjacent microvessels in rodents, Cauli *et al*. showed that increased depolarizing activity of single cortical interneurons results in precise vasomotor responses in neighboring microvessels. [48] They further showed that these neuronally induced vasomotor responses can be mimicked by perivascular application of vasoactive neuropeptides directly on microvascular receptors.

On a larger scale, these changes in blood flow in response to neuronal activation can be observed as the blood oxygen level dependent (BOLD) signal, which is employed in functional magnetic resonance imaging (fMRI). The BOLD response has been adapted in many fMRI studies investigating increased cerebral metabolic demand in cognitive tasks, spatial memory, visual processing, and across various disease states. [49-51]

Interestingly, the neurogenic response exhibits both segmental and regional heterogeneity, as vessel reactivity varies from the pial arteries as they branch into the parenchyma and become arterioles. [30] Regarding segmental variability, pial arteries receive perivascular innervation from the peripheral autonomic system, with roots in the superior cervical, sphenopalatine, otic, and trigeminal ganglia. [47, 52] This anatomic pathway is referred to as extrinsic innervation. The brain's

parenchymal arteries and arterioles, in contrast, are primarily innervated by intrinsic nerves originating from subcortical neurons, such as those found within the locus coeruleus, raphe nucleus, basal forebrain, or local cortical interneurons. These areas then project to the perivascular space surrounding the parenchymal and arteriolar vessels. It follows that this pathway is referred to as intrinsic innervation.

This difference in anatomy entails divergent expression levels of neurotransmitter receptors. For instance, α-adrenoreceptor reactivity is relatively absent in parenchymal arteries due to a shift toward β-adrenoreceptor density. [53] Similar heterogeneity has been shown with serotonin receptor levels. Accordingly, serotonin- and norepinephrine-induced pial vasoconstriction is absent in the parenchymal and arteriolar arteries, sometimes even causing vasodilation. [54] This mosaic topography in neurogenic regulation may provide the brain with the ability to flexibly modulate blood flow to meet local metabolic demand. [30]

Regarding regional heterogeneity, the anterior circulatory system of the brain possesses denser sympathetic innervation than that of the posterior system. The anterior circulation is controlled mostly by adrenergic sympathetic relays from the superior cervical ganglion as they travel up the carotid arteries. The posterior vessels instead depend on the sympathetic chain via the vertebrobasilar arteries. [55] Autoregulation has also been shown to be more effective in the brainstem. For example, in severe hypertension in anesthetized cats, cerebral blood flow significantly increases in the anterior circulation, whereas the brainstem only

requires modest increases in flow. [56] This vascular resistance differential points to a likely regional incongruity in cerebral autoregulation.

This regional variability may play a key role in the development of posterior reversible encephalopathy syndrome (PRES). This syndrome, which parenthetically is not always posterior or even reversible, is otherwise characterized radiologically by transient bilateral subcortical vasogenic edema in the territory of the posterior circulation. [57] Among several etiologic theories involving immunologic dysfunction, vasospasm, and endothelial and blood-brain barrier breakdown, one interesting explanation for the edema's apparent posterior predilection is the relative dearth of sympathetic tone in that area, leading to poor autoregulation of blood flow in the setting of abrupt hypertensive episodes. [55]

3) Metabolic Mechanism

The metabolic mechanism subserving autoregulation occurs in smaller vessels that are subject to changes in the local environment. [58] Most notably, carbon dioxide overtly alters vasomotor responses; every 1 mmHg increase in P_aCO_2 corresponds to a roughly 4% increase in cerebral blood flow. [59] The concentration of cerebral carbon dioxide can accumulate and cause vasodilation in this fashion when, for example, hypotension below the lower autoregulatory limit results in tissue hypoperfusion and thus anaerobic respiration. The opposite physiology transpires in the setting of hyperperfusion with consequent decreases in P_aCO_2 and vasoconstriction. [60, 61]

It is hypothesized that this vasomotor response is regulated by the H^+ concentration in the smooth muscle of cerebral vessels. [59] Proton gradients are regulated by carbonic anhydrase activity, the catalytic activity of which depends on the tight regulation of pH (normally hovering around 7.4 in the human body). Prolonged hypocapnia that generates tissue alkalosis may increase carbonic anhydrase activity. [11]

Additionally, decreased oxygen partial pressures can increase cerebral blood flow, as can be seen in Figure 2. This effect does occur unless there is severe hypoxemia of less than 50 mmHg, or 6.6 kPa. [62] Similarly, severe hypoglycemia at levels of less than 2 mmol/L can lead to increases in cerebral blood flow. [63]

4) Endothelial Mechanism

Lastly, endothelial tissue begets a gamut of signals that affect vascular tone. The endothelium secretes vasodilators like nitric oxide (NO) and vasoconstrictors like thromboxane A2 and endothelin-1 in a paracrine manner. [10, 64]

Further, as an interesting bedside-to-bench endeavor, researchers have looked at the ability of statins to regulate autoregulation. In more detail, statins have the capacity to upregulate nitric oxide synthase, causing cerebral artery dilation and increased cerebral blood flow. [65, 66] This mechanism occurs through the inhibition of small G-proteins known as Rho and Rac. Rho negatively regulates endothelial nitric oxide synthase. Statins inhibit Rho GTPase activity via inhibition

of a process known as geranylgeranylation (a form of prenylation), which ultimately confers nitric oxide synthase upregulation.

At this point, it should be stressed that conventional measurements of cerebrovascular reactivity are not exactly synonymous with measurements of cerebral autoregulation. The response to vasodilatory stimuli like CO_2, nitric oxide, or acetazolamide, has been used traditionally in the quantification of vasomotor reactivity. [6, 66] These agents dilate cerebral arterioles and small arteries to locally increase cerebral blood flow through a variety of neurogenic, metabolic, and endothelial processes. Although an intact endothelium is quite necessary for adequate pressure regulation, this approach does not assess fluctuations in cerebrovascular resistance in strict response to perfusion changes. Therefore, vasomotor reactivity and cerebral autoregulation are non-interchangeable physiologic phenomena. In other words, when vasomotor reactivity is exhausted, brain blood flow becomes dependent on systemic arterial blood pressure. Cerebral autoregulation is one critical aspect of this reactivity and involves vascular tone changes in response to pressure fluctuations. Vessels may continue to exhibit responses to further changes in P_aCO_2, and these responses fall within the domain of the cerebral autoregulatory mechanism protecting the brain. For example, vasodilation may reach its maximum at arterial pressures below the lower limit for constant cerebral blood flow. [6, 12]

C. Methods to measure cerebral autoregulation

Pressure autoregulation has traditionally been assessed by calculating cerebral blood flow at two different equilibrium states of arterial blood pressure. These steady-states

correspond to particular cerebral blood flow values. One pressure measurement could be taken at baseline, and the second could be measured after manual or pharmacologic manipulation of blood pressure, at which point brain blood flow could be measured again. Because this approach involves stable pressures and flows, it is referred to as a static autoregulatory measurement. [67] Other stimuli include body tilt, hand grip, lower body negative pressure, Valsalva, paced breathing, and squat-stand maneuvers. [6, 11] An advantage of these maneuvers is the precise control of the magnitude and time of the hemodynamic response; they are accurate insofar as the stimuli drive a synchronized response of brain blood flow. However, the methods are all temporally limited and, for the most part, cannot be performed more than once per day.

The advent of transcranial Doppler (TCD) ultrasound allowed for visualization of real-time blood-flow velocities (with a temporal resolution of approximately 5 msec), paving the road for dynamic assessments of autoregulation. [6, 68] Dynamic autoregulation refers to short-term, fast responses of the brain's blood flow to changes in systemic pressure. As TCD cannot measure flow directly, blood flow velocity is used as a surrogate. In this manner, methods like carotid compression or inflation of a leg cuff, each followed by release and subsequent autoregulatory hyperemia, can be utilized to induce rapid changes in middle cerebral artery flow velocity (taken as a surrogate for global hemispheric perfusion). [11, 69] Alternatively, one may insonnate intracranial vessels without any particular blood pressure challenges, such that monitoring takes place throughout spontaneous fluctuations of arterial blood pressure. [70] This latter approach renders dynamic assessments of cerebral autoregulation safe and feasible, as pressure

manipulations would be unrealistic and potentially harmful in critically ill patients. For example, a thigh-cuff inflation-deflation might incite a sudden blood pressure drop of up to 30 mmHg. [71] In a patient with an ischemic stroke, this drop could cause secondary brain injury from significant hypoperfusion, particularly in a setting when autoregulatory physiology is compromised in the first place. [13]

This dynamic response is likely complete after 10-15 seconds, suggesting that arterioles are able to counter slower fluctuations in systemic blood pressure. Faster changes, such as those greater than 0.5 Hz, are not compensated – for example, those occurring with each cardiac systole. This selective compensation is referred to as the high-pass filter principle. [72] The cerebrovascular system accordingly buffers against slow hemodynamic oscillations (0.01 to 0.4 Hz), while higher frequencies may pass unfiltered to the brain's circulation. [15] In the literature, the discussion regarding mechanisms underlying dynamic versus static autoregulation is ongoing. [66, 72, 73]

In addition to blood flow velocity, other intracranial signals are frequently used in dynamic vasoregulatory research. Examples include near-infrared spectroscopy (NIRS), local brain tissue oxygenation (PbtO2), and intracranial pressure (ICP) monitoring from a cerebrospinal fluid (CSF) draining system. [74-76] The fundamental principle of these dynamic measurements is the same across methodologies – the input signal is a large, abrupt blood pressure or volume change, and the resulting change in the intracranial compartment acts as the output signal. [66] Analysis of these signals is discussed in the next section.

As NIRS was our method of choice for the studies presented in this thesis, it will be discussed in more detail both here and in Part II. As a primer, near-infrared light (700-950 nanometers) is non-invasively transmitted from a source embedded in a sensor attached to the forehead. The light is then emitted past the skin, cranium, and cerebrospinal fluid to interrogate hemoglobin concentration in the frontotemporal cortex that is usually supplied by the middle cerebral artery. These tissues are essentially and remarkably transparent to light in this spectrum. [12] Many biological molecules have absorption spectra in the near-infrared range. [77] More pertinently, these chromophores include oxyhemoglobin, deoxyhemoglobin, bilirubin, and cytochrome aa_3 (a complex present in mitochondria that plays a role in the oxidative phosphorylation pathway), and they are the most abundant molecules that absorb light between 700 and 1,000 nm. [77, 78] The amount of light detected by sensors positioned at set distances from the light source is a function of chromophore absorption. Because oxy- and deoxyhemoglobin absorb light at different wavelengths, concentrations of these molecules can be derived using the modified Beer-Lambert law. This law generally states that the absorbance of a solution (A) is equal to the product of the molar absorptivity (ε), the distance through which the light travels (l), and the concentration of the absorbing species (c), or $A = \varepsilon lc$. Then, the ratio of oxyhemoglobin to total hemoglobin functions as a surrogate for cerebral blood flow, and it has been shown to be unaffected by extracranial circulation, hemoglobin concentration, cranial thickness, and cerebrospinal fluid. [79, 80] Furthermore, NIRS technology assumes that the hemoglobin measured is contained in a fixed mixture of vessels that are roughly 70-75% venous and 25-30% arterial blood volume. [12, 81] Calculations used to account for this

variability in the ratio of arterial to venous blood are unique to the manufacturer of the monitoring device. Thus, regional cerebral oxygen saturations in different machines are not necessarily equivalent. [82]

Table 1 displays some techniques that are available for analyzing cerebral autoregulation. Each offer different spatiotemporal resolution, radiation exposure, usability in certain patient cohorts, cost and availability, as well as interpretation of output signals. [83-85] It should be noted that for the nuclear (positron emission tomography, or PET) and radiologic (CT or MRI) techniques, the temporal resolution is still insufficient for dynamic measurements. There has also been an absence of simultaneous, non-invasive blood pressure recordings alongside these radiologic measures.

Methods	**Techniques**	**Spatiotemporal Resolution**
Absolute or relative perfusion measurements with isotopes or contrast agents	Nuclear (PET/SPECT/CT) Perfusion MRI MRI with arterial spin labeling fMRI	Excellent spatial resolution, but poor temporal, although arterial spin labeling and the BOLD signal may be promising
Continuous relative perfusion measurements (flow velocity)	TCD ultrasound	Poor spatial resolution, but excellent temporal
Local cerebral oxygenation	NIRS Venous oxygenation saturation (SjVO2) Cerebral oxygenation (PbtO2)	Poor to moderate spatial resolution, with good temporal
Intracranial pressure	ICP monitoring	Poor spatial resolution (global pressure), but excellent temporal

Table 1. Abridged comparison of cerebral autoregulation monitoring techniques. Pros of nuclear and radiologic methods include anatomic images with excellent spatial resolution, but they entail radiation as well as possible allergy reactions to contrast agents. They also only provide

> snapshot evaluations of autoregulation and are not used in patient care settings. Transcranial Doppler (TCD) ultrasound is relatively cheap and is obviously non-invasive with essentially no adverse effects (e.g., no radiation exposure). However, TCD offers no absolute perfusion measurements, and it is sometimes limited by poor window acquisition of the middle cerebral artery through the temporal bone. Cerebral oxygenation with NIRS monitoring is also non-invasive but is quite limited spatially. Intracranial pressure (ICP) monitoring involves excellent temporal resolution and can be used in conjunction with other techniques; however, as its name implies, it is invasive. SPECT, single photon-emission-CT.

Most studies of cerebral autoregulation rely on linear methods (cross-spectral or correlation-based) to assess autoregulatory functionality and integrity. If the pressure-flow relationship displays low coherence, this lack of linear dependence suggests intact autoregulation. In other words, brain blood flow is able to resist changes in blood pressure with an appropriate vasoregulatory response. Nevertheless, it has been argued that autoregulation itself engenders uncertainty with respect to its linear estimates, and so some researchers have put forth non-linear analysis techniques. [30] These approaches are discussed in the following section on autoregulatory indices.

D. Autoregulation indices and signal processing

Using spontaneous fluctuations of blood pressure and cerebral blood flow, researchers have devised a number of mathematical methods for modeling autoregulatory indices. In this section, particular attention will be paid to transfer function analysis and the time-correlation approach, with subsequent nods to wavelet analysis and projection pursuit regression.

1) Transfer Function Analysis

Transfer function analysis (TFA) is based on linear, stationary modeling and a fast Fourier transform algorithm to compute spectral estimates of blood pressure and cerebral blood flow. Autoregulation, when properly functioning, attenuates the influence of blood pressure on brain blood flow velocity by preventing direct propagation of the pressure waveform at lower frequencies (usually under 0.2 Hz). [30] Two key parameters – gain and phase-shift – can be derived from TFA at each frequency. Gain reflects the compression of brain blood flow velocity amplitude changes in response to blood pressure. As an example, a gain of 0.65 denotes that 65% of the relative amplitude of cerebral blood flow velocity is attenuates with regard to unit of change in arterial blood pressure. Phase-shift quantifies the time lag between blood pressure and brain flow velocity at a given frequency and is represented in degrees or radians. Larger phase-shifts between the two signals means that autoregulation is properly buffering the cerebrovascular tree from changes in blood pressure. [15, 86, 87] Of note, TFA can only rationalize linear relationships between arterial blood pressure and mean flow velocity, which is why coherence usually accompanies TFA to test the linearity between the two waveforms. Generally, a coherence above 0.5 is considered acceptable for TFA. Regarding frequency bands, values for gain, phase-shift, and coherence are reported in three bins: very low (0.02-0.07 Hz), low (0.07-0.2 Hz), and high (0.2-0.5 Hz) ranges. [87] The high-pass filter principle of autoregulation translates to reductions in coherence and gain with increases in phase-shift. These modulations result in the relative desynchronization between blood pressure and cerebral blood flow

oscillations. Additionally, because vasomotor adaptation is slow and requires roughly 10-15 seconds, autoregulation is most likely to function at lower frequencies. [6, 15, 87]

2) Time Domain Analysis

The moving Pearson correlation coefficient between blood pressure and various cerebral output signals permits the estimation of autoregulation indices with regard to each variable. [88] The coefficient for mean cerebral blood flow velocity is Mx, while the tissue oxygenation index (TOx) is derived from NIRS. Perhaps the most rigorously studied index is the pressure reactivity index (PRx), which is derived from ICP instead of cerebral blood flow velocity or tissue oxygenation. [11, 89] Cerebral perfusion pressure (CPP = MAP – ICP) may be substituted for arterial blood pressure as well. In all cases, a positive correlation coefficient reflects synchrony between the two signals, suggesting impaired cerebral autoregulation. Meanwhile, a negative or near-zero coefficient implies buffering and thus intact autoregulatory physiology.

The use of a threshold to delineate good versus impaired autoregulation has not been rigorously validated in the literature. In 2014, Sorrentino *et al*. found that an autoregulatory index greater than 0.3 prognosed fatal outcome in a cohort of 459 patients with traumatic brain injury. [90] Subsequent landmark studies adopted this approach when translating autoregulatory index research to individualized thresholds of cerebral perfusion pressure. [91] It is interesting to note that these two studies utilized PRx as their biomarker for autoregulation status, rather than the

NIRS-derived tissue oxygenation index (TOx). As stated above, PRx is derived as the moving correlation coefficient between ICP and mean arterial pressure, and so it is theoretically analogous to tissue oximetry's continuous correlation with mean arterial pressure. Studies will be needed to more scrupulously compare thresholds for impaired autoregulation among multimodal measurements of autoregulation. As one example, Steiner *et al*. in 2009 argued that critical thresholds for the NIRS-derived TOx should be set between 0.2 and 0.3. [92] Thus, in our studies at Yale-New Haven Hospital, we employed the more conservative threshold, using a cutoff of 0.3, [13, 14] rather than 0.2 or 0.25, as some authors have done in the past. [93, 94] Furthermore, in a piglet study using NIRS, the sensitivity and specificity of a NIRS-derived autoregulatory index of >0.3 to detect impaired autoregulation were 77 and 84%, respectively. [95] Table 2 below shows more information about these indices in human studies, as well as their respective cutoff values for impaired autoregulation.

3) Wavelet Analysis

This approach, also known as multimodal pressure flow analysis, represents an alternative to the classical spectral analyses, such as fast Fourier transform, and considers both time and frequency content of the signal. The wavelet analysis produces maps of phase shift and coherence between blood pressure and cerebral blood flow velocity over a range of frequencies and time points. Enforcing a minimal coherence threshold and focusing the analysis on areas in the time-frequency map with a high degree of correlation increases the reliability of the phase-shift estimation. [96] Interestingly, signal decomposition with wavelet

analysis has also been applied to tissue oxygenation using NIRS, paving the way for future wavelet signal processing using NIRS technology. [97]

4) Projection Pursuit Regression

Projection pursuit regression (PPR) is a non-parametric method wherein a model is not specified *a priori* but derived directly from variables of interest (i.e., arterial blood pressure and cerebral blood flow). This analysis modifies a linear transfer function between input (blood pressure) and output (brain blood flow). A linear autoregressive transfer function is passed through kernel functions, also known as ridge functions, that are determined by minimizing the mean squared error. [98] The method characterizes the non-linear relationship between pressure and flow and identifies regions wherein this relationship changes. The gain (i.e., slope) of the pressure-flow relationship within each region provides a measure of the effectiveness of autoregulation within that region. Furthermore, PPR allows for the derivation of five hemodynamic biomarkers of cerebral autoregulation: falling slope, rising slope, autoregulatory gain, as well as the upper and lower limits of autoregulation. An interesting 2016 study by Santos et al. used PPR to show that patients suffering from delayed cerebral ischemia (DCI) after subarachnoid hemorrhage had distinctive hemodynamic profiles with respect to those not suffering from DCI. [99] The authors then invoked previously found pharmacologic effects on PPR-derived autoregulation parameters. After combining their results with those parameters, the research team argued that myogenic dysfunction leads to vasospasm, while sympathetic overaction and cholinergic

dysfunction lead to DCI, while deficits in all three pathophysiologic mechanisms beget both vasospasm and DCI.

All in all, there are over 20 indices of cerebral autoregulation, a situation with obvious pros and cons for autoregulation research. Each index enlists a unique threshold for impaired autoregulation, with a range spanning 0.069 to 0.46, depending on devices used to measure cerebral blood flow or a surrogate thereof. Table 2 below, adapted from an educational 2017 review article by Rivera-Lara *et al.*, illustrates a handful of these indices and how to derive them, together with suggested cutoff values for dysautoregulation. [12, 15]

Cerebral blood flow surrogate	**Autoregulation Index**	**Variables in the Correlation Model**	**Threshold for Dysautoregulation**
NIRS: regional cerebral oxygenation	Tissue oxygenation index (TOx)	Regional oxygen saturation and MAP	>0.3
TCD: cerebral blood flow velocity	Mean flow velocity index (Mx)	Mean cerebral blood flow velocity and MAP or cerebral perfusion pressure	>0.3 or 0.46
ICP monitor: intracranial pressure	Pressure reactivity index (PRx)	Mean ICP and MAP	>0.3
Invasive brain tissue oxygen	Oxygen reactivity index (ORx)	Tissue oxygen pressure and cerebral perfusion pressure or MAP	>0.4

Table 2. Abridged comparison of autoregulation indices, how to derive them, and their suggested cutoff values for impaired autoregulation. MAP, mean arterial pressure; ICP, intracranial pressure; NIRS, near-infrared spectroscopy; TCD, transcranial Doppler. [100, 101]

The time-correlation method is used to quantify TOx, Mx, PRx, and ORx. For Mx, for instance, a Pearson correlation coefficient is taken between 30 time-averaged (10 sec) values of arterial blood pressure and flow velocity. Similarly, for NIRS, a Pearson

correlation coefficient between 30 time-averaged (10 sec) values of arterial blood pressure and tissue oxygenation (TOx) or total hemoglobin concentration (THx). [15]

E. Comparisons between autoregulatory indices

In the past two decades, novel autoregulatory indices have been validated against more weathered ones. These validation studies facilitate the use of newer, possibly superior methods to clinically monitor autoregulation. Of greatest relevance, studies attempting to cross-validate invasive versus non-invasive methods wield the potential to use a non-invasive approach in critically ill patients. Table 3 below presents a summary of said studies. Ultimately, the results shown appear to support the accuracy of non-invasive autoregulation measurements, although the number of indices available renders analytic standardization very challenging.

Study	**Autoregulatory Indices Compared**	**P Value**
Patients with no intracranial injury		
Ono *et al*. 2013 [102]	Mean flow velocity index based on MAP vs. cerebral oximetry index	<0.001
Brady *et al*. 2010 [12]	Mean flow velocity index based on MAP vs. cerebral oximetry index	<0.0001
Steiner *et al*. 2009 [92]	Mean flow velocity index based on MAP vs. tissue oxygen index	<0.0001
Hori *et al*. 2015 [19]	Mean flow velocity index based on MAP vs. cerebral blood flow velocity index	<0.001
Blaine *et al*. 2013 [94]	Mean flow velocity index based on cerebral perfusion pressure vs. hemoglobin volume index	<0.001
Patients with intracranial injuries		
Lang *et al*. 2003 [101]	Mean flow velocity index based on cerebral perfusion pressure vs. mean flow velocity based on MAP	<0.01
Sorrentino *et al*. 2011 [90]	Mean flow velocity index based on cerebral perfusion pressure vs. mean flow velocity based on MAP	<0.001

Lavinio *et al*. 2007 [103]	Mean flow velocity index based on cerebral perfusion pressure vs. mean flow velocity based on MAP	<0.001
Czosnyka *et al*. 2008 [104]	Mean flow velocity index based on cerebral perfusion pressure vs. dynamic autoregulatory index	0.0001
Highton *et al*. 2015 [105]	Mean flow velocity index based on MAP vs. tissue oxygen index	0.004
Soehle *et al.* 2004 [70]	Mean flow velocity index based on MAP vs. systolic flow velocity index	<0.001
Highton *et al.* 2015 [105]	Mean flow velocity index vs. tissue hemoglobin index	<0.001
Budohoski *et al*. 2012 [106]	Pressure reactivity index vs. mean flow velocity index based on cerebral perfusion pressure	<0.001
Lang *et al*. 2012 [107]	Pressure reactivity index vs. low-frequency sample pressure reactivity index	<0.00001
Santos *et al*. 2011 [108]	Pressure reactivity index vs. low-frequency sample pressure reactivity index	<0.001
Barth *et al*. 2010 [109]	Pressure reactivity index vs. brain tissue oxygen pressure reactivity index	0.044
Highton *et al.* 2015 [105]	Pressure reactivity index vs. tissue oxygen index	0.04
Highton *et al.* 2015 [105]	Pressure reactivity index vs. tissue hemoglobin index	<0.001
Zweifel *et al.* 2010 [76]	Pressure reactivity index vs. tissue hemoglobin index	0.0002
Silverman *et al*. 2019 [14]	Pressure reactivity index vs. tissue oxygen index	<0.0001

Table 3. Validation of various autoregulatory indices.

F. Optimal cerebral perfusion pressure

In the last two decades, these autoregulatory indices have also been used to generate optimum cerebral perfusion pressures as well as ideal pressure ranges based on lower and upper limits of autoregulation. Steiner *et al*. published a landmark study in 2002 using continuous autoregulation monitoring as a means of identifying optimal cerebral perfusion pressure (CPP_{OPT}) in patients with traumatic brain injury. [110] This optimal pressure is calculated by plotting cerebral autoregulation indices against a range of blood pressures

over 4-hour monitoring periods and fitting a U-shaped curve to the data. It is possible to retrieve this optimal window at both the population and individual level. The hypothesis surrounding this window of cerebral perfusion pressures is that brain arterioles are capable of maintaining a constant cerebral blood flow with the largest possible autoregulatory reserve at those pressures. At an individual level in the critical care setting, a continuous estimation of an ideal cerebral perfusion pressure presents an attractive target for hemodynamic management. Indeed, this is reflective of the Cambridge hypothesis altogether, which is stated as follows: "Cerebral perfusion pressure (CPP) should be kept at the CPP where an individual patient autoregulates most efficiently." [cppopt.org]

In 2002, Steiner *et al*. monitored upwards of 10,000 hours of continuous data, including mean arterial pressure (MAP), intracranial pressure (ICP), and CPP, in a total of 114 patients with traumatic brain injury. [110] The pressure reactivity index (PRx) was computed as the moving correlation coefficient between time-averaged values of MAP and ICP. CPP_{OPT} was defined as the CPP at which PRx achieved its minimum value when plotted against CPP. This minimum value corresponds to the index at which autoregulation is optimally functioning. In 68 patients (or 60% of the cohort), the authors were able to generate a parabolic curve when plotting PRx against CPP; through the generation of this curve, they were able to determine a CPP_{OPT} for 60% of their cohort. The primary endpoint was 6-month functional outcome on the Glasgow Outcome Scale, which was correlated with the difference between actual CPP and CPP_{OPT}. The team found that outcomes significantly correlated with differences both above ($P<0.05$) and below CPP_{OPT} ($P<0.001$).

In 2012, Aries *et al*. proposed and tested an automated CPP_{OPT} algorithm based on a moving 4-hour window, which updated every minute, in another retrospective cohort of patients with traumatic brain injury. [16] This time around, the team was able to identify CPP_{OPT} for 55% of the total recording period, and they ultimately demonstrated improved outcomes in patients who maintained a CPP near the average, automated CPP_{OPT}.

These relatively low yields of CPP_{OPT} generation posed a considerable problem. In other studies, this yield dipped as low as 44% of the recording period. [111] Weersink *et al*. identified 6 key factors that were independently associated with the absence of the parabolic curve. [112] These factors included absence of slow arterial blood pressure waves, higher PRx values, lower amounts of sedative-analgesic drugs, higher vasoactive medication doses, no administration of maintenance neuromuscular blockers, and decompressive craniectomy operations, all of which associated with the absence of an optimal CPP curve.

Depreitere *et al*. then introduced an innovative and flexible multi-window algorithm for CPP_{OPT} calculation. [111] They utilized a low-resolution version of PRx (termed LAx in their paper) and calculated a moving weight-averaged value of CPP_{OPT} based on windows of different lengths – namely, 2, 4, 6, 8, and 12 hours – instead of a single 4-hour moving window. This weighting system favored two criteria: (1) best-fit U-shaped, second-order polynomial curves, and (2) lower LAx values. In other words, if the U-curve fit the second-order polynomial function well, or if the autoregulatory index was very low, the multi-

window model would preferentially weigh those particular windows, as shown in the equation below (Figure 5). This approach yielded a CPP_{OPT} for a staggering 97% over the total recording period. Perhaps the authors put their approach best: "Hence, autoregulation was investigated in a dynamic way by scanning different time scales to maximally exploit and optimize the potential information on cerebrovascular pressure reactivity capacity within routinely obtained monitoring data."

$$weight = \frac{1}{e^{window\ length}} \times \frac{1}{e^{fit\ error}} \times W_{non-parabolic\ window}$$

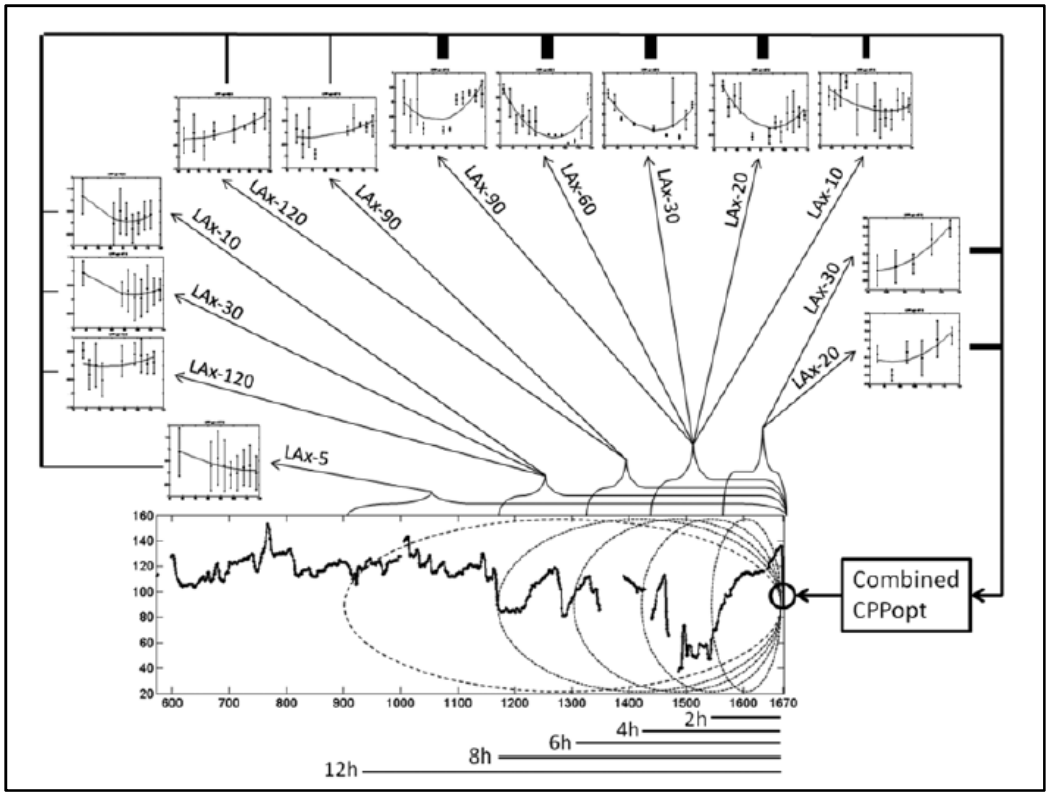

Figure 5. Adapted from Depreitere *et al*., this figure demonstrates the concept underlying the multi-window generation of a weighted CPP_{OPT}. The optimum CPP values received a weighting factor based on the goodness of fit of their U-shaped curve as well as the lower value of the autoregulatory index at CPP_{OPT}. This approach was used in the two Yale cohort studies that will be discussed in Parts II and III.

The evolution of autoregulation-based blood pressure optimization is impressive. With the idea of an individualized, optimal cerebral perfusion pressure range in mind, researchers have carried out many observational studies in both adult and pediatric settings in an effort to personalize hemodynamic care. These studies now stand on the shoulders of Lassen's autoregulatory curve, just now seeing eye-to-eye with society-endorsed guidelines that recommend impersonal, imprecise hemodynamic management of patients with cerebrovascular disease. Nevertheless, randomized controlled trials are lacking. Furthermore, the specialized equipment to monitor and determine optimal pressures is expensive and demanding, not universally available, and requires a moderate degree of training and interpretation abilities. Of course, ICM+ software licenses (University of Cambridge, UK) are required to perform this work, so before widespread distribution of these licenses becomes a reality, data regarding effectiveness in randomized trials is needed.

The primary goal of said feasibility studies was to trend and define an optimal brain perfusion pressure in different patient populations. Secondary goals mostly revolved around investigating whether transgressing the limits of this ideal autoregulatory landscape correlated with functional outcome. Almost needless to say at this juncture, the main hypothesis is that deviation from personalized autoregulatory limits associates with poor functional and radiographic outcomes. This hypothesis will be revisited frequently in the following chapters. Before transitioning to the studies on which this thesis is based, Table

4 below reviews some relevant literature on the published reports attempting to establish feasibility and association with outcome (if applicable).

Study	**Disease Setting**	**Autoregulation Index, Optimal Pressure Used**	**Sample Size**	**Percent Time CPP_{OPT} or MAP_{OPT} Generated**	**Association with Poor Outcome**
Aries *et al*. 2012 [16]	Traumatic brain injury	PRx, CPP_{OPT}	307	55%	Below and above CPP_{OPT}
Depreitere *et al*. 2014 [111]	Traumatic brain injury	Low-frequency autoregulation index, CPP_{OPT}	55	97%	Below and above CPP_{OPT}
Lewis *et al*. 2015 [113]	Traumatic brain injury	PRx, CPP_{OPT}	30	NA	Below CPP_{OPT}
Dias *et al*. 2015 [114]	Traumatic brain injury	PRx, CPP_{OPT}	18	NA	Below CPP_{OPT}
Lang *et al*. 2015 [107]	Traumatic brain injury	Low-frequency sample pressure reactivity index, CPP_{OPT}	307	NA	No association with outcome
Depreitere *et al*. 2014 [111]	Traumatic brain injury	PRx, CPP_{OPT}	55	44%	No association with outcome
Weersink *et al*. 2015 [112]	Traumatic brain injury	PRx, CPP_{OPT}	48	72%	Not performed
Dias *et al*. 2015 [114]	Traumatic brain injury	Cerebral oximetry index, CPP_{OPT}	18	NA	Not performed
Dias *et al*. 2015 [114]	Traumatic brain injury	Brain tissue oxygen pressure reactivity index, CPP_{OPT}	18	NA	Not performed
Dias *et al*. 2015 [114]	Traumatic brain injury	Cerebral blood flow velocity index, CPP_{OPT}	18	NA	Not performed

Jaeger *et al*. 2010 [115]	Traumatic brain injury	PRx, CPP_{OPT}	38	84%	Not performed
Donnelly *et al*. 2017 [91]	Traumatic brain injury	PRx, CPP_{OPT}	729	93%	Below lower limit of autoregulation
Petkus *et al*. 2019 [116]	Traumatic brain injury	PRx, CPP_{OPT}	81	NA	Below CPP_{OPT}
Diedler *et al*. 2014 [17]	Intracerebral hemorrhage	PRx, CPP_{OPT}	38	57%	No association with outcome
Bijlenga *et al*. 2010 [117]	Subarachnoid hemorrhage	PRx, CPP_{OPT}	25	NA	No association with outcome
Hori *et al*. 2015 [19]	Cardiac surgery	Cerebral oximetry index, MAP_{OPT}	121	NA	Below MAP_{OPT}
Hori *et al*. 2015 [118]	Cardiac surgery	Cerebral blood flow velocity index, MAP_{OPT}	69	NA	Not performed
Hori *et al*. 2015 [118]	Cardiac surgery	Mean flow velocity index, MAP_{OPT}	69	NA	Not performed
Hori *et al*. 2017 [119]	Cardiac surgery	Mean velocity index, MAP_{OPT}	614	100%	Below lower limit of autoregulation
Blaine *et al*. 2013 [94]	Cardiac surgery	Mean flow velocity index, MAP_{OPT}	109	87%	Not performed
Blaine *et al*. 2013 [94]	Cardiac surgery	Hemoglobin volume index, MAP_{OPT}	109	100%	Not performed
Burton *et al*. 2015 [21]	Hypoxic-ischemic encephalopathy	Hemoglobin volume index, MAP_{OPT}	17	NA	Below MAP_{OPT}
Lee *et al*. 2013 [120]	Pediatric moyamoya vasculopathy	Cerebral oximetry index, MAP_{OPT}	7	86%	Not performed
Lee *et al*. 2013 [120]	Pediatric moyamoya vasculopathy	Hemoglobin volume index, MAP_{OPT}	7	86%	Not performed
Lee *et al*. 2018 [20]	Pediatric moyamoya vasculopathy	Hemoglobin volume index, MAP_{OPT}	15	100%	Not performed

Rivera-Lara *et al*. 2019 [121]	Acutely comatose*	Cerebral oximetry index, MAP_{OPT}	91	97%	Above and below MAP_{OPT}
Silverman *et al*. 2019 [14]	Subarachnoid hemorrhage	TOx, MAP_{OPT}	31	89.5%	Outside autoregulatory limits
Silverman *et al*. 2019 [14]	Subarachnoid hemorrhage	PRx, MAP_{OPT}	28	87.8%	Outside autoregulatory limits
Petersen *et al*. 2019 [13]	Ischemic stroke	TOx, MAP_{OPT}	65	86.3%	Above upper limit of autoregulation

Table 4. Summary table of relevant studies on optimum CPP or MAP in different patient populations. A handful of the reports went on to examine whether deviation from optimal pressures associated with outcome. *This 2019 study by Rivera-Lara *et al*. enrolled a heterogenous population of acutely comatose patients in their neurocritical care unit. Etiologies included intracerebral hemorrhage (32.5%), aneurysmal subarachnoid hemorrhage (27.7%), traumatic brain injury (14%), acute ischemic stroke (12%), status epilepticus (6.5%), anoxic brain injury (3.1%), and meningitis (2.4%).

PART II

A. Subarachnoid hemorrhage

Subarachnoid hemorrhage (SAH) accounts for approximately 1 to 6% of all stroke subtypes. [122, 123] There are roughly 30,000 adult cases in the United States per year, and 25% die within 24 hours of hemorrhage onset. An additional 40% die within 30 days. Moreover, over one-third of survivors sustain major neurologic deficits. While its incidence falls well below that of ischemic stroke, the young age of afflicted individuals, together with high morbidity and mortality rates, takes a relatively high toll on years of life and functionality lost. [124] As an emergent medical and neurosurgical issue, SAH calls for a multidisciplinary collaboration to achieve favorable patient outcomes.

The incidence of spontaneous SAH in population-based studies is approximately 9.1 cases per 100,000 people annually (95% CI 8.8-9.5) with some regional variation. [125] It is thought that 85% of these cases are aneurysmal in etiology, while 10% are the so-called perimesencephalic type. [122] The latter non-aneurysmal, spontaneous SAH has a specific pattern on imaging and typically entails a better prognosis (Figure 6).

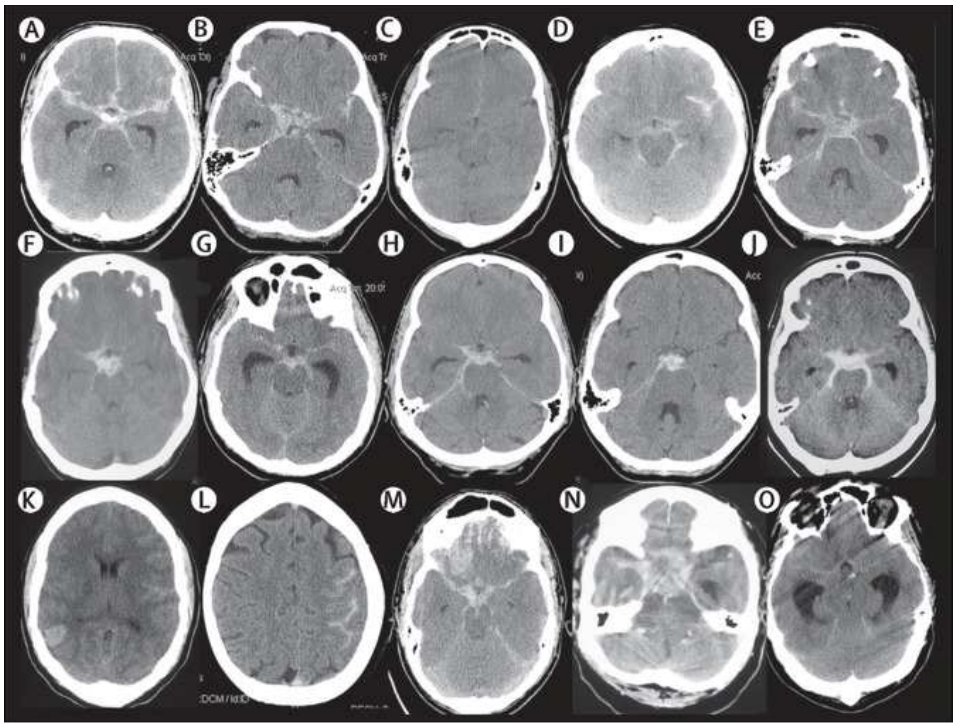

Figure 6. CT scans of different types of subarachnoid hemorrhage, adapted from a 2017 *Lancet* review by R.L. Macdonald and T.A. Schweizer. [122] Panels demonstrate SAH bleeds arising from aneurysms of the right middle cerebral artery (A), right internal carotid artery (B), anterior communicating artery (C), left middle cerebral artery (D), and right superior cerebellar artery (E). Head CT scans of patients with perimesencephalic SAH (F-H, J) resemble an aneurysmal SAH from a basilar bifurcation aneurysm (I), illustrating that CT or catheter angiography are necessary in all patients with this condition. Non-aneurysmal SAH due to cerebral venous thrombosis (K, L), trauma (M), pituitary apoplexy (N), and pseudo-subarachnoid hemorrhage due to increased intracranial pressure, brain swelling, and compression of the basal cisterns (O).

The occurrence of SAH peaks between 50 and 60 years of age. [125] It is 1.6 times more common in females than in males, but this difference becomes most evident only after the fifth decade of life. [125] Risk factors for aneurysm development, aneurysm rupture, and subarachnoid hemorrhage are largely similar. These factors include smoking, hypertension, excess alcohol intake, and increased cholesterol. [126, 127] Non-modifiable risks comprise age, female sex, family history, and a personal medical history of a prior subarachnoid hemorrhage. [125]

When an aneurysm bursts, it is an intracranial catastrophe and an unquestionable emergency. Blood pushes into the subarachnoid space at arterial pressures until the intracranial pressure equalizes across the rupture site and arrests the bleed via thrombosis at the aneurysm rupture site. [128] Subtle prodromal events include headache, dizziness, orbital pain, diploplia, visual loss, sensory or motor disturbance, ptosis, or dysphasia. These symptoms are the results of sentinel leaks, mass effect from aneurysm expansion and growth, emboli, or some combination thereof. Classic presentation of SAH itself can include the canonical "worst headache of life," nausea and vomiting, meningeal irritation, photophobia, visual changes, focal deficits, sudden loss of consciousness, or seizures during the acute phase. Vitals and physical examination findings can include mild to moderate blood pressure elevation, temperature elevation or frank fever, tachycardia, papilledema, retinal or vitreous hemorrhage (e.g., Terson syndrome resulting from either blood tracking through the optic nerve sheath or venous hypertension with rupture of retinal veins), as well as global or focal neurologic abnormalities. In fact, the degree of encephalopathy at presentation is a major determinant of prognosis. [128]

In approximately 11% of events, subarachnoid hemorrhage can be linked to family history, which is defined as two first-degree relatives who have suffered the condition. [129] Another 0.3% of cases result from autosomal dominant polycystic kidney disease. Interestingly, genome wide association studies (GWAS) have identified 6 definite and 1 probable loci with common variants associated with brain aneurysms: 4q31.23 (OR 1.22); 8q11.23–q12.1 (OR 1.28); 9p21.3 (OR 1.31); 10q24.32 (OR 1.29); 12q22 (OR 1.16);

13q13.1 (OR 1.20); 18q11.2 (OR 1.22). [130] A recent study examining messenger RNA (mRNA) expression in whole blood reported that patients with vasospasm following SAH differ from those without vasospasm. [131] Signaling pathways involved in the vasospasm group included, among over one thousand others, adrenergic, P2Y, NO, renin-angiotensin, thrombin, CCR3, CXCR4, MIF, PKA, PKC, and calcium, thereby supporting a role of both coagulation and immunologic systems in those patients suffering from vasospasm. Thus, both genome-wide studies on DNA and RNA wield great potential in SAH studies from a biomarker vantage point and may lead to targetable therapies. [131]

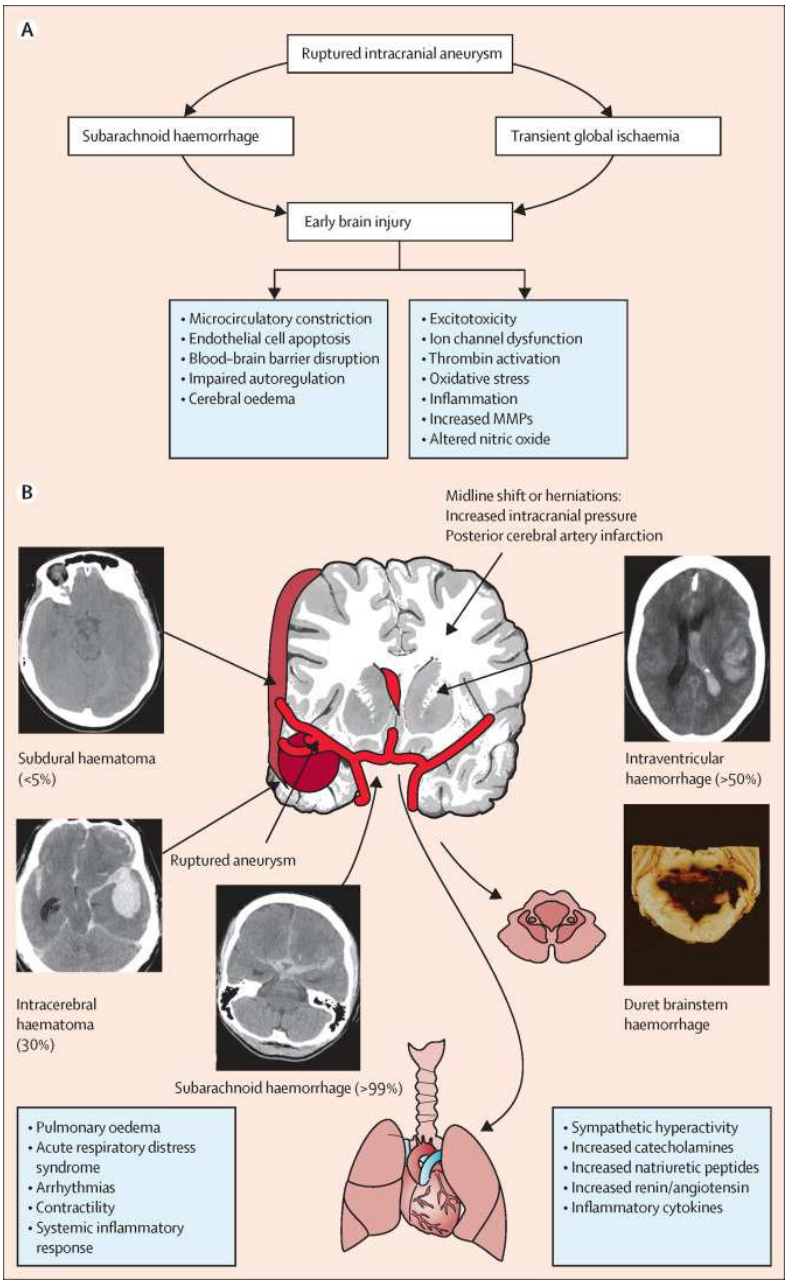

Figure 7. Adapted from Macdonald's *Lancet* review, this figure illustrates the pathophysiology of subarachnoid hemorrhage. [122] Hemorrhage into various compartments (subarachnoid, intraventricular, intracerebral, subdural) can cause brain shift, increased intracranial pressure, herniation, Duret brainstem hemorrhages, and death. Systemic effects of SAH include cardiac and pulmonary complications, including potentially fatal arrhythmias, contractility abnormalities, Takotsubo cardiomyopathy, pulmonary edema, and acute respiratory distress syndrome. Brain injury is initially due to transient global ischemia and effects of the hemorrhage. Delayed neurological complications can ensue, for example, vasospasm and delayed cerebral ischemia.

The brain injury shown in Figure 7 occurs in two phases, the first of which is termed early brain injury. Early injury is caused by transient global ischemia and toxic effects of the subarachnoid blood on brain parenchyma. The delayed phase can result in deterioration in up to a third of patients about 3 to 14 days after the hemorrhage. [132] Delayed cerebral ischemia (DCI), in particular, is the most important complication because no effective preventative measure or treatment exists. It is diagnosed when other causes are ruled out or deemed insufficient to cause observed neurologic worsening. Cerebral infarction from delayed ischemia remains a grave cause of morbidity in patients surviving the initial subarachnoid bleed. [133, 134] The pathophysiology of delayed brain infarction is postulated to involve a multifactorial constellation of vasospasm, dysfunctional autoregulation, microthrombosis, cortical spreading depolarizations and ischemia, as well as well capillary transit time heterogeneity. [11, 132, 135, 136] Despite many randomized trials, the only pharmacologic agent shown to reduce the risk of DCI and poor outcome is the calcium channel blocker nimodipine. Indeed, guidelines recommend oral nimodipine within 96 hours of a subarachnoid bleed in all patients. [25]

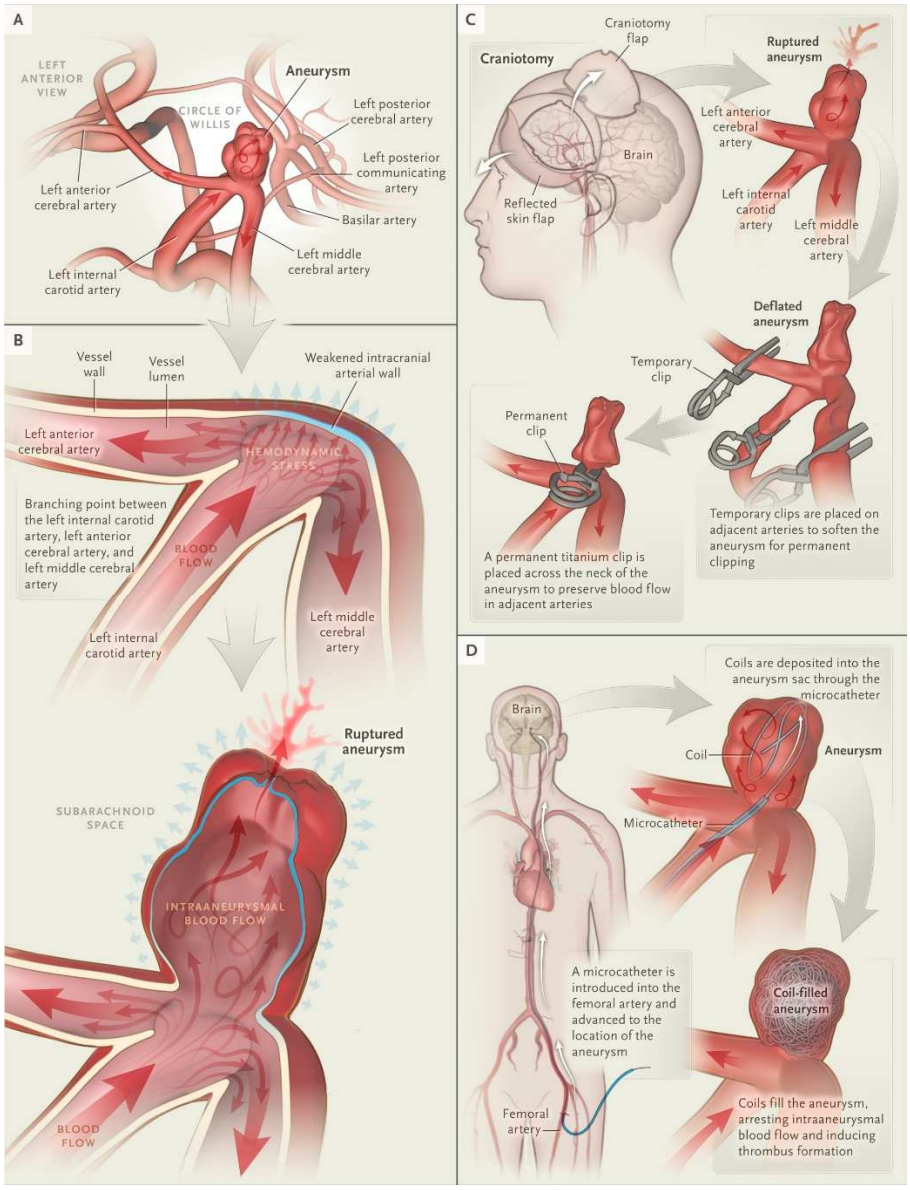

Figure 8. Adapted from the *New England Journal of Medicine*'s 2017 review on subarachnoid hemorrhage by M.T. Lawton and G.E. Vates. [128] Panels A and B display the anatomy of the subarachnoid space and the circle of Willis. High pulsatile pressures at arterial branch points lacking tunica media promote the formation of saccular aneurysms in susceptible persons. Open surgical repair of an aneurysmal bleed (C) involves exposing the aneurysm and adjacent normal arteries so that the neurosurgeon can apply a titanium clip on the neck of the aneurysm. Endovascular repair (D) involves the navigation of an intra-arterial catheter through the circulation under fluoroscopic guidance until the catheter tip is in the lumen of the aneurysm. Platinum coils are then delivered and packed into the lumen of the aneurysm, which slows or prevents blood flow and leads to local thrombus formation.

Management principles in cases of DCI revolve around counteracting reduced oxygen and glucose delivery to the brain. [132, 137] Measures include monitoring of the neurologic exam, maintenance of euthermia, euvolemia, adequate hemoglobin, glucose, electrolytes (especially sodium and magnesium), nutrition, and patient mobilization. These values are important because SAH can be associated with natriuresis and decreased body water secondary to raised natriuretic peptides, renin activity, aldosterone, catecholamines, and arginine vasopressin. [138] However, prophylactic treatments for DCI, such as the purported triple-H therapy for vasospasm (hypertension, hypervolemia, hemodilution), as well as hypermagnesemia and hypothermia, have not been beneficial in studies and are thus no longer officially recommended. [122, 132] Guidelines from the American Heart Association nevertheless state that induced hypertension should be carried out in patients with DCI unless they have pre-existing high blood pressures. [25] If induced hypertension is not possible or ineffective, endovascular pharmacological or mechanical angioplasty is recommended.

Another common complication following SAH is hydrocephalus, stemming from extravasated blood blocking cerebrospinal fluid absorption through subarachnoid cisterns. Parenthetically, recent findings have invoked cerebrospinal hypersecretion as well as immunologic pathways in the pathogenesis of hydrocephalus. [139] Regardless of exact molecular etiology, hydrocephalus following SAH occurs in a wide range of 15 to 85% of cases, though fortunately, most of these cases are not clinically significant. [25] In cases causing encephalopathy, management usually calls for placement of an external ventricular drain (EVD) to drain cerebrospinal fluid and monitor intracranial pressure. [128] Beyond

the brain bleed and the risks of DCI and hydrocephalus, patients with SAH are at risk for serious medical and systemic complications. They should be treated in an intensive care unit and preferably one that specializes in neurocritical care, as is the usual case for patients at Yale-New Haven Hospital. [128]

B. Clinical relevance of autoregulation following subarachnoid hemorrhage

In 1951 at Syracuse Memorial Hospital in New York, Ecker and Riemenschneider first described arterial vasospasm in 7 patients with subarachnoid hemorrhage. [140] Given that vasospasm's peak risk window transpires 5-7 days after the hemorrhage, a causal relationship between spasm and DCI historically has been assumed. [141] However, the fact that some patients with spasm can do well while others deteriorate without spasm casts that relationship into apocryphal light. Furthermore, the CONCIOUS-1 and -2 trials of 2008 and 2011, respectively, showed that clazosentan failed to efficaciously prevent ischemia and infarction after SAH, suggesting that arterial narrowing is insufficient to explain all the possible mechanisms leading to DCI. The trial acronym stands for Clazosentan to Overcome Neurological Ischemia and Infarct Occurring After Subarachnoid Hemorrhage. This drug is an endothelin receptor antagonist used to block arterial vasoconstriction, and while the drug arm in the trials saw a 36% reduction in the need for medical management of vasospasm, both treatment and control groups carried similar rates of DCI and poor outcome. [142, 143]

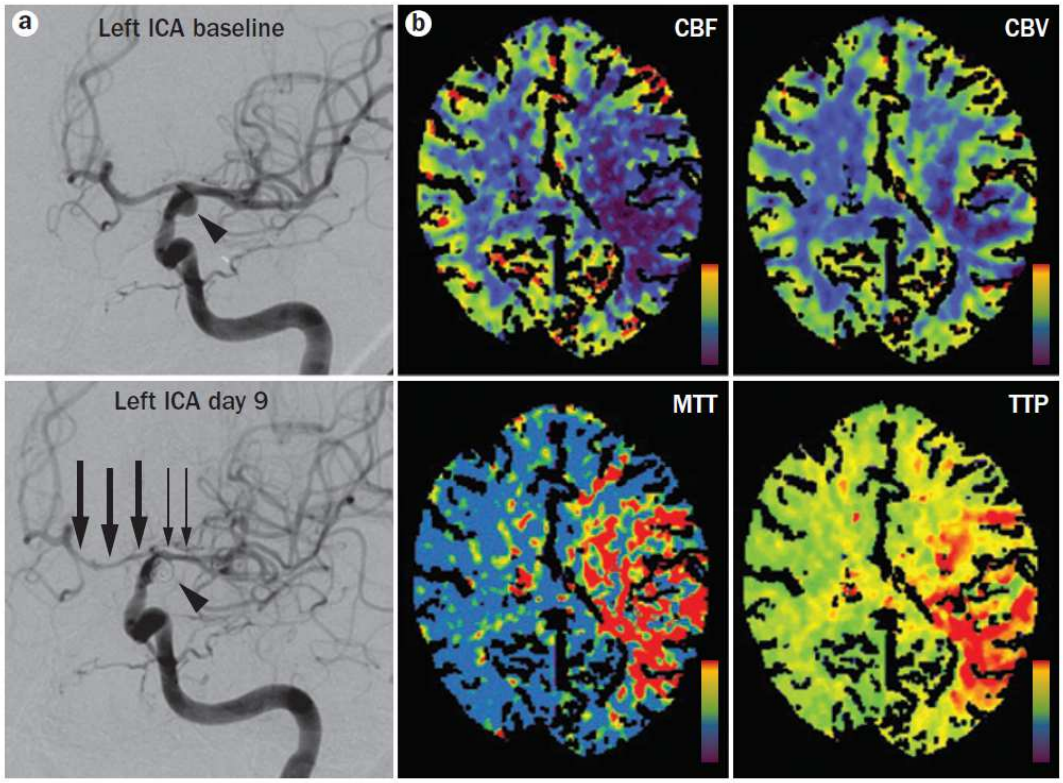

Figure 9. Adapted from a 2013 *Nature Neurology* review on subarachnoid hemorrhage and cerebral autoregulation. Panel A shows a digital subtraction angiography (DSA) at baseline with an aneurysm arising from the left posterior communicating artery. Angiography at day 9 shows the embolized aneurysm with severe vasospasm in the left anterior cerebral artery and moderate spasm in the left middle cerebral artery. Panel B shows perfusion scans performed to assess the hemodynamic consequences of the patient's hemorrhage. There is clearly reduced cerebral blood flow and velocity (CBF and CBV, respectively) in the left parietal lobe, with a corresponding prolongation of mean transit time and time to peak (MTT and TTP, respectively). The findings are in agreement with reversible ischemia in the left middle cerebral artery territory but not in the left anterior cerebral artery, where more severe vasospasm was seen. Thus, this patient illustrates an example of dissociation between cerebral vasospasm and perfusion deficits seen in DCI.

Experimentally, vasospasm does not diminish cerebral blood flow unless there is a secondary insult, such a drop in systemic blood pressure. [144] See Figure 9 for an exemplary dissociation between spasm and perfusion deficits on perfusion imaging. Together with the CONSCIOUS trial findings, this dual insult concept supports Harper's

dual-control hypothesis from the 1970's, whereby distal autoregulatory vasodilation compensates for proximal vasospasm. [145-147] These compensations have their limits, however, and vasodilatory reserve, so to speak, may be exhausted in the setting of severe vasospasm. Consequently, when hemodynamic instability occurs, such as a fall in blood pressure, cerebral blood flow can drop and lead to ischemia and DCI. Of note, autoregulatory impairment as a result of SAH is an insult in its own right, predisposing to cerebral infarction irrespective of a dual insult. [11] In 1985 in Denmark, Voldby *et al.* showed that although spasm alone did not predict DCI, the combination of spasm and impaired autoregulation led to DCI in a large proportion of enrolled patients (admittedly only 38 in total), again supporting Harper's hypothesis. [148] The authors invoke central lactic acidosis secondary to vasospasm as a possible cause of autoregulatory impairment and vasoparalysis. Although concrete experimental data are lacking, a plausible idea is that autoregulatory and vasodilatory exhaustion translate to shortening of the autoregulatory plateau. Conversely, microvascular vasospasm not apparent on angiography could shift the plateau towards higher pressures. [11] While it is unclear how exactly the autoregulatory curve changes post-SAH, experts assume the curve follows one of three patterns, shown in Figure 10.

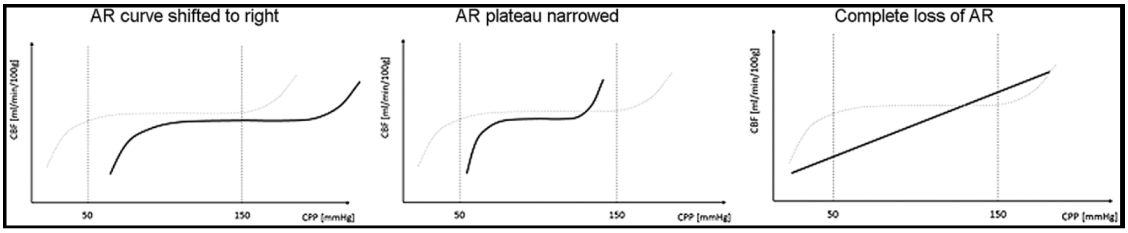

Figure 10. Adapted from Budohoski *et al.*, this figure shows possible effects of SAH on the autoregulatory curve, either via a shift to higher pressures in the left panel, a narrowing of the autoregulatory plateau in the middle, or a complete loss of autoregulatory capacity with passive pressure-

flow propagation in the right panel. [149] AR, autoregulation; CBF, cerebral blood flow; CPP, cerebral perfusion pressure.

The majority of studies that have measured dynamic cerebral autoregulation after SAH have reported impairment in autoregulatory physiology (Table 5, adapted from the 2013 Budhoski *et al.* review and expanded to include more recent studies). The findings described in the table ultimately support autoregulation's clinical import in prognosticating and possibly identifying patients at risk for DCI and poor outcome. Additionally, two retrospective projects showed that an optimal cerebral perfusion pressure increases post-SAH. [117, 150] These studies also demonstrated that more time spent above or below that optimal pressure is associated with worse outcome, but this finding has not yet been replicated in a prospective manner. After SAH, hemodynamic augmentation therapy is often implemented to treat vasospasm and prevent DCI, and so it follows a personalized cerebral perfusion pressure target, based on autoregulatory physiology, is a reasonable strategy. [149] Thus, we set out to monitor autoregulation and personalized limits of hemodynamic compensation in a prospective cohort of SAH patients.

Cerebral autoregulation following SAH: review of relevant literature			
Study	**Sample size**	**Cerebral blood flow measurement**	**Pertinent findings**
Giller *et al.* 1991 [69]	25	TCD	Absence of autoregulatory hyperemic response in all poor-grade patients (n=14) but only in approximately 60% of favourably graded patients
Lam *et al.* 2000 [151]	20	TCD	Patients with impaired autoregulation (n = 5) and vasospasm (n = 6) developed DCI; no patients without impaired autoregulation (n = 14) had DCI
Rätsep *et al.* 2001 [152]	55	TCD	Spasm was associated with DCI only if reduced hyperemic response (n=14)

			was present; in all cases spasm and reduced hyperemic response were associated with DCI (n=12) and poor outcome in 68%
Lang *et al.* 2001 [153]	12	TCD	Testing divided into early (days 1-6) and late (day 7-13); 88% of patients with intact autoregulation (n=8) had good outcomes; impaired autoregulation was predictive of Glasgow Outcome Scale 1 and 2; late phase autoregulation did not have predictive value
Soehle *et al.* 2004 [70]	32	TCD	Spasm caused impairments in autoregulation, which was more affected ipsilateral to spastic vessel, as the authors hypothesized
Tseng *et al.* 2005, 2006 [154-156]	80	TCD	Shorter duration of autoregulatory impairment was associated with lower incidence of DCI in the pravastatin group (n=40)
Jaeger *et al.* 2007, 2012 [157, 158]	67	$PbtO_2$	Impaired autoregulation on day 5-6 post-SAH was an independent predictor of DCI (n = 20); impaired autoregulation was an independent predictor of outcome at 6 months (n=56); these were critical studies in forming our hypotheses
Christ *et al.* 2007 [159]	6	TCD	Dynamic autoregulation was impaired (n=6) compared to healthy controls (n=9)
Tseng *et al.* 2007 [160]	35	TCD, ICP	Impaired autoregulation was found ipsilateral to aneurysm; hypertonic saline improved blood flow but not autoregulation (n=35)
Tseng *et al.* 2009 [161]	80	TCD	Shorter duration of autoregulatory impairments and decreased incidence of severe vasospasm resulted in a reduced incidence of new infarctions in the EPO group (40% vs. 7.5%, n = 40)
Bijelinga *et al.* 2010 [117]	25	ICP	Intact autoregulation had 87.5% positive predictive value for survival (n=16); impaired autoregulation in the first 48 hours correlated with outcome on the modified Rankin scale (n=16)

Barth *et al.* 2010 [109]	21	ICP, $PbtO_2$, TD-rCBF	No differences were found in dynamic autoregulation between infarction (n=8) and no infarction groups (n=13)
Rasulo *et al.* 2011 [162]	29	ICP	Duration of impaired autoregulation was longer in patients with poor outcome (n=14); more time spent below optimal cerebral perfusion pressure was associated with poor outcome (n=14)
Budohoski *et al.* 2012, 2015 [163-165]	98	TCD, NIRS	Disturbed autoregulation in the first 5 days post-SAH was an independent predictor of DCI; these are key studies as well
Steinmeier *et al.* 1996 [166]	10	TCD, ICP, ABP	Spontaneous fluctuations of blood pressure can be used for assessment of autoregulation using continuous intracranial pressure signal
Soehle *et al.* 2003 [167]	NN	$PbtO_2$	$PbtO_2$ autoregulation can be harnessed to titrate cerebral perfusion pressure levels
Zweifel *et al.* 2010 [79]	27	TCD, NIRS	Dynamic autoregulation assessed with NIRS correlates with TCD-based autoregulatory measures; this was a critical study using NIRS to effectively track autoregulation after SAH
Hecht *et al.* 2011 [168]	5	$PbtO_2$, TD-rCBF	Improved correlation of dynamic indices of autoregulation after temporal synchronization
Johnson *et al.* 2016 [169]	47	ICP	All patients were poor-grade and mechanically ventilated; high PRx indices associated with low cerebral blood flow, as measured by xenon-CT, but PRx did not significantly differ between patients with or without DCI
Calviere *et al.* 2015 [170]	30	TCD	Neither autoregulatory impairment nor vasospasm alone as associated with DCI, but the combination of both was significantly correlated with DCI, supporting Harper's dual insult hypothesis
Sugimoto *et al.* 2016 [171]	1	ICP	Cortical spreading depolarization (CSD) and high PRx indices preceded development of DCI in a single patient, lending support to the idea that both CSD and autoregulation should be monitored simultaneously

Liu *et al*. 2018 [172]	81	NIRS	Impaired autoregulation trended toward patients with poorer grades of SAH; DCI occurred in 39 of 51 (48%) patients with impaired autoregulation vs. 6 of 30 (7%) patients with intact autoregulation
Al-Jehani *et al*. 2018 [173]	15	TCD	Six patients developed vasospasm, and 5 (83%) of these patients had abnormal transient hyperemic response tests on initial TCD assessment, performed 24-48 hours of admission for SAH
Otite *et al*. 2014 [174]	68	TCD	Patients with vasospasm had higher transfer function gain, while patients with DCI had lower transfer function phases; in decision tree modelling, gain and phase were strongly predictive of vasospasm and DCI
Ortega-Gutierrez *et al*. 2020 [175]	8	TCD	Lower phase shifts were associated with symptomatic vasospasm and DCI, with a larger cohort on the way
Rynkowski *et al*. 2019 [176]	40	TCD	Impaired hyperemic response found in 19 patients (preserved in n=21) and associated with age, infarction, APACHE II score, and worse outcome
Gaasch *et al*. 2018 [177]	43	ICP, ABP, $PbtO_2$	High pressure reactivity indices (PRx) but not oxygen reactivity indices (ORx), were associated with DCI and worse outcome in poor-grade patients
Abbreviations: DCI, delayed cerebral ischemia; EPO, erythropoietin; ICP, intracranial pressure; NIRS, near-infrared spectroscopy; PbtO2, partial pressure of oxygen in brain tissue; PW-MRI, proton weighted MRI; SAH, subarachnoid hemorrhage; TCD, transcranial Doppler; TD-rCBF, thermal diffusion regional cerebral blood flow; APACHE, acute physiology and chronic health evaluation score.			

Table 5. Indirect cerebral blood flow methods for measurement of dynamic autoregulation in patients with subarachnoid hemorrhage.

C. Pilot study on autoregulation monitoring in subarachnoid hemorrhage

The initial SAH bleed triggers inflammatory cascades, vasospasm, microthrombosis, and cortical spreading depolarizations, all of which likely contribute to DCI. [14] As reviewed in the previous section, the relationship between DCI and any one of these

pathophysiologic mechanisms is nonlinear. Instead, these mechanisms likely represent a constellation of pathophysiology, rendering patients vulnerable to secondary neurological injury. In particular, early impairment of cerebral autoregulation in the setting of vasospasm may compromise the brain's ability to compensate for hemodynamic instability, as may occur during an episode of hypotension. [11] Following aneurysmal SAH (aSAH), local decline in perfusion pressure from vasospasm and/or global reductions of perfusion pressure from hydrocephalus can overwhelm an individual's autoregulatory capacity. Furthermore, the autoregulatory curve can dynamically shift across and within individual patients, providing a strong rationale for personalizing blood pressure management after aSAH. Nevertheless, the role of cerebral autoregulation in aSAH is not fully understood. It has been shown that autoregulatory failure is associated with secondary brain injury, possibly leading to cerebral infarctions and poor outcome. [163, 178] One of the most commonly used autoregulatory indices is the pressure reactivity index (PRx) based on intracranial pressure (ICP); high PRx indices, which reflect dysautoregulation, have been associated with morbidity and mortality in aSAH. [177] Like PRx, the non-invasively acquired NIRS-derived autoregulatory index (TOx) has been linked to DCI and poor outcomes in aSAH. [79, 89] Prior work by our group has shown that NIRS monitoring can be used to identify BP ranges in individual patients at which autoregulation is optimally functioning. Such an autoregulation-derived, personalized BP range may provide a favorable physiological environment for the injured brain. [110] This concept is critical in the evolving era of personalized medicine, particularly as it remains unclear which patients are ideal candidates for therapeutic BP manipulation.

Statement of Purpose

In this prospective, observational study, we employ a novel methodology to trend autoregulatory blood pressure (BP) thresholds in individuals with aneurysmal SAH to determine patient-specific blood pressure targets. This approach involves both invasive (ICP) and non-invasive (NIRS) continuous measures of cerebral autoregulation and optimal BP ranges. Overall, then, the purpose of this study is to define individual BP thresholds in patients with SAH and examine how deviating from those thresholds affects functional and radiographic outcomes. The primary hypothesis is that deviation from personalized autoregulatory limits associates with worse functional and radiographic outcomes following SAH. A secondary hypothesis is that invasive and non-invasive measures of autoregulatory limits correlate with one another.

Specific Aim 1: to evaluate the feasibility of our personalized approach (continuous pressure-flow autoregulation monitoring) in a prospective, observational pilot study in the neuroscience intensive care unit.

Specific Aim 2: to correlate invasive (ICP) and non-invasive (NIRS) measures of autoregulatory indices and blood pressure limits.

Specific Aim 3: to assess the impact of deviating from individualized BP targets on radiographic and clinical outcomes following aSAH.

The first aim serves to further establish feasibility at Yale, as several studies listed in the prior section have done, while the second and third strive to fill more pressing knowledge gaps in the field of autoregulatory research.

Methods

Study Design and Subjects

This was a single-center, prospective cohort study. All patients presenting to the Yale-New Haven Hospital Emergency Department with the diagnosis of acute SAH were screened. Patents were eligible for enrollment if they were older than 18, were diagnosed with an aneurysmal SAH secondary to a ruptured aneurysm, required invasive BP monitoring in the Neuroscience ICU, and were able to have optimal BP monitoring initiated within 48 hours of symptom onset (prior to possible development of vasospasm). An overview of the study timeline is provided below in Figure 11.

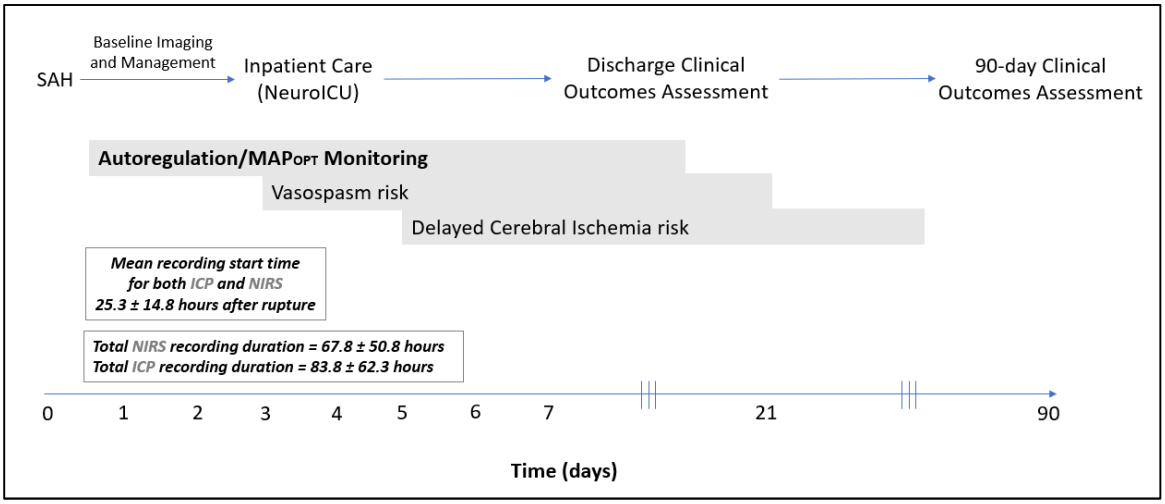

Figure 11. SAH Autoregulation Monitoring: Study Timeline.

Per standard of care, all patients received PO nimodipine. Treatment protocol aimed to maintain ICP less than 22 mmHg and cerebral perfusion pressure (CPP) greater than 50 mmHg. If CPP dropped below 50 mmHg, IV norepinephrine or phenylephrine was administered. To treat clinical vasospasm, hypertension with the same vasopressors was induced. If unsuccessful, verapamil was administered during angiography; in 29.0% of cases in our cohort, balloon angioplasty was also performed.

Patients were excluded in the event of a traumatic SAH or other non-aneurysmal condition. History of prior SAH or a modified Rankin scale >2 before admission were additional exclusion criteria. The institutional review board at the Yale School of Medicine approved this study prior to patient recruitment (HIC number 2000022972). All patients or their legally authorized representatives provided written informed consent.

Near-Infrared Spectroscopy and Intracranial Pressure

Adhesive NIRS probes were placed on the frontotemporal skull covering cortex typically supplied by the middle cerebral artery (Figure 12). These probes connected to the Casmed Foresight Elite monitor (Edwards Lifesciences, USA), which measured oxy- and deoxyhemoglobin concentrations (Figure 13). The ratio of oxyhemoglobin to total hemoglobin (TOI) functions as a cerebral blood flow surrogate and is unaffected by extracranial circulation, hemoglobin concentration, cranial thickness, and cerebrospinal fluid. [80, 179] Cerebral vasoreactivity mediates autoregulation through local vasoconstriction and vasodilation with ensuing fluctuations in cerebral blood flow and volume. [95] Autoregulatory function, therefore, can be measured by interrogating changes in TOI or ICP in response to MAP fluctuations. Arterial BP was monitored invasively through the femoral or radial artery. NIRS, ICP, and BP data were collected continuously for up to 1 week following symptom onset, beginning within 48 hours of symptom onset. All signals were sampled at a frequency of 200 Hz and recorded using ICM+ software (Version 8.4, Cambridge, UK).

Figure 12. Image of NIRS sensor placement. NIRS probes are placed over the frontal scalp, above the eyebrows and just below the hairline, curving around to the temples. In this manner, the probes sense oxy- and deoxyhemoglobin optical densities in the territory most frequently supplied by the middle cerebral artery. This placement does not require shaving of eyebrows or the hairline, nor does it interfere with routine clinical care.

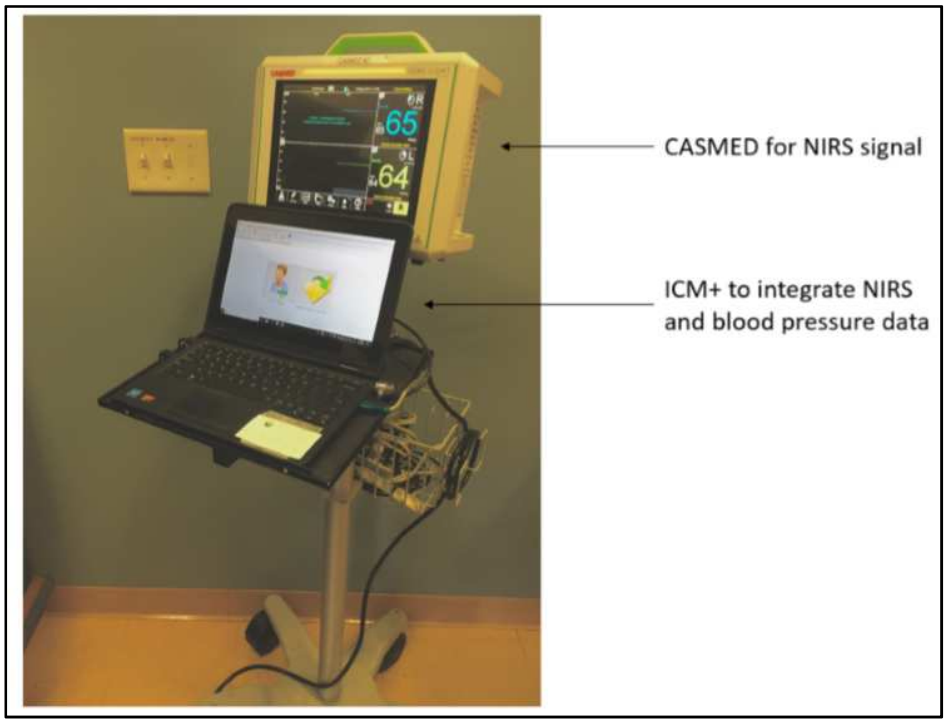

Figure 13. Neuromonitoring setup. The monitoring currently requires one NIRS monitoring device and one laptop computer running ICM+ software (Cambridge Enterprise, Cambridge, UK) per patient. The laptop computer is connected to the patient's bedside monitor to collect continuous physiologic variables including blood pressure. The integrating ICM+ software computes the limits of autoregulation from continuous NIRS and

BP data. These thresholds can be displayed in real-time on the laptop monitor as dynamically updating visual targets for BP management.

ICP was recorded using an external ventricular drain (EVD) in 28 patients. The remaining 3 individuals in our total cohort of 31 patients did not require EVD placement as part of their clinical care and so were not included in ICP-PRx analysis. At Yale, the neurosurgical service handles placement of EVDs by tunneling catheters through the scalp (typically via Kocher's point) and into a lateral ventricle; the neurosurgeon subsequently connects the catheter to a drainage and pressure monitoring system, which, in turn, is primarily handled by specially trained nurses in the Yale-New Haven Hospital Neuro ICU. This connection allows for ICP measurements as well as therapeutic drainage and sampling of cerebrospinal fluid (CSF). In each patient, the height of the EVD was adjusted such that the pressure transducer was anatomically in line with the foramen of Monro, approximately at the level of the external auditory meatus (Figure 14).

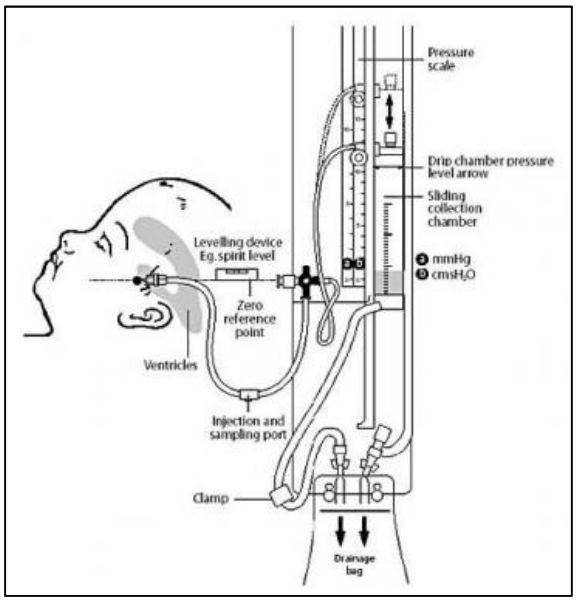

Figure 14. Intracranial pressure monitoring via EVD placement. Image source: Medscape page on intracranial pressure monitors. (URL: https://emedicine.medscape.com/article/1983045-overview).

In the 28 patients with EVDs, ICP was recorded on ICM+ software at a standard frequency of 200 Hz, directly from the pressure transducer illustrated above. (It should be noted that NIRS signals and blood pressure data were also recorded at this standard frequency.) Other than sampling at a frequency of 200 Hz, the ICP signal did not undergo statistical correction.

Regarding artefact in our signal processing, rejecting blood pressure artefact was far more commonly encountered than ICP artefact in our cohort. Blood pressure artefact rejection occurred via a two-step process: (1) automated ICM+ software detection of pulsatility loss in the mean arterial pressure (MAP) waveform, followed by (2) visual inspection of the resultant signal in retrospect. An example of blood pressure artefact is provided in an ICM+ screenshot below, illustrating a rapid, sharp spike in systolic and diastolic pressure. This abrupt increase to a systolic reading of up to 300 mmHg could represent patient movement or flushing or kinking of the line. The representative screenshot in Figure 15 shows a lack of the MAP signal (red) in the highlighted region, demonstrating that ICM+ automatically recognized a lack of pulse pressure pulsatility and, therefore, removed the MAP calculation from display. Following this automated detection of MAP artefact, we visually inspected the MAP signal for obvious, abrupt and large changes.

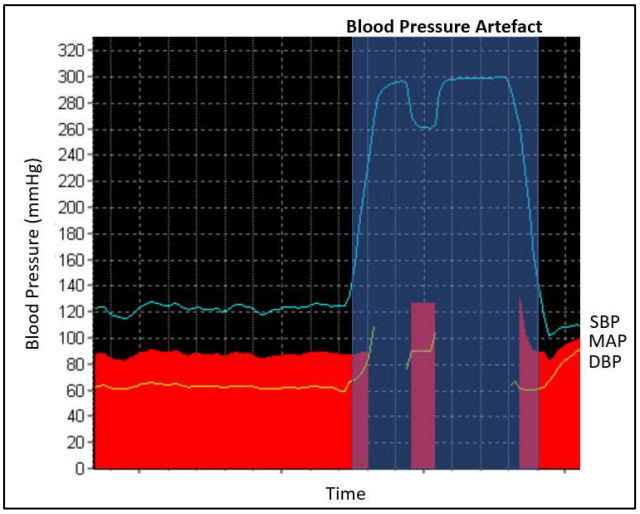

Figure 15. Removal of blood pressure artefact. (ICM+ screenshot)

Compared to blood pressure, accurately identifying ICP artefact is a more complex task, in particular when using an open EVD system. Accordingly, our ICM+ software did not automatically recognize artefacts in the ICP waveform as it did for blood pressure in the above screenshot. We thus had to rely on retrospective visual inspection of the ICP waveform to identify and splice out artefactual signal. Firstly, abrupt drops in the ICP recording to zero or rapid increases to non-physiologic values were excluded from further analysis. Otherwise, we accepted a degree of noise in this data, while rejecting overtly non-physiologic readings, which were not frequently encountered in patients' ICM+ files. In only 3 patients, the ICP signal dropped to zero at several times during the recording. These junctures were spliced out of the recording period. In several other patients, we edited out abrupt, large spikes in the ICP signal that otherwise returned to a normal reading in a matter of seconds; this also occurred infrequently in our cohort. Below, in Figure 16, we have provided a screenshot example of a sudden spike in the ICP reading that was felt to be non-physiologic**.** The remainder of the recording periods were left untouched, as we felt that subjectively edited data (without absolute clear guidance of what constitutes artefactual

signal in the ICP waveform in subarachnoid hemorrhage in particular) could potentially make our approach more challenging from a technical standpoint. Interestingly, various "deep-learning" algorithms are currently being developed to aid in the identification and removal of ICP artefact, but these are not yet incorporated into ICM+ software updates. [180]

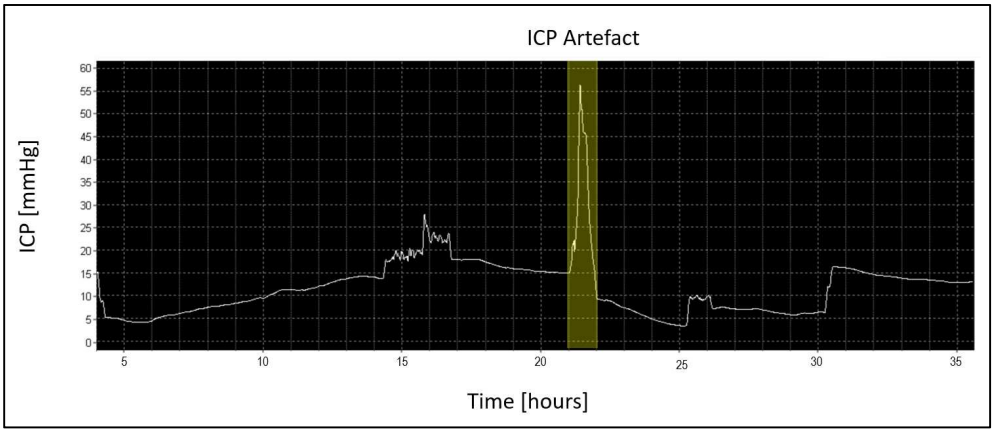

Figure 16. An example of ICP artefact that was removed prior to further signal processing. (ICM+ screenshot)

Regarding EVD status, two recent publications, as well as observations from patients in our cohort, led us to including ICP measurements when the EVD was both open and closed. These papers will be revisited in the discussion (Part II, Section E). In 2015, Aries *et al*. effectively demonstrated that open and closed EVD systems can be harnessed to calculate autoregulatory indices due to the relatively preserved slow fluctuations in the ICP signal. [181] As a follow-up study in 2018, Klein *et al*. described very good agreement of PRx indices obtained via intraparenchymal and EVD measurements of ICP. [182] In fact, 3 patients in our cohort underwent invasive multimodal monitoring with intraparenchymal measurements of ICP. These patients also had EVDs to measure ICP. In these patients, the ICP waveforms derived from the parenchymal probe and the open EVD system appeared

to track each other fairly well. Below, a screenshot of one of said patients is shown (Figure 17). Times during which the EVD was closed are indicated by arrows; one can appreciate that the ICP waveform derived from an open EVD (orange) indeed tracks the ICP waveform derived from the parenchyma (white).

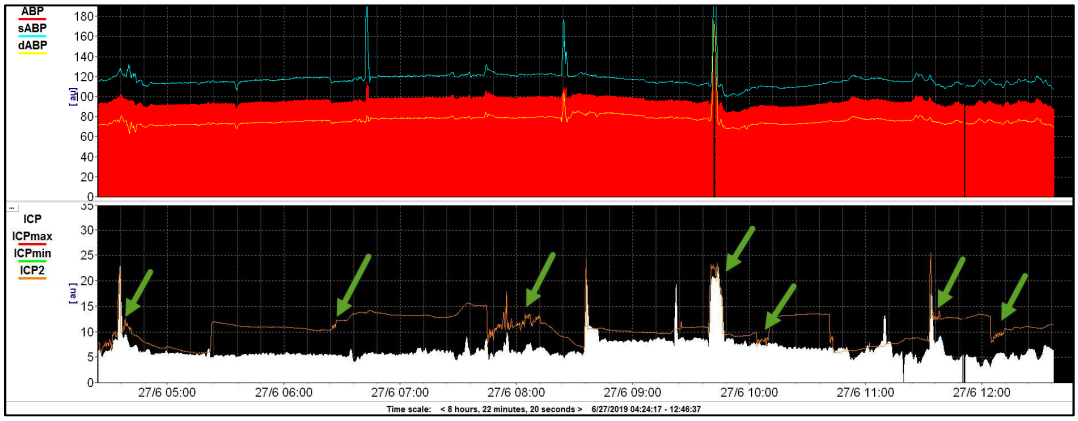

Figure 17. Mirrored intracranial pressure waveforms derived from an open EVD (orange) and the parenchyma (white). (ICM+ screenshot)

Therefore, in considering the aforementioned publications together with our observation that intraparenchymal and open EVD systems exhibit similar ICP waveforms, we included continuous ICP data to derive optimal blood pressure parameters, regardless of EVD status. This approach was both more inclusive and analytically practical and resulted in longer ICP monitoring periods.

Calculation of Autoregulatory Indices

Arterial BP and cerebral blood flow emerge as dynamic physiologic oscillations, and their relationship can be characterized via time-correlation analysis. Indices of autoregulation, including the pressure reactivity index (PRx) and tissue oxygenation index (TOx), are calculated as rolling correlation coefficients between successively averaged MAP values and corresponding ICP or TOI signals, as previously described by Czosnyka et al. [79, 95,

183] MAP maintains a negative or near-zero correlation with ICP or TOI when autoregulation is functional, indicating pressure-reactive brain blood flow. In contrast, MAP positively correlates with ICP or TOI when autoregulation is impaired, whereby systemic pressures passively propagate to cerebral vasculature.

Calculation of Optimal Blood Pressure (MAP_{OPT})

Regarding determination of MAP_{OPT} in individual patients, 5-minute median MAP time trends were computed alongside PRx and TOx. MAP values were allotted into bins of 5 mmHg; corresponding PRx and TOx indices were averaged within these groups. [110] Parabolic curve fitting was applied to the binned pressures to illustrate the MAP value with the lowest associated PRx or TOx (i.e., the MAP at which autoregulation was most preserved). [16] The nadir of this curve reflects MAP_{OPT}. The MAP at which PRx or TOx crosses a threshold for impaired autoregulation (set at PRx or TOx=+0.30) yields lower and upper limits of autoregulation (LLA, ULA). A continuous time trend of MAP_{OPT} and its limits is thus calculated and recorded using a moving 4-hour window that is updated every minute (Figure 18).

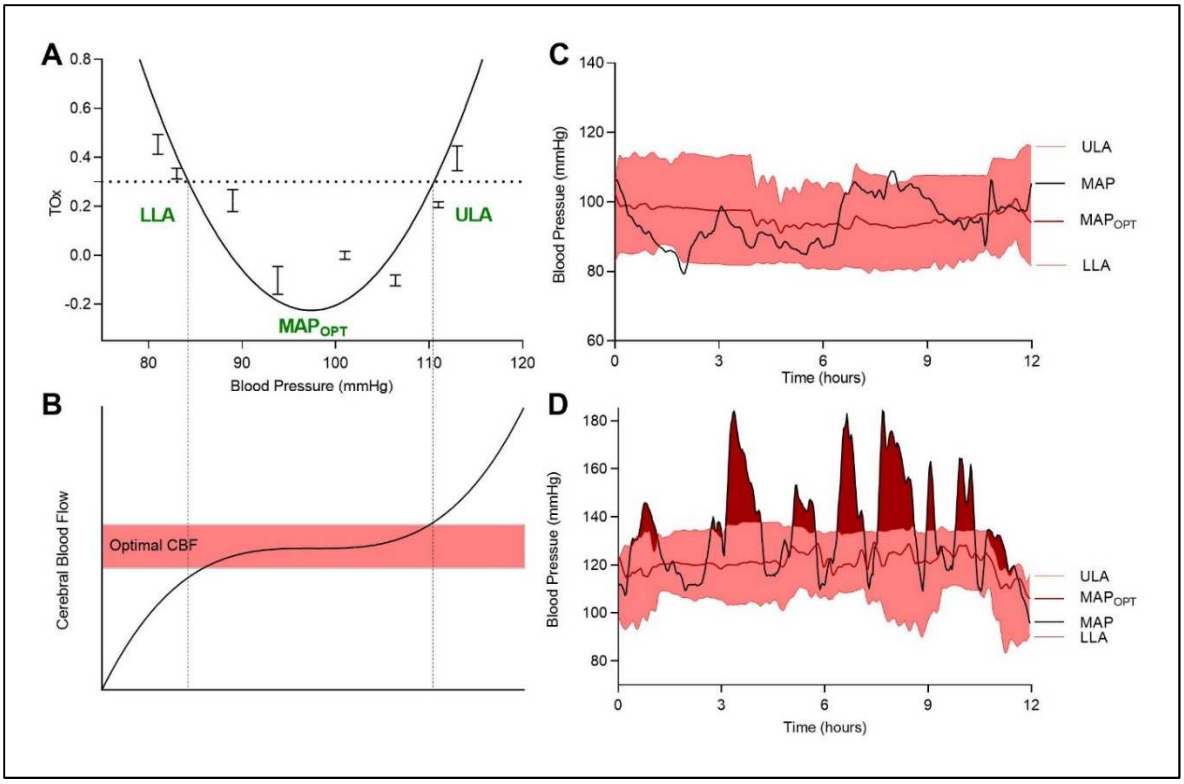

Figure 18. Generation of MAP_{OPT} and personalized limits of autoregulation. Panel A shows the characteristic parabolic curve that is generated when plotting an autoregulatory index against a range of binned blood pressures during a 4-hour recording. The vertex of this U-curve is located at the point with the lowest autoregulatory index and thus represents the optimum blood pressure (MAP_{OPT}). By setting a threshold for impaired autoregulation at TOx=+0.30, intersecting MAP values provide estimates of lower and upper limits of autoregulation (LLA, ULA). These intersections correspond with the inflection points of Lassen's autoregulatory curve, as shown by the dotted vertical lines between Panels A and B. In Panel C, a continuous time trend of these limits can be displayed in real-time, while superimposing the patient's actual BP in black, to provide clinicians with a dynamically updating BP target. Panel D shows another patient's 12-hour recording, during which the patient's blood pressure frequently oscillated outside personalized limits of autoregulation (regions highlighted in dark red above ULA).

Clinical Outcomes

The modified Rankin scale (mRS) was used to assess functional outcome at discharge and 3 months (see figure below for details on the scale). Unfavorable outcome was defined as mRS ≥3. A blinded member of the research team determined 90-day mRS outcomes via

telephone interview. Patients were also assessed for shifts across the entire mRS spectrum. [184]

Clinical Scores and Radiographic Outcomes

All patients were assigned a Hunt & Hess (HH), modified Fisher (mF), and World Federation of Neurologic Surgeons (WFNS) score upon diagnosis of SAH. All patients underwent diagnostic and/or therapeutic cerebral angiogram as part of routine clinical care. When possible, daily transcranial Dopplers (TCD) were performed during the week after aSAH treatment. Further imaging with CT, MRI, or additional angiograms was dependent on the treating clinical team and, therefore, patient-specific. Sonographic cerebral vasospasm was defined using acceleration of TCD mean blood flow velocity using previously defined thresholds, while radiographic vasospasm was defined using CTA, MRA, or catheter angiography, as previously delineated.[19,34] Clinical vasospasm was noted as new focal neurologic signs or deterioration in level of consciousness when other causes of worsening had been excluded. Irrespective of vasospasm, delayed cerebral ischemia (DCI) was defined as cerebral infarction on CT or MRI associated with neurologic worsening that could not otherwise be explained.[20,21] All clinical scores and radiographic definitions were confirmed in regular adjudication meetings, including two staff neurointensivists (Dr. Emily Gilmore and Dr. Nils Petersen) blinded to further analyses.

Statistical Analysis

In each patient, we calculated percent time spent outside the limits of autoregulation (%time outside LA). We used χ^2- or Fisher's exact tests, t-tests, and Mann-Whitney U tests as appropriate. We used generalized linear models (GLM) to test for associations

among %time outside LA and vasospasm, DCI, discharge and 3-month outcome. The GLM modeled ordinal logistic regression to assess for shifts across the mRS range. In multivariate analysis, we accounted for independent variables that have been associated with outcome after aSAH, including age, WFNS, clinical vasospasm, and DCI. Predictive performance of %time outside LA for poor outcome was analyzed via area under the receiver operating characteristic (ROC) curve.

D. Results of the subarachnoid hemorrhage pilot study

Demographics

Thirty-one patients were enrolled (Table 6). Mean NIRS monitoring time was 67.80 (±50.83) hours. Optimal BP could be calculated for a mean of 89.53 (±6.69) % of the total NIRS monitoring period. Patients spent on average 69.13 (±18.93) % of their monitored time within LA (Table 7). Among patients with good and poor outcome at discharge and 90 days, lower and upper limits of autoregulation were not different. BP variability, computed as the standard deviation of MAP during the monitoring period, was also not significantly different between these groups, though a trend toward greater variability was observed in patients with worse discharge outcomes (8.1 *vs.* 16.6 mmHg, P=0.106). Patients with favorable outcome at discharge were younger and experienced angiographic vasospasm and DCI less frequently. They also had lower TOx and PRx indices (i.e., more intact autoregulation), wider NIRS-derived optimal BP ranges, and spent less time outside their dynamic optimal BP ranges (Tables 8 and 9).

Table 6. SAH Cohort: Patient Characteristics.	
Total patients	31
90-day outcomes, n (%)	28 (90.3)
Sex, F (%)	23 (74.2)
Age, mean ± SD	57.5 ± 13.4
Race White Black or African American Hispanic Asian	 18 (58.1) 6 (19.4) 5 (16.1) 2 (6.5)
Admission WFNS, mean ± SD	2.2 ± 1.2
Admission HH, mean ± SD	2.7 ± 0.9
Admission mF, mean ± SD	3.2 ± 1.1
Admission MAP, mean ± SD	97.6 ± 19.6
Aneurysm Location, n (%) Acomm Pcomm MCA ICA Pericallosal Basilar tip PICA No definitive lesion on angiogram with aneurysmal bleed pattern on head CT	 12 (38.7) 5 (16.1) 5 (16.1) 4 (12.9) 1 (3.2) 2 (6.5) 1 (3.2) 1 (3.2)
Medical History*, n (%) Hypertension Coronary Artery Disease Myocardial Infarction Congestive Heart Failure Atrial Fibrillation Hyperlipidemia Diabetes Mellitus (I&II) Cancer Thyroid Disease Migraine Fibromuscular Dysplasia Current Smoker Past Smoker Alcohol Intake (1 drink~12 grams)	 13 (41.9) 1 (3.2) 3 (9.7) 1 (3.2) 1 (3.2) 11 (35.5) 4 (12.9) 4 (12.9) 4 (12.9) 3 (9.7) 1 (3.2) 7 (22.6) 13 (41.9)

1 (no alcohol consumption) 2 (consumption≤150 grams/week) 3 (consumption≥150 grams/week)	21 (67.7) 7 (22.6) 3 (9.7)
Ictal loss of consciousness, n (%)	13 (41.9)
Endovascular coiling, n (%)	24 (77.4)
Surgical clipping, n (%)	3 (9.7)
EVD placed, n (%)	28 (90.3)
Intubated, n (%)	28 (90.3)
Treated for pneumonia, n (%)	13 (41.9)
Treated for *C. difficile*, n (%)	1 (3.2)
Rebleed, n (%)	2 (6.5)
VP shunt placed, n (%)	1 (3.2)
Length of stay, mean days ± SD	19.3 ± 11.3
Early hydrocephalus, n (%)	17 (54.8)
Vasospasm on TCD, CTA, or MRA, n (%)	15 (48.4)
Angiographic vasospasm, n (%)	9 (29.0)
Clinical vasospasm, n (%)	8 (25.8)
DCI, n (%)	6 (19.4)
In-hospital mortality, n (%)	5 (16.1)
90-day mortality, n (%)	5 (19.2) †

Table 6. Patient Characteristics. Baseline demographics are shown. SD: standard deviation; F: female; Acomm: anterior communicating artery; Pcomm: posterior communicating artery; MCA: middle cerebral artery; ICA: internal carotid artery; PICA: posterior inferior cerebellar artery; CT: computed tomography; VP: ventriculoperitoneal; CTA: computed tomography angiography; MRA: magnetic resonance angiography. *Percentages may add to more than 100% due to comorbidity. † Percentage indicates the 90-day mortality of the 26 patients who survived post-discharge from the hospital.

Table 7. Neuromonitoring & Hemodynamic Variables.	
NIRS Neuromonitoring (n = 31)	
Monitoring time (hours)	67.80 ± 50.83
Percent MAP_{OPT} calculated	89.53 ± 6.69
Mean ABP (mmHg)	94.25 ± 13.62
Mean TOx	0.083 ± 0.338
Mean MAP_{OPT} (mmHg)	93.72 ± 12.57
Mean LLA (mmHg)	82.16 ± 12.18
Mean ULA (mmHg)	105.29 ± 11.62
Mean Range (ULA-LLA, mmHg)	23.13 ± 6.74
Percent time MAP<LLA	13.02 ± 9.41
Percent time MAP>ULA	17.82 ± 13.54
Percent time MAP within LA	69.13 ± 18.93
Percent time MAP outside LA	30.83 ± 18.87
ICP Neuromonitoring (n = 28)	
Monitoring time (hours)	83.78 ± 62.26
Percent MAP_{OPT} calculated	87.80 ± 7.25
Mean ABP (mmHg)	95.65 ± 13.93
Mean PRx	0.061 ± 0.401
Mean MAP_{OPT} (mmHg)	94.99 ± 13.25
Mean LLA (mmHg)	82.70 ± 12.91
Mean ULA (mmHg)	106.82 ± 11.70
Mean Range (ULA-LLA, mmHg)	23.97 ± 5.14
Percent time MAP<LLA	12.44 ± 7.04
Percent time MAP>ULA	15.44 ± 9.12
Percent time MAP within LA	72.12 ± 12.79
Percent time MAP outside LA	27.88 ± 12.79

Table 7. NIRS and ICP Neuromonitoring & Hemodynamic Variables. Neuromonitoring and hemodynamic measures are displayed as means ± standard deviations for both NIRS and ICP modalities. NIRS: near-infrared spectroscopy; ICP: intracranial pressure; MAP_{OPT}: optimal mean arterial pressure; ABP: arterial blood pressure; TOx: tissue oxygenation index; PRx: pressure reactivity index; LLA: lower limit of autoregulation; ULA: upper limit of autoregulation; LA: limits of autoregulation.

Table 8. Comparison of patients with good (mRS 0-2) and poor (mRS 3-6) functional outcome at discharge (n=31).

	Good Outcome	*Poor Outcome*	*P VALUE*
Age, median (IQR)	50.0 (40.0-59.5)	63.5 (55.5-73.3)	**0.005**
Sex, n (%) Female Male	 11 (84.6) 2 (15.4)	 12 (66.7) 6 (33.3)	0.412
Admission MAP, median (IQR)	96.0 (76.5-113.5)	94.0 (86.5-104.5)	0.869
WFNS, median (IQR)	2.0 (1.0-2.0)	2.0 (1.3-3.8)	0.215
HH, median (IQR)	2.0 (2.0-3.0)	3.0 (2.0-4.0)	0.258
mF, median (IQR)	3.0 (2.0-4.0)	4.0 (3.0-4.0)	0.082
Ictal LoC, n (%) Yes No	 4 (30.8) 9 (69.2)	 9 (50.0) 9 (50.0)	0.462
Vasospasm on TCD, CTA, or MRA, n (%) Yes No	 6 (46.2) 7 (53.8)	 9 (50.0) 9 (50.0)	0.833
Angiographic Vasospasm, n (%) Yes No	 1 (7.7) 12 (92.3)	 8 (44.4) 10 (55.6)	**0.045**
Clinical Vasospasm, n (%) Yes No	 1 (7.7) 12 (92.3)	 7 (38.9) 11 (61.1)	0.095
DCI, n (%) Yes No	 0 (0.0) 13 (100.0)	 6 (33.3) 12 (66.7)	**0.028**
Early hydrocephalus, n (%) Yes No	 7 (53.8) 6 (46.2)	 10 (55.6) 8 (44.4)	0.925
Length of Stay, median (IQR)	14.0 (12.0-17.0)	17.5 (13.8-29.0)	0.125
NIRS			
TOx, median (IQR)	0.006 (-0.04-0.04)	0.150 (0.06-0.23)	**0.002**
LLA, median (IQR)	80.4 (76.4-82.2)	81.6 (74.0-90.5)	0.679
ULA, median (IQR)	108.4 (98.0-114.0)	101.3 (96.1-111.8)	0.352

Range, median (IQR)	28.4 (23.6-30.7)	19.6 (15.7-25.4)	**0.010**
MAP_{OPT}, median (IQR)	92.8 (86.1-98.7)	91.4 (80.5-100.5)	0.622
MAP, median (IQR)	94.6 (86.2-99.0)	91.2 (81.8-100.8)	0.514
MAP Variability, median (IQR)	11.0 (8.9-12.4)	13.4 (10.2-15.6)	0.106
%time MAP<LLA, median (IQR)	8.1 (3.1-15.5)	16.6 (6.0-24.7)	0.051
%time MAP>ULA, median (IQR)	9.7 (5.6-11.3)	22.9 (11.6-29.1)	**0.002**
%time outside limits of autoregulation, median (IQR)	17.9 (13.2-21.8)	40.5 (19.8-54.4)	**0.002**
Monitoring Time, median (IQR)	42.1 (13.6-61.2)	68.5 (36.0-145-9)	**0.034**
ICP			
PRx, median (IQR)	0.014 (-0.005-0.049)	0.075 (0.04-0.12)	**0.001**
LLA, median (IQR)	81.5 (74.8-84.6)	80.9 (72.6-89.6)	0.963
ULA, median (IQR)	107.7 (95.8-113.6)	107.3 (96.9-118.7)	0.890
Range, median (IQR)	24.5 (21.3-26-9)	25.0 (18.0-29.4)	0.861
MAP_{OPT}, median (IQR)	96.3 (84.5-100.0)	90.0 (84.2-105.9)	0.926
%time MAP<LLA, median (IQR)	6.9 (2.6-13.3)	13.9 (11.0-19.0)	**0.029**
%time MAP>ULA, median (IQR)	10.8 (6.2-16.6)	15.8 (11.0-22.3)	0.111
%time outside limits of autoregulation, median (IQR)	22.1 (10.3-29.1)	30.9 (24.4-42.2)	**0.015**
Monitoring Time, median IQR	42.7 (16.0-70.0)	93.8 (47.7-172.0)	**0.019**

Table 8. Comparison of patients with good (mRS 0-2) and poor (mRS 3-6) functional outcome at discharge. Utilizing non-parametric statistics (Mann Whitney U, chi-squared, or Fisher's exact test, when appropriate), baseline demographic, clinical outcome measures, neuromonitoring as well as hemodynamic variables were compared were compared in patients good vs. poor outcome at discharge, as determined by a modified Rankin Scale (mRS) or 0-2 vs. 3-6, respectively. IQR: interquartile range; WFNS: World Federation of Neurologic Surgeons; HH: Hunt & Hess; mF: modified Fisher; LoC: loss of consciousness; TCD: transcranial Doppler; CTA:

computed tomography angiography; MRA: magnetic resonance angiography; DCI: delayed cerebral ischemia; TOx: tissue oxygenation index; LLA: lower limit of autoregulation; ULA: upper limit of autoregulation; MAP_{OPT}: optimal mean arterial pressure; ICP: intracranial pressure; PRx: pressure reactivity index.

Table 9. Comparison of patients with good (mRS 0-2) and poor (mRS 3-6) functional outcome at 90-day follow-up (n=28).

	Good Outcome	*Poor Outcome*	*P VALUE*
Age, median (IQR)	56.0 (45.0-64.0)	67.0 (60.0-74.5)	0.061
Sex, n (%) Female Male	 15 (78.9) 4 (21.1)	 6 (66.7) 3 (33.3)	0.646
Admission MAP, median (IQR)	97.5 (83.0-112.8)	94.0 (81.0-104.5)	0.820
WFNS, median (IQR)	2.0 (1.0-2.0)	2.0 (2.0-3.0)	0.172
HH, median (IQR)	2.0 (2.0-3.0)	3.0 (2.0-3.5)	0.263
mF, median (IQR)	3.0 (2.0-4.0)	4.0 (4.0-4.0)	**0.048**
Ictal LoC, n (%) Yes No	 7 (36.8) 12 (63.2)	 4 (44.4) 5 (55.6)	0.700
Vasospasm on TCD, CTA, or MRA, n (%) Yes No	 8 (42.1) 11 (57.9)	 4 (44.4) 5 (55.6)	1.000
Angiographic Vasospasm, n (%) Yes No	 3 (15.8) 16 (84.2)	 4 (44.4) 5 (55.6)	0.165
Clinical Vasospasm, n (%) Yes No	 3 (15.8) 16 (84.2)	 3 (33.3) 6 (66.7)	0.352
DCI, n (%) Yes No	 1 (5.3) 18 (94.7)	 3 (33.3) 6 (66.7)	0.084
Early hydrocephalus, n (%) Yes No	 9 (47.4) 10 (52.6)	 6 (66.7) 3 (33.3)	0.435
Length of Stay, median (IQR)	14.0 (12.0-18.0)	17.0 (13.5-26.0)	0.308

NIRS			
TOx, median (IQR)	0.034 (-0.03-0.09)	0.229 (0.10-0.27)	**0.002**
LLA, median (IQR)	80.4 (76.2-82.4)	84.7 (76.4-108.9)	0.129
ULA, median (IQR)	107.9 (97.5-113.3)	100.9 (93.8-125.3)	0.847
Range, median (IQR)	19.6 (15.7-25.4)	15.8 (13.4-21.1)	**0.001**
MAP_{OPT}, median (IQR)	92.8 (86.9-98.4)	91.5 (85.6-119.6)	0.735
MAP, median (IQR)	93.7 (84.3-98.7)	92.2 (83.1-121.6)	0.847
MAP Variability, median (IQR)	12.2 (10.3-14.9)	14.0 (9.3-15.0)	0.664
%time MAP<LLA, median (IQR)	10.0 (3.3-17.5)	24.1 (11.0-25.8)	**0.048**
%time MAP>ULA, median (IQR)	9.9 (6.6-17.4)	27.8 (18.4-36.6)	**0.004**
%time outside limits of autoregulation, median (IQR)	17.9 (14.6-33.3)	52.0 (39.3-65.0)	**0.001**
Monitoring time, median (IQR)	42.5 (25.9-87.7)	93.4 (35.3-162.9)	0.105
ICP			
PRx, median (IQR)	0.027 (0.007-0.067)	0.075 (0.05-0.14)	**0.032**
LLA, median (IQR)	81.6 (74.6-84.2)	80.9 (72.5-101.0)	1.000
ULA, median (IQR)	108.3 (97.4-113.5)	107.3 (96.9-124.6)	0.934
Range, median (IQR)	25.0 (17.9-29.4)	24.5 (17.0-30.8)	1.000
MAP_{OPT}, median (IQR)	96.0 (85.7-100.2)	90.0 (84.7-114.4)	0.890
%time MAP<LLA, median (IQR)	12.4 (5.1-17.3)	16.4 (11.6-19.7)	0.229
%time MAP>ULA, median (IQR)	11.8 (8.1-16.4)	17.3 (13.5-34.5)	**0.037**
%time outside limits of autoregulation, median (IQR)	24.6 (14.7-30.4)	38.5 (29.8-44.8)	**0.012**
Monitoring time, median (IQR)	60.1 (40.6-108.2)	93.8 (42.1-172.0)	0.419

Table 9. Comparison of patients with good (mRS 0-2) and poor (mRS 3-6) functional outcomes at 90-day follow-up. Utilizing non-parametric statistics (Mann Whitney U, chi-squared, or Fisher's exact test, when appropriate), baseline demographic, clinical outcome measures, neuromonitoring as well

as hemodynamic variables were compared were compared in patients good vs. poor outcome at 90 days, as determined by a modified Rankin Scale (mRS) or 0-2 vs. 3-6, respectively. IQR: interquartile range; WFNS: World Federation of Neurologic Surgeons; HH: Hunt & Hess; mF: modified Fisher; LoC: loss of consciousness; TCD: transcranial Doppler; CTA: computed tomography angiography; MRA: magnetic resonance angiography; DCI: delayed cerebral ischemia; TOx: tissue oxygenation index; LLA: lower limit of autoregulation; ULA: upper limit of autoregulation; MAP_{OPT}: optimal mean arterial pressure; ICP: intracranial pressure; PRx: pressure reactivity index.

Autoregulatory Indices and Outcome

In univariate analysis, TOx associated significantly with functional outcome at discharge (*P*=0.001, OR 3.0, 95% CI 1.5-5.8) and 90 days (*P*=0.006, OR 2.5, 95% CI 1.3-4.8). These associations held when adjusting separately for age, WFNS, vasospasm, and DCI (Tables 10 and 11). PRx significantly associated with discharge mRS (*P*=0.010, OR 6.3, 95% CI 1.6-25.6) and 90-day mRS (*P*=0.016, OR 5.6, 95% CI 1.4-22.6). These associations held when adjusting separately for age, WFNS, and vasospasm.

Table 10. Predictors of functional outcome at discharge in univariate ordinal regression analysis (n = 31).

VARIABLE	*P VALUE*
Age	**0.016**
Sex	0.647
Admission MAP	0.525
Ictal loss of consciousness	0.347
WFNS	**0.007**
Hunt-Hess	0.055
Modified Fisher	0.082
Length of stay	0.280
Early hydrocephalus	0.277
Radiographic vasospasm (TCD, CTA, or MRA)	0.725
Angiographic vasospasm	**0.023**
Clinical vasospasm	**0.028**
Delayed cerebral ischemia	**0.004**
Re-bleed	0.167
Extraventricular drain placed	0.053
Intubated	0.053
Treated with surgical clipping	0.252

Treating with endovascular coiling	0.834
Past Medical History	
Hypertension	0.533
Coronary Artery Disease	1.000
Myocardial Infarction	0.406
Congestive Heart Failure	0.705
Atrial Fibrillation	0.705
Hyperlipidemia	**0.010**
Diabetes Mellitus (I & II)	0.892
Cancer	0.477
Thyroid Disease	0.076
Migraine	0.681
Current Smoker	0.428
Past Smoker	**0.020**
Excessive Alcohol Intake	0.868
NIRS	
TOx	**0.001**
Percent time MAP_{OPT} calculated	0.633
Mean MAP_{OPT}	0.246
Mean MAP	0.293
Mean upper limit of autoregulation (ULA)	0.970
Mean lower limit of autoregulation (LLA)	**0.043**
Autoregulatory range (ULA – LLA)	**0.001**
Percent time MAP > ULA	**0.005**
Percent time MAP < LLA	**0.011**
Percent time MAP within limits of autoregulation	**0.0004**
Percent time MAP outside limits of autoregulation	**0.0004**
ICP	
PRx	**0.010**
Percent time MAP_{OPT} calculated	0.785
Mean MAP_{OPT}	0.368
Mean MAP	0.208
Mean upper limit of autoregulation (ULA)	0.295
Mean lower limit of autoregulation (LLA)	0.176
Autoregulatory range (ULA – LLA)	0.243
Percent time MAP > ULA	**0.010**
Percent time MAP < LLA	**0.046**
Percent time MAP within limits of autoregulation	**0.003**
Percent time MAP outside limits of autoregulation	**0.003**

Table 10. Predictors of functional outcome at discharge in univariate ordinal regression analysis. Univariate predictors of worse discharge mRS include age, WFNS, angiographic vasospasm, clinical vasospasm, delayed cerebral ischemia, and hyperlipidemia. NIRS-derived predictors include TOx, LLA, the autoregulatory optimal blood pressure range, %time MAP > ULA, %time MAP < LLA, and %time MAP outside autoregulatory limits. IPC-derived predictors include PRx, %time MAP > ULA, %time MAP < LLA, and %time MAP outside autoregulatory limits.

Table 11. Predictors of functional outcome at 90-day follow-up in univariate ordinal regression analysis (n = 28).

VARIABLE	*P VALUE*
Age	**0.007**
Sex	0.648
Admission MAP	0.785
Ictal loss of consciousness	0.635
WFNS	0.071
Hunt-Hess	0.530
Modified Fisher	0.088
Length of stay	0.347
Early hydrocephalus	0.311
Radiographic vasospasm (TCD, CTA, or MRA)	0.749
Angiographic vasospasm	0.058
Clinical vasospasm	0.126
Delayed cerebral ischemia	**0.011**
Re-bleed	1.000
Extraventricular drain placed	0.105
Intubated	0.105
Treated with surgical clipping	0.920
Treating with endovascular coiling	0.914
Past Medical History	
Hypertension	0.148
Coronary Artery Disease	1.000
Myocardial Infarction	0.168
Congestive Heart Failure	0.513
Atrial Fibrillation	0.513
Hyperlipidemia	**0.007**
Diabetes Mellitus (I & II)	0.697
Cancer	0.505
Thyroid Disease	0.079
Migraine	0.858
Current Smoker	0.266
Past Smoker	**0.032**
Excessive Alcohol Intake	0.830

NIRS	
TOx	**0.006**
Percent time MAP_{OPT} calculated	0.883
Mean MAP_{OPT}	0.577
Mean MAP	0.621
Mean upper limit of autoregulation (ULA)	0.658
Mean lower limit of autoregulation (LLA)	0.125
Autoregulatory range (ULA – LLA)	**0.002**
Percent time MAP > ULA	**0.031**
Percent time MAP < LLA	**0.006**
Percent time MAP within limits of autoregulation	**0.002**
Percent time MAP outside limits of autoregulation	**0.002**
ICP	
PRx	**0.016**
Percent time MAP_{OPT} calculated	0.914
Mean MAP_{OPT}	0.849
Mean MAP	0.761
Mean upper limit of autoregulation (ULA)	0.999
Mean lower limit of autoregulation (LLA)	0.672
Autoregulatory range (ULA – LLA)	0.266
Percent time MAP > ULA	**0.028**
Percent time MAP < LLA	**0.039**
Percent time MAP within limits of autoregulation	**0.004**
Percent time MAP outside limits of autoregulation	**0.004**

Table 11. Predictors of 90-day functional outcome in univariate ordinal regression analysis. Univariate predictors of worse 3-month mRS include age, delayed cerebral ischemia, and hyperlipidemia. NIRS-derived predictors include TOx, the autoregulatory optimal blood pressure range, %time MAP > ULA, %time MAP < LLA, and %time MAP outside autoregulatory limits. IPC-derived predictors include PRx, %time MAP > ULA, %time MAP < LLA, and %time MAP outside autoregulatory limits.

Given the heterogeneity in autoregulation monitoring techniques, we sought to correlate our invasive and non-invasive autoregulatory indices. Beyond just the indices, we were interested to ascertain whether the NIRS- and ICP-derived personalized blood pressure limits correlated well with one another. Non-parametric regression analysis revealed that NIRS- and ICP-derived MAP_{OPT} (Spearman 0.92, $P<0.0001$), LLA (Spearman 0.88,

P<0.0001), and ULA (Spearman 0.92, *P*<0.0001) demonstrated strong correlations with one another (Figure 19). To further illustrate agreement, Bland-Altman plots were constructed (Figure 20). Overall, the low bias values and relatively narrow 95% confidence intervals (dotted lines on the Bland-Altman plots) underscore collinearity between NIRS- and ICP-based limits of autoregulation. Moreover, there is apparent scattered variability surrounding the x-axis in all Bland-Altman plots shown, adding to the validity of the analysis.

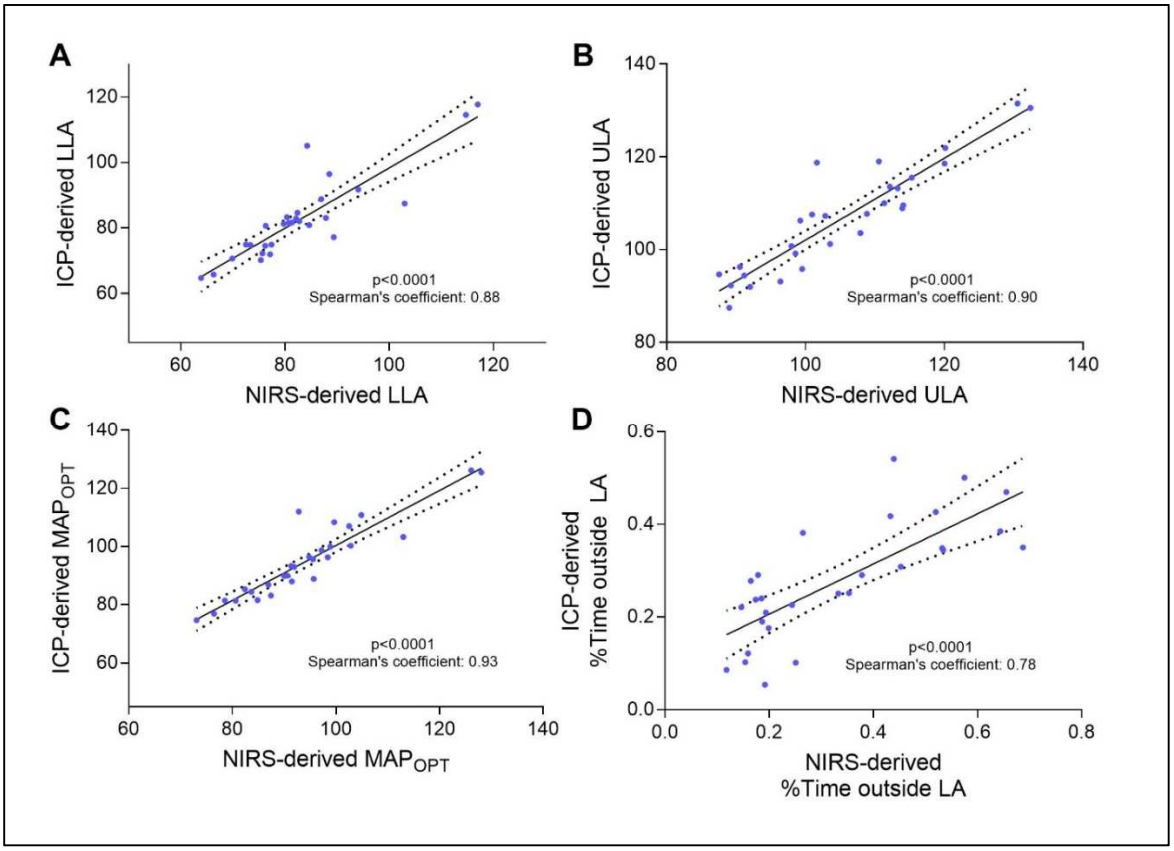

Figure 19. Correlation between ICP- and NIRS-derived limits of autoregulation. ICP- and NIRS-derived autoregulatory parameters significantly correlated in bivariate non-parametric analysis (Panels A-C). Both ICP- and NIRS-derived %time outside LA also correlated with one another; the axes in this panel are shown as decimals (Panel D). Best-fit lines and corresponding 95% confidence intervals are displayed to illustrate linear relationships. LA: limits of autoregulation.

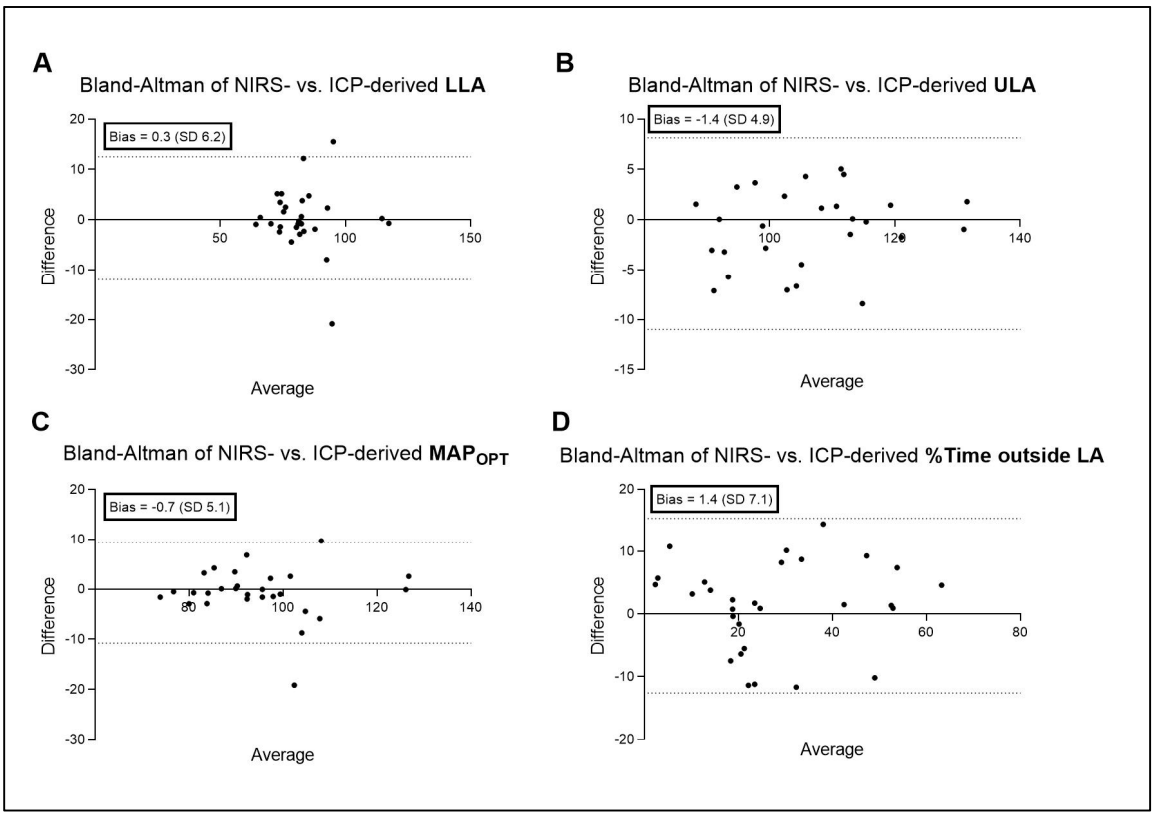

Figure 20. Bland-Altman analyses of NIRS- vs. ICP-derived autoregulatory parameters. Panels A-D display Bland-Altman plots (difference vs. average) for NIRS- vs. ICP-derived LLA, ULA, MAP_{OPT}, and percent time MAP spent outside LA. The dotted lines in each plot represent 95% confidence intervals. LLA: lower limit of autoregulation; ULA: upper limit of autoregulation; MAP_{OPT}: mean arterial pressure; %time MAP outside LA: percent time MAP spent outside limits of autoregulation.

Limits of Autoregulation and Clinical Outcome

Using ICP-derived optimal blood pressures, %time outside LA was a significant predictor of unfavorable outcome at discharge (*P*=0.003, OR 2.6, 95% CI 1.4-4.9) and 90 days (*P*=0.004, OR 2.8, 95% CI 1.4-5.5) (Figure 21, panels A and B). Every 10% increase in time spent outside LA was associated with a 2.8-fold increase in the odds of shifting towards a worse outcome on the 90-day mRS. These associations remained significant after separate adjustments for age, WFNS, vasospasm, and DCI (Tables 12 and 13).

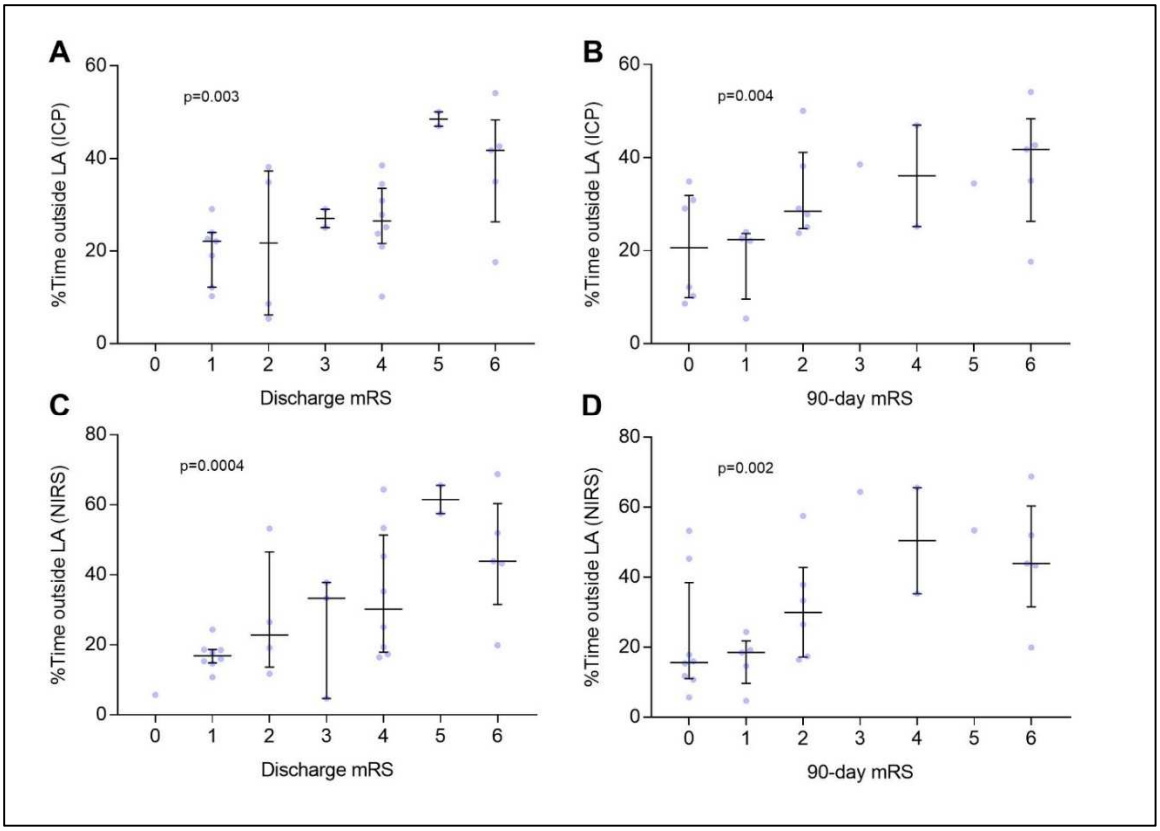

Figure 21. Percent time MAP spent outside limits of autoregulation associates with discharge and 90-day functional outcome following aSAH. A&B: Deviating from ICP-derived autoregulatory limits associated with discharge and 90-day outcome. C&D: Deviating from NIRS-derived autoregulatory limits associated with discharge and 90-day outcome. P-values shown demonstrate statistical significance in univariate ordinal regression. Error bars represent 95% confidence intervals. OR: odds ratio; CI: confidence interval.

Table 12. Multivariate association between NIRS- and ICP-derived autoregulatory parameters and functional outcome at discharge.

Variables included in multivariate model	*aOR*	*95% CI*	*P VALUE*
NIRS (n=31)			
TOx, Age	2.6	1.3-5.1	**0.006**
TOx, WFNS	2.4	1.2-4.9	**0.013**
TOx, Radiographic Vasospasm	3.0	1.5-5.8	**0.001**
TOx, Angiographic Vasospasm	3.1	1.5-6.1	**0.002**

TOx, Clinical Vasospasm	3.4	1.7-6.8	**0.001**
TOx, DCI	2.7	1.4-5.4	**0.005**
%time outside LA, Age	2.2	1.4-3.5	**0.001**
%time outside LA, WFNS	2.1	1.3-3.3	**0.002**
%time outside LA, Radiographic Vasospasm	2.2	1.4-3.5	**0.0004**
%time outside LA, Angiographic Vasospasm	2.4	1.5-3.9	**0.0003**
%time outside LA, Clinical Vasospasm	2.6	1.6-4.3	**0.0001**
%time outside LA, DCI	2.4	1.5-3.9	**0.0004**
ICP (n=28)			
PRx, Age	6.5	1.6-27.1	**0.010**
PRx, WFNS	5.2	1.2-22.3	**0.028**
PRx, Radiographic Vasospasm	7.2	1.7-30.1	**0.007**
PRx, Angiographic Vasospasm	4.9	1.1-20.9	**0.034**
PRx, Clinical Vasospasm	4.3	1.1-21.0	**0.033**
PRx, DCI	4.2	0.9-19.0	0.064
%time outside LA, Age	2.6	1.3-4.9	**0.004**
%time outside LA, WFNS	2.3	1.2-4.5	**0.010**
%time outside LA, Radiographic Vasospasm	2.7	1.4-5.1	**0.003**
%time outside LA, Angiographic Vasospasm	2.3	1.2-4.5	**0.012**
%time outside LA, Clinical Vasospasm	2.4	1.2-4.6	**0.016**
%time outside LA, DCI	2.4	1.2-4.7	**0.011**

Table 12. Multivariate association between autoregulatory parameters and functional outcome at discharge. This table shows multivariate ordinal

regression analysis of autoregulatory indices TOx and PRx as well as %time outside autoregulatory limits versus discharge mRS. Separate adjustments were performed for age, WFNS, radiographic vasospasm, angiographic vasospasm, clinical vasospasm, and DCI due to the small cohort in this pilot study. TOx: tissue oxygenation index; PRx: pressure reactivity index; WFNS: World Federation of Neurologic Surgeons; DCI: delayed cerebral ischemia; MAP: mean arterial pressure; %time outside LA: percentage of time that MAP spent outside limits of autoregulation; aOR: adjusted odds ratio; CI: confidence interval.

Table 13. Multivariate association between NIRS- and ICP-derived autoregulatory parameters and functional outcome at 90-day follow-up.

Variables included in multivariate model	*aOR*	*95% CI*	*P VALUE*
NIRS (n=28)			
TOx, Age	2.0	1.1-3.9	**0.033**
TOx, WFNS	2.3	1.1-4.6	**0.022**
TOx, Radiographic Vasospasm	2.5	1.3-4.8	**0.006**
TOx, Angiographic Vasospasm	2.4	1.3-4.7	**0.007**
TOx, Clinical Vasospasm	2.6	1.3-5.0	**0.005**
TOx, DCI	2.1	1.1-4.2	**0.026**
%time outside LA, Age	2.0	1.3-3.1	**0.002**
%time outside LA, WFNS	1.9	1.2-2.9	**0.007**
%time outside LA, Radiographic Vasospasm	1.9	1.3-3.0	**0.002**
%time outside LA, Angiographic Vasospasm	1.9	1.3-2.9	**0.003**
%time outside LA, Clinical Vasospasm	2.0	1.3-3.0	**0.007**
%time outside LA, DCI	1.8	1.2-2.8	**0.008**
ICP (n=25)			
PRx, Age	6.2	1.5-25.8	**0.013**
PRx, WFNS	5.2	1.2-22.4	**0.027**

PRx, Radiographic Vasospasm	6.3	1.5-26.2	**0.012**
PRx, Angiographic Vasospasm	4.4	1.0-19.6	**0.050**
PRx, Clinical Vasospasm	4.7	1.1-20.8	**0.041**
PRx, DCI	3.6	0.7-18.1	0.113
%time outside LA, Age	3.0	1.5-6.3	**0.003**
%time outside LA, WFNS	2.8	1.3-6.1	**0.008**
%time outside LA, Radiographic Vasospasm	2.9	1.4-5.9	**0.003**
%time outside LA, Angiographic Vasospasm	2.5	1.2-5.5	**0.020**
%time outside LA, Clinical Vasospasm	2.8	1.3-6.1	**0.012**
%time outside LA, DCI	2.2	1.0-5.0	**0.047**

Table 13. Multivariate association between autoregulatory parameters and functional outcome at 90-day follow-up. This table shows multivariate ordinal regression analysis of autoregulatory indices TOx and PRx as well as %time outside autoregulatory limits versus 90-day mRS. Separate adjustments were performed for age, WFNS, radiographic vasospasm, angiographic vasospasm, clinical vasospasm, and DCI due to the small cohort in this pilot study. TOx: tissue oxygenation index; PRx: pressure reactivity index; WFNS: World Federation of Neurologic Surgeons; DCI: delayed cerebral ischemia; MAP: mean arterial pressure; %time MAP outside LA: percentage of time that MAP spent outside limits of autoregulation; aOR: adjusted odds ratio; CI: confidence interval.

Using NIRS-derived optimal blood pressures, %time outside LA significantly associated with poor discharge (*P*=0.0004, OR 2.2, 95% CI 1.4-3.4) and 90-day outcome (*P*=0.002, OR 1.9, 95% CI 1.3-2.9) (Figure 21, panels C and D). These associations remained significant after separate adjustments for the same covariates (Tables 12 and 13). Deviating from NIRS-derived autoregulatory limits predicted poor discharge and 90-day outcome with high sensitivity and specificity (area under ROC 0.82, 95% CI 0.67-0.98, *P*=0.003

and 0.88, 95% CI 0.76-1.00, *P*=0.001, respectively; Figure 22). It is interesting to note the high degree of similarity across ICP and NIRS modalities with regard to ROC-based thresholds for predicting poor outcome at discharge and 90 days. Overall, after rounding up to 30% as a conservative threshold, it seems that MAP > 30% outside the limits of autoregulation predicts poor outcome with moderately high sensitivity and specificity in our cohort.

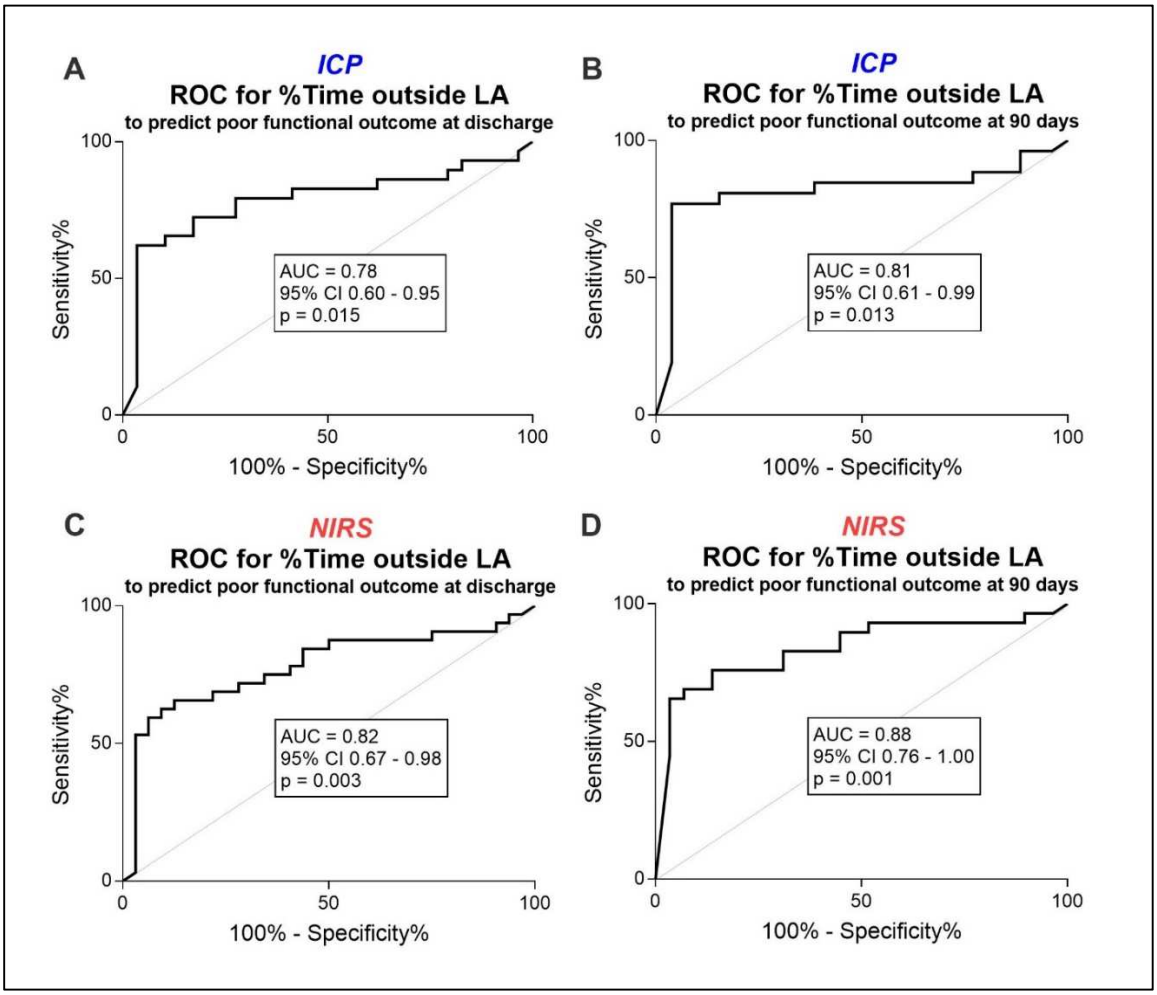

Figure 22. Receiver operating characteristic (ROC) curves of deviating from personalized ICP- and NIRS-derived autoregulatory thresholds to predict poor functional outcome (mRS 0-2) at discharge and 90 days. Panels A and B display ROC curves for ICP-derived percent time MAP spent outside autoregulatory limits for discharge and 90-days. Regarding thresholds, for Panel A, spending >26.5% MAP outside LA predicted poor outcome at discharge with a sensitivity of 64.7% and specificity of 72.7%.

For Panel B, spending >29.1% MAP outside LA predicted poor outcome at 90 days with a sensitivity of 77.8% and a specificity of 68.7%. Panels C and D show similar curves for NIRS data. For Panel C, spending >24.7% MAP outside LA predicted poor outcome at discharge with a sensitivity of 72.2% and a specificity of 84.6%. For Panel D, spending >29.9% MAP outside LA predicted poor outcome at 90 days with a sensitivity of 88.9% and a specificity of 68.4%. ROC: receiver operating characteristics; MAP: mean arterial pressure; %time MAP outside LA: percent time MAP spent outside limits of autoregulation; AUC: area under the curve; CI: confidence interval.

Three patients underwent treatment for clinical vasospasm during the neuromonitoring period; the remaining cohort did not undergo hemodynamic interventions for vasospasm during recordings. Given the possible effect of BP interventions on autoregulatory function, a sensitivity analysis was performed excluding these patients. After separate adjustments for age, WFNS, vasospasm, and DCI, NIRS- and ICP-derived %time outside LA remained significantly associated with discharge and 90-day outcomes (Tables 14 and 15).

Table 14. Multivariate association between NIRS- and ICP-derived autoregulatory parameters and functional outcome at discharge, excluding 3 patients who underwent treatment for clinical vasospasm during neuromonitoring.

Variables included in multivariate model	*aOR*	*95% CI*	*P VALUE*
NIRS (n=28)			
TOx, Age	2.4	1.2-4.7	**0.016**
TOx, WFNS	2.5	1.2-5.1	**0.014**
TOx, Radiographic Vasospasm	2.8	1.4-5.5	**0.004**
TOx, Angiographic Vasospasm	2.8	1.4-5.7	**0.004**
TOx, Clinical Vasospasm	3.1	1.5-6.3	**0.002**
TOx, DCI	2.7	1.3-5.4	**0.006**

%time outside LA, Age	2.2	1.4-3.5	**0.001**
%time outside LA, WFNS	2.2	1.3-3.6	**0.002**
%time outside LA, Radiographic Vasospasm	2.3	1.4-3.7	**0.001**
%time outside LA, Angiographic Vasospasm	2.4	1.4-4.0	**0.001**
%time outside LA, Clinical Vasospasm	2.5	1.5-4.3	**0.0004**
%time outside LA, DCI	2.4	1.4-3.9	**0.001**
ICP (n=25)			
PRx, Age	6.9	1.4-33.0	**0.016**
PRx, WFNS	5.9	1.2-29.6	**0.031**
PRx, Radiographic Vasospasm	8.7	1.7-44.8	**0.010**
PRx, Angiographic Vasospasm	6.5	1.3-32.0	**0.022**
PRx, Clinical Vasospasm	6.8	1.4-33.6	**0.019**
PRx, DCI	5.8	1.1-29.6	**0.036**
%time outside LA, Age	2.0	1.0-4.1	**0.046**
%time outside LA, WFNS	2.0	1.0-3.9	**0.050**
%time outside LA, Radiographic Vasospasm	2.2	1.1-4.4	**0.028**
%time outside LA, Angiographic Vasospasm	2.0	1.0-4.1	**0.042**
%time outside LA, Clinical Vasospasm	2.1	1.1-4.2	**0.037**
%time outside LA, DCI	2.1	1.1-4.2	**0.035**

Table 14. Multivariate association between autoregulatory parameters and functional outcome at discharge, excluding 3 patients who underwent treatment for clinical vasospasm during the neuromonitoring period. This sensitivity analysis shows multivariate ordinal regression analysis of autoregulatory indices TOx and PRx as well as %time outside

autoregulatory limits versus discharge mRS after excluding 3 patients who underwent hemodynamically relevant interventions for clinical vasospasm during the neuromonitoring period. Separate adjustments were recursively performed for age, WFNS, radiographic vasospasm, angiographic vasospasm, clinical vasospasm, and DCI.

Table 15. Multivariate association between NIRS- and ICP-derived autoregulatory parameters and functional outcome at 90-day follow-up, excluding 3 patients who underwent treatment for clinical vasospasm during neuromonitoring.

Variables included in multivariate model	*aOR*	*95% CI*	*P VALUE*
NIRS (n=25)			
TOx, Age	1.8	0.9-3.6	0.076
TOx, WFNS	2.7	1.3-5.6	**0.009**
TOx, Radiographic Vasospasm	2.3	1.2-4.5	**0.015**
TOx, Angiographic Vasospasm	2.3	1.2-4.4	**0.015**
TOx, Clinical Vasospasm	2.3	1.2-4.4	**0.017**
TOx, DCI	2.4	1.2-4.7	**0.014**
%time outside LA, Age	2.0	1.3-3.1	**0.003**
%time outside LA, WFNS	2.2	1.3-3.6	**0.002**
%time outside LA, Radiographic Vasospasm	1.9	1.2-2.9	**0.004**
%time outside LA, Angiographic Vasospasm	1.9	1.2-2.9	**0.004**
%time outside LA, Clinical Vasospasm	1.9	1.2-3.0	**0.004**
%time outside LA, DCI	2.0	1.3-3.2	**0.003**
ICP (n=22)			
PRx, Age	5.2	3.3-24.0	**0.035**
PRx, WFNS	8.9	1.6-50.5	**0.014**

PRx, Radiographic Vasospasm	6.2	1.3-29.6	**0.022**
PRx, Angiographic Vasospasm	5.7	1.2-28.3	**0.033**
PRx, Clinical Vasospasm	10.9	1.7-72.1	**0.013**
PRx, DCI	11.3	1.5-83.3	**0.017**
%time outside LA, Age	2.2	1.0-4.7	**0.043**
%time outside LA, WFNS	2.7	1.2-6.2	**0.016**
%time outside LA, Radiographic Vasospasm	2.2	1.1-4.7	**0.036**
%time outside LA, Angiographic Vasospasm	2.4	1.1-5.3	**0.032**
%time outside LA, Clinical Vasospasm	3.0	1.3-7.0	**0.009**
%time outside LA, DCI	2.5	1.1-5.8	**0.028**

Table 15. Multivariate association between autoregulatory parameters and functional outcome at 90-day follow-up, excluding 3 patients who underwent treatment for clinical vasospasm during the neuromonitoring period. This sensitivity analysis shows multivariate ordinal regression analysis of autoregulatory indices TOx and PRx as well as %time MAP spent outside autoregulatory limits versus discharge mRS after excluding 3 patients who underwent hemodynamically relevant interventions for clinical vasospasm during the neuromonitoring period. Separate adjustments were recursively performed for age, WFNS, radiographic vasospasm, angiographic vasospasm, clinical vasospasm, and DCI.

Limits of Autoregulation and Radiographic Outcomes

Six patients suffered from DCI (19.4%). Percent time with MAP outside LA did not significantly differ between patients with and without any short-term radiographic outcomes (Table 16). Nonetheless, when comparing patients with and without DCI, a trend toward more time spent outside LA can be seen for NIRS and ICP modalities (Figure 23).

Table 16. Percentage of time MAP spent outside LA in patients with and without short-term radiographic and clinical outcomes.

ICP-derived %time outside LA	Median	IQR	*P VALUE*
Ictal LoC			0.537
Yes	30.0%	13.0-41.6%	
No	24.6%	19.8-35.0%	
Early Hydrocephalus			1.000
Yes	30.9%	22.1-38.2%	
No	24.0%	15.6-35.9%	
Radiographic Vasospasm			0.701
Yes	31.8%	22.3-40.8%	
No	24.6%	13.5-36.3%	
Angiographic Vasospasm			0.089
Yes	41.8%	29.1-50.1%	
No	24.0%	18.3-32.9%	
Clinical Vasospasm			0.126
Yes	42.2%	27.1-51.1%	
No	24.6%	16.3-34.6%	
DCI			0.126
Yes	45.9%	26.2-53.1%	
No	25.1%	18.0-34.8%	
NIRS-derived %time outside LA	Median	IQR	*P VALUE*
Ictal LoC			0.737
Yes	25.1%	15.9-52.7%	
No	22.1%	17.0-39.2%	
Early Hydrocephalus			0.118
Yes	35.3%	19.2-53.4%	
No	18.6%	15.5-36.7%	
Radiographic Vasospasm			0.740
Yes	24.4%	15.9-53.3%	
No	22.5%	17.0-39.2%	
Angiographic Vasospasm			0.334
Yes	43.6%	19.7-53.0%	
No	19.4%	16.0-37.8%	
Clinical Vasospasm			0.611
Yes	43.3%	17.9-52.0%	
No	22.1%	16.1-43.4%	
DCI			0.105
Yes	43.6%	25.3-54.1%	
No	19.9%	16.0-45.3%	

Table 16. Deviation from autoregulatory limits in patients with and without short-term radiographic and clinical outcome measures. Using non-parametric comparisons, %time outside LA did not significantly differ in patients with and without ictal loss of consciousness (LoC), early hydrocephalus, radiographic vasospasm, angiographic vasospasm, clinical vasospasm, or delayed cerebral ischemia. IQR: interquartile range.

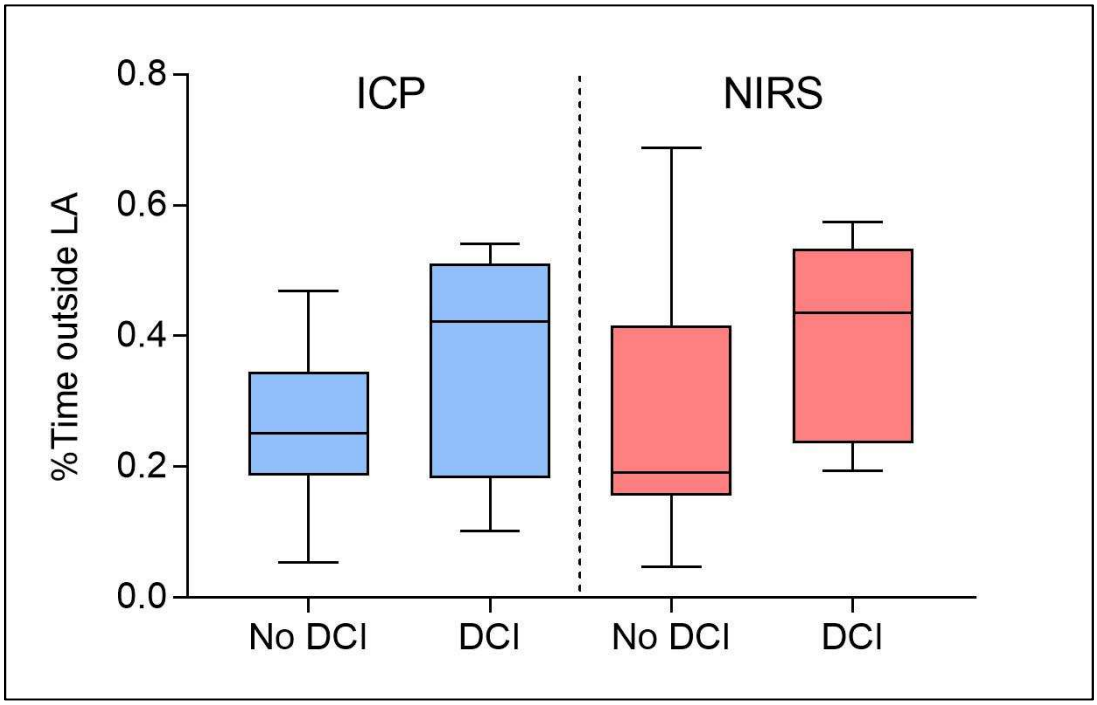

Figure 23. Percent time with MAP outside limits of autoregulation (LA) in patients with and without delayed cerebral ischemia (DCI). While %time with MAP deviating from personalized LA did not significantly differ between patients with and without DCI in the Mann Whitney U test, there was a readily appreciable trend towards spending more time outside LA in patients with DCI in both ICP and NIRS modalities. Error bars represent 95% confidence intervals.

E. Discussion

In this pilot feasibility study of 31 patients with aneurysmal SAH (aSAH), we demonstrated that continuous estimation of optimal blood pressure and limits of cerebral autoregulation is feasible and that deviating from personalized thresholds of autoregulation strongly

associates with worse functional outcome, even after adjusting for important prognostic covariates. We also showed collinearity between invasively (ICP) and non-invasively (NIRS) derived optimal blood pressures and limits of autoregulation, providing support for non-invasive measures of autoregulation in patients who may not be candidates for invasive procedures.

Studies performed in patients with traumatic brain injury suggest that autoregulatory physiology can be harnessed to optimize cerebral perfusion. [185, 186] Although not yet proven in prospective studies, retrospective data suggest that this treatment avenue may ameliorate outcome after brain injury. Similar findings in patients with aSAH have posited that intact autoregulation improves clinical outcomes. [11, 15, 178] Furthermore, autoregulatory function was invoked as a secondary endpoint in aSAH clinical trials of pravastatin and erythropoietin, both of which reduced the duration of impaired autoregulation in tandem with improved discharge outcomes, a decrease of in-hospital mortality, and a marked decrease in the incidence of DCI. [154-156] Of note, functional improvements were not sustained in 6-month follow-up. These two trials, therefore, illustrate that targeting autoregulation is achievable as a therapeutic paradigm, but the ultimate benefit of such a strategy remains unclear.

While these studies considered autoregulation in their design, no prospective study has examined personalized BP thresholds based on autoregulatory physiology following aneurysmal rupture. Optimal BP ranges are unique to individual patient physiology and likely influenced by numerous factors. [11, 15, 187] For example, disturbances in

autoregulation may be exacerbated when cerebral vessels are unable to adjust for vasoconstriction caused by proximal spasm. This dual insult of vasospasm and dysfunctional autoregulation may shorten the autoregulatory plateau and render patients vulnerable to distal ischemia. In comparison, microvascular spasm may shift the autoregulatory curve towards higher pressures. [188, 189] For these reasons, evaluating individual patients' hemodynamics and maintaining BP within autoregulatory limits would provide the optimal physiologic environment for the injured brain.

Indeed, in our study, for every 10% increase in time spent outside ICP-derived limits of autoregulation, there was a 2.6-fold and 2.8-fold increased likelihood of shifting towards worse outcomes on the discharge and 3-month mRS, respectively. Importantly, our neuromonitoring was initiated within the first 48 hours of aneurysm rupture, well before the vasospasm risk window. In addition, a sensitivity analysis excluding patients who underwent treatment for clinical vasospasm revealed persistent significance between %time outside LA and functional outcome. These results suggest that deviation from optimal BP targets in the early days following aSAH may represent a marker of impaired buffering capacity of the cerebral vasculature, potentially helping to identify patients who are more susceptible to further damage from hemodynamic instability throughout their hospital course. Additionally, patients with worse discharge and 90-day outcomes exhibited narrower NIRS-derived optimal BP target ranges consistent with a shortening of their autoregulatory plateau. Overall, frequent episodes of hypo- and hyperperfusion may manifest as deviation from personalized autoregulation-based thresholds, indicating perturbed autoregulatory physiology, which may aid in

prognosticating poor outcome.

Although associations between PRx and functional outcome are well established in patients with traumatic brain injury, less robust evidence exists for patients with SAH. [177] Mixed results have been reported in recent literature, but in general studies have demonstrated a strong relationship among high PRx indices, DCI, and poor outcome. [109, 117, 190] Most of these studies used measurements of ICP when the EVD is closed, but Aries *et al*. effectively showed that an open EVD system can be used to calculate autoregulatory indices due to preserved slow fluctuations in the ICP signal. [181] More recently, Klein *et al*. revealed good agreement of PRx indices obtained via parenchymal and EVD measurements of ICP. [182] In our study, then, we included continuous ICP data to derive dynamically updating optimal BP parameters regardless of whether the EVD was open. This inclusive approach resulted in longer monitoring periods and an increased capacity to determine ideal BP in real-time. Ultimately, higher PRx indices correlated with worse outcomes in our cohort.

Similar findings have been reported using non-invasive technologies like TCD and NIRS. Budohoski *et al*. found that perturbed autoregulation in the first 5 days after aSAH increased the risk of DCI and poor outcome. [163] These authors not only highlighted the feasibility of detecting dysautoregulation using NIRS, but they also observed collinearity between TCD- and NIRS-based indices of autoregulation. Using these results as a launchpad, our study underscores the feasibility of using both invasive and non-invasive measures of autoregulation-based optimal BP. Further, we showed that target BP ranges

significantly correlated between NIRS and ICP modalities, providing an argument for non-invasive measures of optimal cerebral perfusion pressure in future studies.

Limitations

This study has several limitations, including a small sample size. Given the study's observational design, conclusions about the effect of autoregulation-guided therapy on outcome are beyond its scope. While inferences about autoregulatory mechanisms underlying DCI are clouded because only 6 patients suffered from this complication, a recent 2019 meta-analysis found that autoregulatory impairment likely constitutes an accurate predictor of DCI and poor outcome. [191] These authors performed a summary receiver operating characteristic of autoregulation disturbances for DCI prediction, reporting an area under the curve of 0.87, underlining autoregulation's clinical import in prognostication. In our study, while %time outside LA did not significantly differ in patients with and without DCI, there was an appreciable trend towards spending more time outside LA in patients with DCI (Figure 21). This interesting observation would align with Harper's dual insult theory, whereby dysautoregulation distal to proximal vasospasm results in infarction. [11, 15, 145, 146] In a larger cohort, prospective randomized trials using continuous monitoring strategies to calculate optimal BP targets may help to bridge this knowledge gap. Lastly, our neuromonitoring was performed early after admission before patients were at risk for vasospasm; beginning at this time point was by design, but completing some recordings prior to vasospasm was dictated by practical issues, including discontinuation of ICP monitoring by the clinical team, recording equipment availability, and discharge from the ICU. More longitudinal monitoring is warranted to capture granular temporal dynamics of optimal BP targets during and after risk periods of spasm and DCI.

Conclusion of the subarachnoid hemorrhage neuromonitoring study

Our method of continuous estimation of autoregulatory limits in aSAH patients provides an optimal BP range tailored to patients' individual hemodynamics. This study thus constitutes an innovative approach to determine patient-specific dynamic BP targets. Findings from this research could ultimately lead to a clinical trial of autoregulation-based treatment strategies, including tailored pharmacologic BP augmentation and lowering based on patients' real-time autoregulatory status after SAH.

PART III

A. Large-vessel occlusion (LVO) ischemic stroke

Globally, the proportion of all strokes attributable to ischemia is 68%, while the incidence of hemorrhagic stroke is 32%, which includes intracerebral hemorrhage and subarachnoid hemorrhage. In the United States, the proportion of strokes due to ischemia is 87%, which stands in contrast to the incidence of other subtypes like intracerebral hemorrhage (10%) and subarachnoid hemorrhage (3%). [192, 193] The lifetime risk for adult males and females aged over 25 is approximately 25%. [194] On the global stage, stroke is the second most common cause of mortality and third most common cause of disability. [195] Zooming in on the United States, as of 2017, the annual incidence of new or recurrent stroke is approximated to be 795,000 cases. [193] Historically, there has also been an increased regional prevalence and higher mortality rate in the southeast, often referred to as the "stroke belt" of the US. [196-198] Males exhibit a higher rate of strokes than females at younger ages, the incidence being reversed for females over 75 years of age. [193] Within the United States alone, disability and long-term complications of stroke cost more than $34 billion each year. [193]

According to the TOAST (Trial of Org 10172 in Acute Stroke Treatment) criteria, there are five predominant subtypes of ischemic stroke: 1) large-artery atherosclerosis, 2) cardioembolism, 3) small-vessel occlusion, 4) stroke of other determined etiology, and 5) stroke of undetermined etiology. [199] Regardless of the etiology, the dictum that "time is brain!" is autologically critical, as every passing minute of an untreated large-vessel occlusion (LVO) leads to the death of two million neurons. It follows that the main

principles of acute care in stroke are to achieve timely recanalization and thus reperfusion of the ischemic territory, to optimize collateral flow, and to avoid secondary brain injury. LVO strokes (occlusions in the basilar artery, internal carotid artery, and middle cerebral artery) account for about half of all ischemic events, and they are independently associated with poor outcome. [200] These stroke subtypes are often life-changing and debilitating from both physical and emotional perspectives. Indeed, over half of patients fail to regain functional independence, and almost a quarter pass away 6 months after the stroke. [201]

Regarding recanalization, it is virtually incontrovertible that thrombolysis and thrombectomy improve neurologic outcomes. [202] The past few decades have witnessed recombinant tissue plasminogen activator's (tPA) premier role in improving these outcomes when administered within 4.5 hours of stroke symptom onset. [203, 204] Randomized controlled trials followed by meta-analyses support the therapeutic indications of tPA, so long as clinicians ascertain proper eligibility. [205] Necessary information to collect includes time last known well, recent surgeries, medical comorbidities, blood thinners, NIHSS score, glucose level, blood pressure, and brain imagining. While tPA has become standard of care, the treatment has its limitations. In addition to the short time window and weighty list of contraindications, pharmacologic thrombolysis frequently fails to fully recanalize proximal artery occlusions caused by large clots. As stated above, these strokes tend to be some of the most disabling. [202] There is now strong evidence that these patients should be considered for endovascular treatment via mechanical thrombectomy.

Mechanical thrombectomy preceded by intravenous tPA has become standard of care treatment in stroke patients with acute ischemia secondary to LVO. [206] This shift occurred after 2015, a year that witnessed five randomized trials (MR CLEAN, ESCAPE, SWIFT PRIME, REVASCAT, and EXTEND IA) showing efficacy of endovascular thrombectomy over standard medical care. [207-211] A subsequent *Lancet* meta-analysis in 2016 [HERMES (Highly Effective Reperfusion Evaluated in Multiple Endovascular Stroke Trials)] included a total of 1,287 patients and demonstrated a significant reduction in 90-day disability compared to controls (adjusted common odds ratio 2.49, 95% CI 1.76-3.53, $P<0.0001$), though 90-day mortality and risk of parenchymal hematoma and symptomatic intracranial hemorrhage did not differ between the two study populations. [206] Another landmark trial occurred in 2018 from the DAWN investigators, investigating the effect of thrombectomy performed in the 6-24 hour window after the onset of ischemic stroke. In this study, 107 patients underwent standard medical care plus thrombectomy (the thrombectomy group), while 99 patients received medical care alone (the control group), for a total of 206 enrolled patients. The thrombectomy group had to fulfill mismatch criteria between severity of clinical deficit and infarct volume on initial brain imaging. The trial was halted at 31 months because interim analysis showed significant improvement in the thrombectomy group with respect to utility-weighted modified Rankin scale score at 90 days (5.5 vs. 3.4, posterior probability of superiority >0.999). Further, the rate of functional independence at 90 days was 49% in the thrombectomy group as compared to 13% in the control group. [212]

Current AHA guidelines recognize that vasopressor therapy may be useful to improve

cerebral blood flow "in exceptional cases," but parameters regarding patient selection and blood pressure targets have not been established. [213] Similarly, at this time, post-stroke hypertension management does not consider patients' unique hemodynamic physiology. Instead, current guidelines recommend maintaining BP <180/105 mmHg for all patients treated with IV t-PA or endovascular therapy to promote perfusion to ischemic territories while mitigating potential risks of intracranial hemorrhage, but acknowledge the lack of prospective trials to substantiate this position. The following excerpts from the *2018 Guidelines for the Early Management of Patients With Acute Ischemic Stroke* illustrate current, endorsed practices for blood pressure (BP) management in ischemic stroke.

> **Initial BP management**
> *"Patients who have elevated BP and are otherwise eligible for treatment with IV alteplase should have their BP carefully lowered so that their systolic BP is <185 mmHg and their diastolic BP is <110 mmHg before IV fibrinolytic therapy is initiated."*
>
> **Post-alteplase BP management**
> *"BP should be maintained <180/105 mmHg for at least the first 24 hours after IV alteplase treatment."*
>
> **Post-EVT BP management**
> *"In patients who undergo mechanical thrombectomy, it is reasonable to maintain the BP ≤180/105 mmHg during the first 24 hours after the procedure. In patients who undergo mechanical thrombectomy with successful reperfusion, it might be reasonable to maintain BP at a level <180/105 mmHg."*

The recommendations go on to acknowledge that very little data is available to guide blood pressure therapy during and after thrombectomy. [213] Randomized controlled trials are not available in this setting. The vast majority of patients enrolled in under 6-hour randomized trials received intravenous thrombolytic therapy, and the trial protocols stipulated management according to local guidelines with pressures generally under

180/105 mmHg for the first 24 hours after the procedure. Importantly, two trial protocols provided additional recommendations. The ESCAPE protocol states that systolic blood pressure ≥150 mmHg is probably useful in promoting and sustaining adequate collateral flow while the artery remains occluded. [208] The protocol further states that controlling pressure once reperfusion has been achieved and aiming for a normal pressure is a reasonable route for individual patients. Labetalol or metoprolol in low doses are recommended for this purpose. Second, the DAWN protocol endorses maintaining systolic pressures under 140 mmHg in the first 24 hours for subjects who achieve successful reperfusion after thrombectomy. [214] Of note, these blood pressure thresholds from the ESCAPE and DAWN protocols will be used as comparisons in our pilot study on personalized autoregulatory thresholds in patients with ischemic stroke.

B. Clinical relevance of autoregulation following ischemic stroke

Cerebral autoregulation in acute stroke is critical for the maintenance of stable blood flow in the ischemic penumbra and for avoidance of excessive hyperperfusion. [15, 30] Unfortunately, there seems to be fairly widespread agreement that stroke is associated with impaired autoregulation, even in cases of minor stroke. This impairment may exist ipsilateral to the stroke site in a focal fashion, or globally throughout both hemispheres. [30] Interestingly, Immink *et al*. reported dynamic autoregulatory disturbance ipsilateral to middle cerebral artery territory strokes but bilaterally in lacunar ischemic strokes. [215] This study utilized transfer function analysis (TFA) within the first 72 hours in 10 patients with large MCA strokes (mean NIHSS 17), 10 patients with lacunar strokes (mean NIHSS

9), and 10 healthy control subjects. Autoregulatory failure was determined via phase shift delay. These results were bolstered in more recent analyses by Guo *et al*. in 2014. This paper showed that dynamic autoregulatory markers were impaired ipsilaterally in stroke of large artery atherosclerosis but bilaterally in stroke of small artery occlusion. [216] Petersen *et al*. then examined autoregulation on a more longitudinal basis, reporting dynamic autoregulatory failure up to 1 week following acute LVO strokes in the MCA. More specifically, this investigation showed that phase was lower in the affected cerebral hemisphere compared to the contralateral hemisphere (29.6 vs. 42.5 degrees, P=0.004). [86] Normalization of autoregulation was observed by the second week after vessel occlusion.

Furthermore, in stroke patients with impaired cerebral autoregulation, recovery tends to be delayed for up to 3 months, underlining the clinical relevance of autoregulation in stroke research. [6, 217] That said, only a handful of studies have looked at functional outcome prognostication with respect to autoregulation physiology in stroke. For example, Reinhard *et al*. enrolled 45 patients within 48 hours of LVO MCA ischemic strokes and showed that ipsilateral lower phase shifts were related to worse mRS outcomes. [218] In light of the prolonged enrollment timeframe, the authors conceded that autoregulatory impairment may reflect initial stroke severity, rather than functioning as an independent contributing factor to outcome. To help resolve this question, Castro *et al*. measured autoregulation in 30 patients with LVO MCA ischemic stroke within just 6 hours of symptom onset. [217] This report demonstrated that autoregulatory impairment operated as a statistically independent predictor of functional autonomy at the 90-day endpoint (odds ratio 14.0, 95%

CI 1.7-74.0, *P*=0.013). In yet another study, these authors reported that final infarct volume is significantly lower in patients with preserved autoregulation in a similar acute window after the cerebrovascular accident. [219] In a review summarizing these findings, Castro *et al*. conclude that early measures of cerebral autoregulation likely entail considerable impact for the guidance of acute management, prognostication, prevention of secondary injury, and ultimate improvement of clinical outcomes. [6]

Hemorrhagic transformation and cerebral edema are feared secondary complications of ischemic stroke. Much like vasospasm and delayed cerebral ischemia, prognostic and preventative measures are lacking, as are mechanistic underpinnings. Autoregulatory physiology has thus been invoked as a biological avenue with possible deterrent and/or restorative benefits. In an invasive neuromonitoring study, Dohmen *et al*. enrolled 15 patients with MCA ischemic strokes and calculated the cerebral perfusion pressure-oxygen reactivity index (COR). [220] They found that COR indices were higher in the 8 patients with a malignant course (i.e., massive brain edema formation) compared to the 7 patients with a relatively benign course (COR 1.99 vs. 0.68, *P*<0.05). The study concludes that impaired autoregulation appears to play an important role in the development of cerebral edema. In an aforementioned study, Castro *et al*. calculated cerebrovascular resistance, coherence, gain, and phase in 46 patients within 24 hours of MCA ischemic stroke. [219] At admission, phase was lower (indicative of worse autoregulation status) in patients with hemorrhagic transformation (6.6 vs. 45.0 degrees, *P*=0.023). Also, progression to edema was related to lower cerebrovascular resistance values (1.4 vs. 2.3 mmHg/cm/sec, *P*=0.033) and increased blood flow velocities (51 vs. 42 cm/sec, *P*=0.033) at initial

presentation. These lower resistances, the authors submit, reflect paradoxical cerebral vasodilation, as resistance is equal to the quotient between mean arterial pressure and mean flow velocity (CVR = MAP/MFV). Thus, they argue that breakthrough hyperperfusion and microvascular injury may underlie the development of malignant edema and hemorrhagic transformation.

Table 17 below displays some of the most relevant literature on autoregulation studies with regard to ischemic stroke, together with major findings from each representative study. Cumulatively, the evidence for impaired autoregulation following ischemic stroke is strong, just as it is for subarachnoid hemorrhage. It follows that the Cambridge hypothesis – that an optimum cerebral perfusion pressure exists at a pressure that allows for functional cerebral autoregulation – can also be applied to the cerebrovascular hemodynamics of stroke pathophysiology.

Cerebral autoregulation following ischemic stroke: review of relevant literature			
Study	**Sample size**	**Cerebral blood flow measurement**	**Pertinent findings**
Immink *et al*. 2005 [215]	30	TCD	Study compared gain and phase in 10 patients with lacunar ischemic strokes, 10 patients with MCA ischemic strokes, and 10 healthy control subjects; autoregulatory impairment shown ipsilateral to MCA stroke and bilateral in lacunar stroke cases
Dohmen *et al*. 2007 [220]	15	Pressure-oxygen reactivity (COR)	Using invasive probes in patients with MCA infarction, authors found early impairment of autoregulation in peri-infarct tissue of patients who developed malignant edema, while autoregulation was preserved in patients with more benign courses; autoregulation measured via time-correlation between CPP and tissue oxygen pressure

Reinhard *et al*. 2012 [218]	45	TCD	Autoregulatory impairment found in ipsilateral hemisphere, and low phase as well as high Mx indices associated with higher NIHSS scores, larger final infarct volumes, and worse mRS outcomes
Guo *et al*. 2014 [216]	41	TCD	Phase shifts up to 40 degrees indicative of autoregulation impairment were found in the ipsilateral hemisphere of large infarcts; impairment further shown in patients with bilateral lacunar infarcts
Guo *et al*. 2015 [221]	71	TCD	In unilateral MCA stroke patients, dynamic autoregulatory failure was shown up to 6 months post-stroke in both MCA and PCA; in lacunar infarction, autoregulatory impairments were diffuse and sustained
Petersen *et al*. 2015 [86]	28	TCD	Low phase was shown in affected hemisphere, and autoregulatory impairment was demonstrated up to 7 days after stroke, with resolution at 2 weeks
Castro *et al*. 2017 [219]	46	TCD	Autoregulatory impairment with low phase shifts shown in affected hemisphere, associated with hemorrhage and edema at 24 hours post-stroke; autoregulatory disturbance resolved at 3-month follow-up
Castro *et al.* 2017 [217]	30	TCD	Low phase shifts in ipsilateral hemisphere correlated with worse functional outcome at 90 days post-stroke as well as large infarct volume at 24 hours
Xiong *et al*. 2017 [222]	60	TCD	Bilateral autoregulatory impairment shown via low phase shifts; also, small vessel disease correlated with worse autoregulation impairment

Table 17. Cerebral blood flow methods for measurement of dynamic autoregulation in patients with ischemic stroke. For further review, Castro *et al*. and Xiong *et al*. published extensive articles summarizing these studies. [6, 30]

C. Pilot study on autoregulation monitoring in ischemic stroke

Endovascular thrombectomy (EVT) has markedly changed the landscape of acute stroke therapy and is now considered standard of care for patients with stroke from large-vessel intracranial occlusion (LVO). [207, 209-211] However, many patients with LVO stroke

have poor functional outcome despite successful EVT. [206] Loss of cerebral autoregulation in the acute phase of stroke leaves patients vulnerable to changes in blood pressure (BP) with consequent neurologic worsening from hypo- or hyperperfusion. [223] Observational studies have found increased rates of hemorrhagic transformation (HT) and worse outcomes in patients with higher peak systolic blood pressure (SBP) values or hemodynamic variability in the first 24 hours after EVT, suggesting that BP optimization may represent a neuroprotective strategy. [224, 225] Current guidelines recommend a BP <180/105mmHg for at least 24 hours after EVT but acknowledge the lack of randomized trials on this aspect of management. Following reperfusion, lower BP targets may be warranted to prevent reperfusion injury and promote penumbral recovery, but optimal targets remain unclear, and individual patient factors such as degree of reperfusion, infarct size, and hemodynamic status may need to be considered. As a result, there is considerable practice variation in post-EVT BP management within the United States. [226]

Prior work has shown that near-infrared spectroscopy (NIRS) monitoring can be used to identify a dynamic BP range in individual patients at which autoregulation is optimally functioning. [13, 14] Such an autoregulation-derived, personalized BP range may provide a favorable physiologic environment for the injured brain following LVO stroke.

Statement of Purpose

This pilot study seeks to further establish the feasibility of our autoregulation-guided algorithm with respect to real-time hemodynamic neuromonitoring in the neuroscience intensive care unit. An additional purpose of this study is to examine the impact of

exceeding individualized thresholds on radiographic and functional outcomes after thrombectomy for LVO ischemic stroke. Our primary hypothesis is that percent time spent outside of dynamic blood pressure targets correlates with worse outcome at discharge and 90-day follow-up. Secondary hypotheses are that percent time above and below the upper and lower limits of autoregulation associate with hemorrhagic transformation and infarct progression, respectively. Finally, we hypothesize that our autoregulation-based approach represents a more personalized alternative to the currently endorsed practice of maintaining systolic blood pressures below fixed thresholds after stroke.

Specific Aim 1: to recapitulate feasibility of autoregulation neuromonitoring and derivation of personalized BP limits in patients undergoing EVT for LVO ischemic stroke.

Specific Aim 2: to evaluate the association between deviation from these BP targets on radiographic as well as clinical outcomes.

Specific Aim 3: to compare personalized, autoregulation-guided BP management with two commonly used clinical approaches: (1) maintaining BP below a fixed, pre-determined value as recommended by current guidelines and (2) stratifying BP thresholds based on reperfusion status.

The first two aims reflect those of the subarachnoid hemorrhage pilot study, while the third aim is unique in its endeavor to compare our individualized method to current clinical practices.

Methods

Study Design and Subjects

This was a single-center, prospective cohort study. All patients presenting to the Yale-New

Haven Hospital Emergency Department with the diagnosis of acute anterior circulation LVO stroke were screened. Patients ≥18 years were eligible if they underwent EVT, had MRI or CT contrast imaging obtained before EVT, and optimal BP monitoring could be initiated within 12 hours of procedure completion. History of prior stroke within 3 months or a baseline modified Rankin scale (mRS) ≥3 were exclusion criteria. All stroke management decisions including post-procedural BP targets were made by the patients' clinical team in accordance with current American Heart Association (AHA) guidelines. [213] Approval for the study was obtained from the institutional review board at the Yale School of Medicine (HIC number 1503015485). All patients or their legally authorized representatives provided written informed consent.

Near-infrared spectroscopy

Similar to the pilot study involving neuromonitoring of patients with subarachnoid hemorrhage, the Casmed Foresight Elite monitor was used to monitor oxygenated and deoxygenated hemoglobin concentrations in patients with LVO stroke. [80, 179] Autoregulatory function was measured by interrogating changes in the NIRS-derived tissue oxygenation index in response to arterial BP fluctuations. Arterial BP was monitored invasively with a radial or femoral artery catheter. NIRS and BP data were collected continuously for up to 48 hours after EVT. All signals were sampled at a frequency of 200Hz using ICM+ software (Cambridge, UK).

Calculation of autoregulatory indices

As a brief review, continuous recordings of arterial BP and cerebral blood flow demonstrate spontaneous oscillations, and their relationship can be characterized using

time-correlation analysis. First, the two signals were subjected to a 10-second average filter. Then, the tissue oxygenation autoregulatory index (TOx) was computed as a moving correlation coefficient between 30 consecutive time-averaged values of mean arterial pressure (MAP) and corresponding TOI signals. The index was updated every 10 seconds when a new set of hemodynamic variables was added. In this way, a continuous time-trend of autoregulatory function was calculated for each patient. [79, 95, 183] MAP has a near-zero or negative correlation with TOI when autoregulation is intact with pressure-reactive cerebral blood flow and volume. In contrast, MAP positively correlates with TOI when autoregulation is impaired, signifying that fluctuations in systemic pressure are able to transmit passively into the cerebral circulation.

Calculation and continuous trending of optimal blood pressure and limits of autoregulation

Regarding determination of optimal mean arterial pressure (MAP_{OPT}), a BP trend was recorded alongside TOx in each patient. Using a moving 4-hour window that was updated every 1-minute, a continuous time trend of MAP_{OPT} and the limits of autoregulation (LA) was recorded, similar to the time trends used in patients with aneurysmal subarachnoid hemorrhage (Figure 24). In each patient with LVO ischemic stroke, we calculated the percent time MAP was below the LLA (%time<LLA), within LA, and above the ULA (%time>ULA).

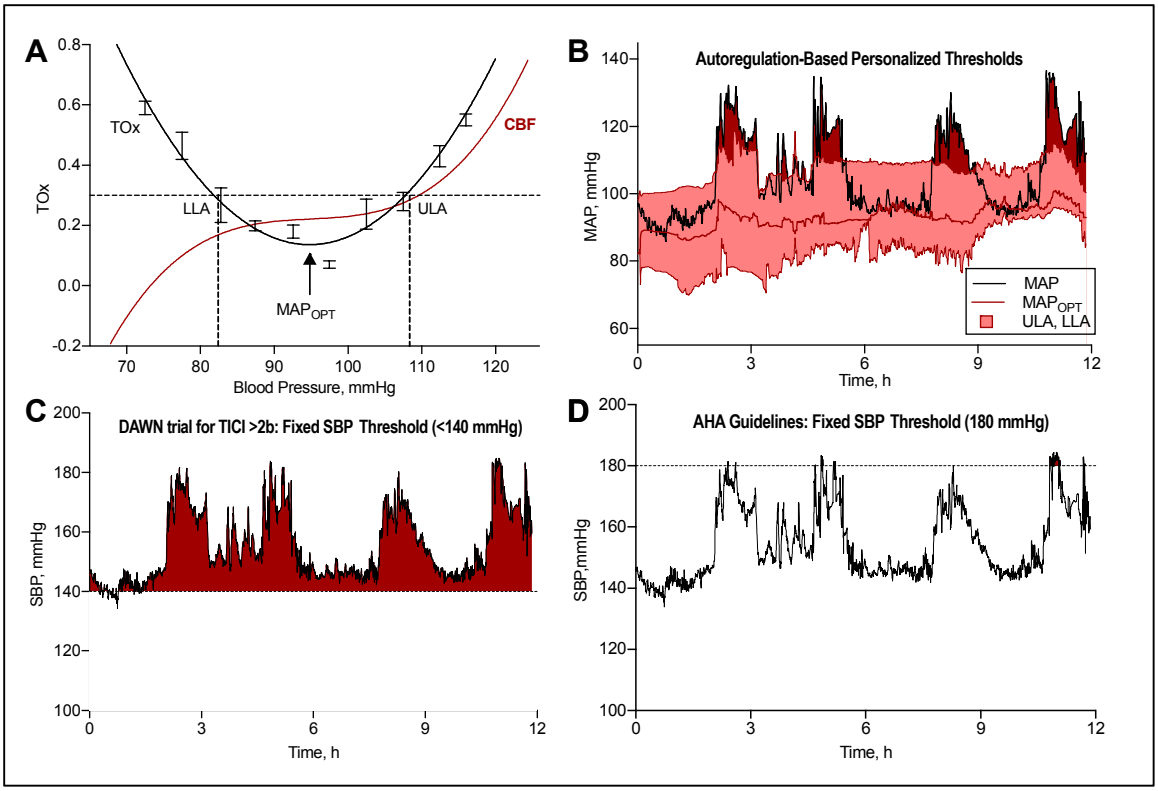

Figure 24. Calculating optimal blood pressure and limits of autoregulation. Time-correlation analysis allowed for the calculation of a moving Pearson correlation coefficient between continuous recordings of mean arterial pressure (MAP) and the NIRS-derived tissue oxygenation index (TOI). The resultant tissue oxygenation autoregulatory index (TOx), derived as said rolling coefficient between 30 successive, time-averaged values of MAP and TOI, can then be displayed as a time series alongside MAP and TOI (not shown). Limits of autoregulation (Panel A) were subsequently calculated by dividing MAP values into groups of 5mmHg and plotting them against corresponding TOx indices, resulting in a characteristic U-shaped curve. After superimposing a threshold for impaired autoregulation (TOx=+0.30), intersecting MAP values provide estimates of the lower and upper limits of autoregulation (LLA, ULA), which correspond to the inflection points of the classic autoregulatory curve (red line, CBF=cerebral blood flow). In Panel C, a continuous time trend of optimal MAP (red line), ULA and LLA (red lines surrounding MAP_{OPT}) can be calculated in this manner, while superimposing the patient's real-time MAP (black line). This trend provides clinicians with a dynamically updating, visual blood pressure target, and areas of relative hypo- or hyperperfusion can be readily interpreted at the bedside (see highlighted red areas between patient's MAP and ULA, signifying periods in which the patient exceeded personalized limits of autoregulation). This approach can be compared to the current approach to systolic blood pressure (SBP) management, whereby clinicians titrate SBP below certain thresholds, disregarding individual factors like cerebral autoregulation. Panels C and D display the same patient's blood

> pressure recording over a 12-hour period; while SBP oscillated below fixed systolic targets of 180mmHg, as currently recommended, it is clear that the patient's MAP frequently exceeded personalized targets, potentially rendering an injured brain vulnerable to further damage from relative hyperperfusion. In contrast, the patient's SBP was above the SBP threshold of 140mmHg during periods where his MAP was within limits of autoregulation and further lowering of BP in that setting may result in cerebral hypoperfusion.

Static Blood Pressure Thresholds

To compare our model of identifying optimal BP targets with a more pragmatic approach, we chose several fixed SBP thresholds, including thresholds commonly used in clinical practice, in recent EVT trials, [211, 212] or those recommended by current guidelines. [213] We calculated the percent time that SBP exceeded fixed thresholds of 140 mmHg, 160 mmHg, and 180 mmHg. We applied these thresholds either to the entire group of patients, or to groups stratified by reperfusion status, with lower BP for patients who achieved successful reperfusion (TICI 2b or 3). For the latter tiered approach, we applied BP parameters of <140 mmHg vs. <185 mmHg and <160 mmHg vs. <185 mmHg that were used in the DAWN (DWI or CTP Assessment with Clinical Mismatch in the Triage of Wake Up and Late Presenting Strokes Undergoing Neurointervention) and REVASCAT (Revascularization with Solitaire FR Device versus Best Medical Therapy in the Treatment of Acute Stroke Due to Anterior Circulation Large Vessel Occlusion Presenting within Eight Hours of Symptom Onset) trials, respectively. [211, 212]

Clinical Outcomes

Functional outcome was measured using the mRS at discharge and 90 days. Endpoints were determined via telephone interview at 3 months by a research associate blinded to monitoring results. We also assessed for shifts across the mRS range. [184]

Radiographic Outcomes

All patients underwent repeat CT imaging at 24 hours as part of routine care. HT has been associated with poor outcome after EVT. [227, 228] We classified HT using the European Cooperative Acute Stroke Study (ECASS) scale and divided patients into three groups: no HT, hemorrhagic infarction (HI), and parenchymal hematoma (PH). [228] HT was further classified as symptomatic (sICH) if the hemorrhage was associated with clinical worsening or an increase of ≥4 points on the NIHSS, as commonly defined. [207, 210, 211] Additionally, since 2016, the clinical protocol for EVT pre-evaluation has also included CT perfusion imaging, which was processed with the use of fully automated software (RAPID, iSchemaView, Menlo Park, CA). Irreversibly injured brain (ischemic core) was diagnosed if the relative cerebral blood flow was <30% of that in normal tissue. In addition, all patients underwent magnetic resonance imaging as part of their routine clinical workup at 24 hours postintervention. Final infarct volumes were measured using RAPID software and defined as pixels with apparent diffusion coefficient values below 680×10^{-6} mm^2/s. Since automated volume computation based on apparent diffusion coefficient threshold values can become inaccurate in the setting of significant hemorrhagic transformation, manual tracings were employed in these instances to calculate the final infarct volume (Analyze 11.0, AnalyzeDirect, Overland Park, KS). Infarct growth was calculated as the difference between pre-EVT infarct core and final infarct volume on follow-up imaging.

Statistical analysis

Baseline characteristics were summarized by means and standard deviations (SD) for normally distributed continuous variables, medians and interquartile ranges (IQR) for

skewed continuous variables, and numbers (%) for categorical variables. We dichotomized mRS scores into favorable (mRS 0-2) and unfavorable (mRS ≥3) outcomes. We used χ^2- or Fisher's exact tests, t- or Mann-Whitney U tests, and Kruskal-Wallis tests as appropriate for comparisons between groups. We performed ordinal, binary logistic, or linear regression modeling, as appropriate. We accounted for common confounders and known predictors of outcome after LVO stroke, including age, admission NIHSS, Alberta Stroke Program Early CT (ASPECT) score, and thrombolysis in cerebral infarction (TICI) score. All statistics were computed using SPSS (Version 24, IBM Corp). Statistical significance was set at $P<.05$ (two-tailed) for all analyses, including the primary hypothesis that percent time above fixed thresholds or outside of dynamic BP targets correlate with functional outcome.

D. Results of the ischemic stroke pilot study

Subject characteristics

Ninety patients were initially enrolled in the study (Table 18). Twelve patients were excluded from analysis due to insufficient monitoring time (n=6), poor signal quality (n=5), and early withdrawal of care (n=1). The mean monitoring time was 28.0±18.4 hours. Optimal BP and LA could be calculated for mean of 83.2±14.7% of the total monitoring period. Patients spent a mean of 65.7±22.9% of their monitored time within personalized limits of autoregulation, 16.5±13.4% above their upper limit, and 17.9±15.2% below their lower limit of autoregulation (Table 19).

Table 18. Patient Characteristics	
Total patients	90
90-day outcomes, n (%)	78 (86.7)
Sex, F (%)	42 (46.7)
Age, mean ± SD	71.6 ± 16.2
Race	
White	72 (80.0)
Black or African American	10 (11.1)
Hispanic	7 (7.8)
Asian	1 (1.1)
Admission NIHSS, mean ± SD	13.9 ± 5.7
Admission ASPECTS, mean ± SD	8.8 ± 1.6
Admission MAP, mean ± SD	107.3 ± 17.2
Admission Glucose, mean ± SD	137.3 ± 68.3
Affected Side, Left (%)	45 (50.0)
Occlusion on Angiography*, n (%)	
ICA	5 (5.6)
tICA	11 (12.2)
ACA	0 (0)
ACA+MCA	3 (3.3)
M1 MCA	43 (47.8)
M2	28 (31.1)
Medical History*, n (%)	
Hypertension	65 (72.2)
Coronary Artery Disease	11 (12.2)
Myocardial Infarction	6 (6.7)
Congestive Heart Failure	10 (11.1)
Atrial Fibrillation	47 (52.2)
Hyperlipidemia	36 (40.0)
Diabetes Mellitus (I & II)	20 (22.2)
Ischemic Stroke	17 (18.9)
Cancer	14 (15.6)
Thyroid Disease	9 (10.0)
Current Smoker	19 (21.1)
Past Smoker	19 (21.1)
Treated with tPA, n (%)	38 (42.2)

Mean time to reperfusion (minutes), mean ± SD	575.98 ± 407.7
Successful recanalization, n (%)	67 (74.4)
TICI Score, n (%) 0 1 2a 2b 3	 15 (16.7) 3 (3.3) 6 (6.7) 41 (45.6) 25 (27.8)
Hemorrhagic transformation, n (%) HI I HI II PH I PH II None	 18 (20.0) 9 (10.0) 7 (7.8) 5 (5.6) 51 (56.7)
Symptomatic hemorrhagic transformation, n (%)	8 (8.9)
Cerebral edema, n (%)	10 (11.1)
In-hospital mortality, n (%)	14 (15.6)
90-day mortality, n (%)	23 (25.6)

Table 18. Demographic and baseline characteristics. Data are mean (SD) and n (%). SD, standard deviation; F, female; NIHSS = National Institutes of Health Stroke Scale; ASPECTS = Alberta Stroke Program Early CT Score; MAP, mean arterial pressure; ICA, internal carotid artery; tICA, terminal internal carotid artery; ACA, anterior cerebral artery; MCA, middle cerebral artery; tPA, alteplase; TICI = thrombolysis in cerebral infarction score; HI = hemorrhagic infarction, PH = parenchymal hematoma. * Percentages may add up to more than 100% due to comorbidity.

Table 19. Neuromonitoring and Hemodynamic Variables	
Mean monitoring time (hours), mean ± SD	28.0 ± 18.4
Patients with sufficient monitoring (> 6 hours)	90 patients
Optimization curve calculated successfully, mean ± SD	83.2 ± 14.7%
Patients with sufficient monitoring and discharge outcomes, n (%)	90 (100)
Patients with sufficient monitoring and 90-day outcomes, n (%)	78 (86.7)

Mean MAP (mmHg), mean ± SD	93.7 ± 12.1
Mean upper limit of autoregulation (mmHg), mean ± SD	104.7 ± 11.5
Mean lower limit of autoregulation (mmHg), mean ± SD	83.7 ± 12.1
Mean MAP_{OPT} (mmHg), mean ± SD	93.3 ± 12.0
Percent time SBP above 120 mmHg, mean ± SD	81.8 ± 24.1%
Percent time SBP above 130 mmHg, mean ± SD	68.7 ± 30.9%
Percent time SBP above 140 mmHg, mean ± SD	54.9 ± 33.5%
Percent time SBP above 160 mmHg, mean ± SD	23.7 ± 26.8%
Percent time SBP above 180 mmHg (AHA guideline), mean ± SD	6.0 ± 14.7%
Percent time SBP above DAWN thresholds, mean ± SD	41.0 ± 35.2%
Percent time SBP above REVASCAT thresholds, mean ± SD	17.9 ± 24.1%
Percent time MAP within limits of autoregulation, mean ± SD	65.7 ± 22.9%
Percent time MAP above the upper limit of autoregulation, mean ± SD	16.5 ± 13.4%
Percent time MAP below the lower limit of autoregulation, mean ± SD	17.9 ± 15.2%

Table 19. Neuromonitoring and hemodynamic variables. Data are mean (SD) and n (%). SD, standard deviation.

Blood pressure, limits of autoregulation, and functional outcome

Twenty-seven (30%) patients achieved functional independence (mRS 0-2) at 3 months. Patients with good outcome were younger (63 vs. 77 years, $P<0.001$) and had lower admission NIHSS scores (12 vs. 16, $P=0.001$). They also had lower rates of HT (25.9% vs. 58.0%, $P=0.007$), smaller infarct volumes (35.4 vs. 106.5 mL, $P<0.001$), and less infarct progression (32.8 vs. 103.2 mL, $P=0.001$). The average percent time spent within autoregulatory limits among patients with favorable outcomes was 79.0±12.4% compared to 60.0±24.1% among patients with unfavorable outcomes ($P<0.001$; Table 20).

Table 20. Univariate comparisons between groups of good (mRS 0-2) and poor (mRS 3-6) functional outcome to determine predictors of outcome at 90-days

Variable	*Good Outcome (n=27)*	*Poor Outcome (n=51)*	*p Value*
Age, mean ± SD	63.1 (17.3)	77.1 (13.1)	**<0.001**
Sex, F (%)	10 (37.0)	27 (52.9)	0.181
Admission NIHSS, mean ± SD	11.6 (5.6)	15.6 (5.5)	**0.004**
Admission ASPECTS, mean ± SD	9.0 (1.5)	8.8 (1.4)	0.445
Admission MAP, mean ± SD	106.5 (18.0)	107.8 (16.9)	0.761
Admission Glucose, mean ± SD	125.3 (33.1)	148.0 (85.5)	**0.021**
Affected Side, n (%)			
Left	14 (51.9)	24 (47.1)	0.687
Right	13 (48.1)	27 (52.9)	
Medical History, n (%)			
Hypertension	15 (55.6)	39 (76.5)	0.057
Coronary Artery Disease	1 (3.7)	10 (19.6)	0.055
Myocardial Infarction	2 (7.4)	3 (5.9)	1.000
Congestive Heart Failure	2 (7.4)	7 (13.7)	0.485
Atrial Fibrillation	14 (51.9)	29 (56.9)	0.672
Hyperlipidemia	9 (33.3)	23 (45.1)	0.315
Diabetes Mellitus (I & II)	7 (25.9)	10 (19.6)	0.520
Ischemic Stroke	2 (7.4)	13 (25.5)	0.072
Cancer	4 (14.8)	7 (13.7)	1.000
Thyroid Disease	3 (11.1)	5 (9.8)	1.000
Current Smoker	6 (22.2)	8 (15.7)	0.474
Past Smoker	8 (29.6)	8 (15.7)	0.147
Mean monitoring time (hours), mean ± SD	25.4 (14.4)	30.0 (20.5)	0.221
Percent time MAP within limits of autoregulation, mean ± SD	79.0 (12.4)	60.0 (24.1)	**<0.001**
Percent time MAP above the upper limit of autoregulation, mean ± SD	8.2 (5.3)	19.5 (12.6)	**<0.001**
Percent time MAP below the lower limit of autoregulation, mean ± SD	12.9 (12.1)	20.8 (16.8)	**0.026**
Mean MAP (mmHg), mean ± SD	91.7 (14.3)	93.9 (10.6)	0.445
Mean upper limit of autoregulation (mmHg), mean ± SD	104.6 (14.3)	104.2 (10.1)	0.801
Mean lower limit of autoregulation (mmHg), mean ± SD	80.3 (12.3)	84.8 (11.2)	0.086
Mean MAP_{OPT} (mmHg), mean ± SD	91.5 (14.0)	93.9 (10.5)	0.384
Treated with tPA, n (%)	13 (48.1)	20 (39.2)	0.447
Time to reperfusion (minutes), mean ± SD	475.0 (271.9)	640.6 (474.7)	0.103
Successful recanalization, n (%)	23 (85.2)	36 (70.6)	0.178
TICI Score, n (%)			
0	4 (14.8)	10 (19.6)	

1 2a 2b 3	0 (0.0) 1 (3.7) 12 (44.4) 10 (37.0)	2 (3.9) 3 (5.9) 23 (45.1) 13 (25.5)	0.690
Hemorrhagic transformation, n (%) HT I HT II PH I PH II None	 3 (11.1) 2 (7.4) 1 (3.7) 1 (3.7) 20 (74.1)	 11 (21.6) 7 (13.7) 5 (9.8) 4 (7.8) 24 (47.1)	 0.078
Symptomatic hemorrhagic transformation, n (%)	1 (3.7)	6 (11.8)	0.411
Cerebral edema, n (%)	1 (3.7)	8 (15.7)	0.152
Final infarct volume (mL), mean ± SD	35.4 (46.3)	106.5 (92.8)	**<0.001**
Infarct progression (mL), mean ± SD	32.8 (44.7)	103.2 (87.9)	**0.001**

Table 20. Univariate analysis of predictors of good functional outcome 90 days after endovascular therapy for large vessel occlusion stroke. Significant differences between groups were determined using T-tests and chi-squared analysis for normally distributed data, while Mann-Whitney U tests were used for non-parametric variables. Fisher's exact test was employed for cross tables containing fewer than five patients.

After adjusting for age, admission NIHSS, ASPECT score, and degree of reperfusion, %time>ULA was independently associated with higher (worse) mRS scores at discharge (adjusted OR per 10% time>ULA 1.53, 95% CI 1.13-2.07, *P*=0.006) and 90 days (adjusted OR per 10% time>ULA 1.91, 95% CI 1.29-2.84, *P*=0.001; Table 21 and Figure 25A&B). While we observed no significant association between %time<LLA and functional outcome, there was a general trend toward decreasing time within limits of autoregulation with higher mRS scores.

Table 21. Association of hemodynamic variables with functional outcome						
Likelihood of a shift towards worse outcome on discharge mRS						
Variables	*OR*	*95% CI*	*p Value*	*aOR*	*95% CI*	*p Value*
%time MAP>ULA, per 10-percent	1.5	1.1-2.1	0.005	1.53	1.13-2.07	0.006
%time SBP>160, per 10-percent	1.1	1.0-1.3	0.148	1.1	0.9-1.3	0.272
%time SBP>180, per 10-percent	1.2	0.9-1.5	0.268	1.2	0.9-1.6	0.162
%time SBP>DAWN threshold	1.0	0.9-1.1	0.988	0.9	0.9-1.2	0.699
Likelihood of a shift towards worse outcome on 90-day mRS						
Variables	*OR*	*95% CI*	*p Value*	*aOR*	*95% CI*	*p Value*
%time MAP>ULA, per 10-percent	1.84	1.3-2.7	0.002	1.91	1.29-2.84	0.001
%time SBP>160, per 10-percent	1.2	1.0-1.4	0.050	1.1	0.9-1.3	0.239
%time SBP>180, per 10-percent	1.0	0.74-1.4	0.929	0.9	0.6-1.2	0.498
%time SBP>DAWN threshold	1.1	1.0-1.2	0.311	1.0	0.9-1.2	0.549

Table 21. Association of hemodynamic variables with functional outcome. aOR, adjusted odd ratio (adjusted for age, admission NIHSS, ASPECT score, and TICI score); OR, odds ratio; MAP, mean arterial pressure; mRS, modified Rankin scale; ULA, upper limit of autoregulation; LA, limits of autoregulation; LLA, lower limit of autoregulation; CI, confidence interval.

Exceeding the upper limit of autoregulation and risk of hemorrhagic transformation

HT was seen in 39 (43.3%) of patients and was overall associated with poor outcome. We observed a progressive increase in %time>ULA with worsening grades of HT (11.4% for

no HT, 13.5% for HI1&2, and 20.9% for PH1&2; *P*=0.03; Figure 23C). Patients who developed sICH appeared to spend more time above the ULA when compared to patients without sICH (11.9% vs. 24.6%, *P*=0.1; Figure 25C).

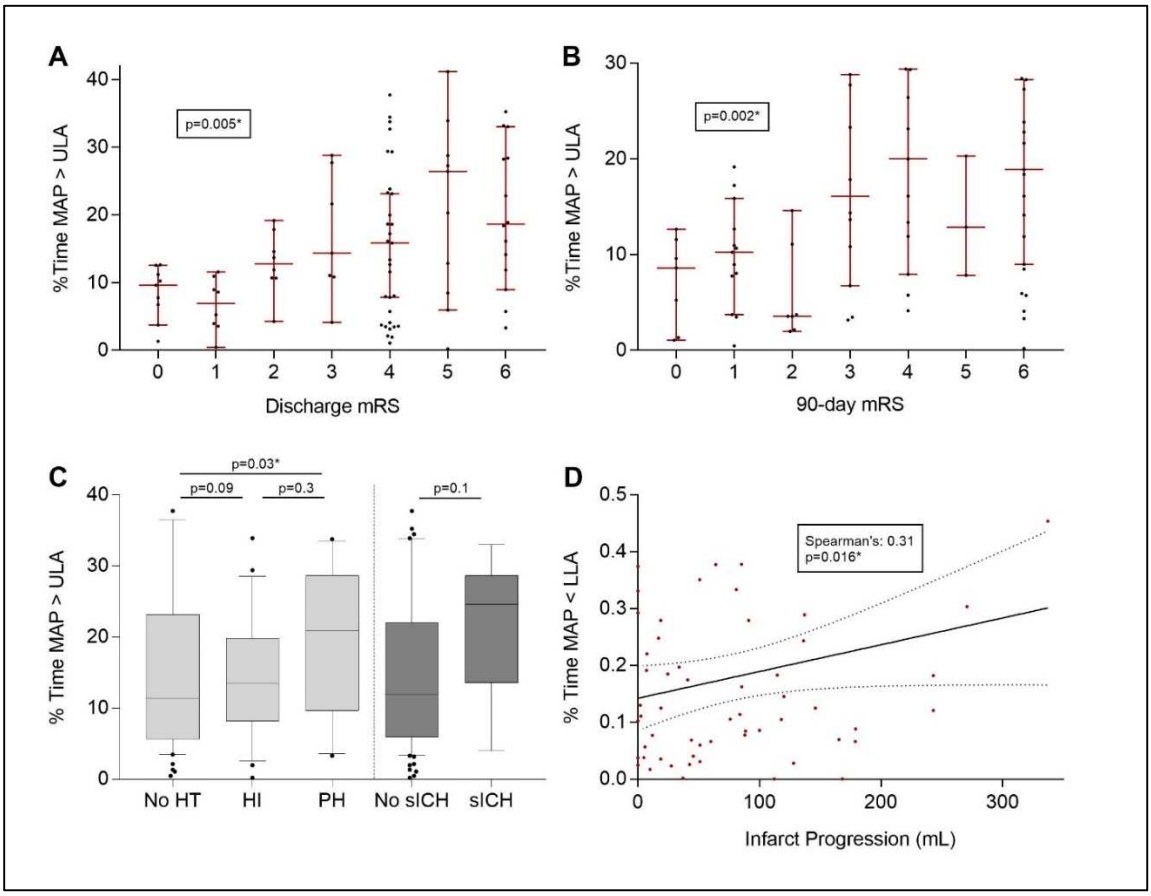

Figure 25. Associations of individualized limits of autoregulation with functional outcome at discharge and 90 days, hemorrhagic transformation, and infarct volume. Percent time spent above ULA was plotted as medians with 95% confidence intervals per each mRS score at discharge and 90 days (Panel A&B). Panel C shows the %time MAP>ULA among degrees of hemorrhagic transformation (HT) and symptomatic intracerebral hemorrhage (sICH). Final infarct volume did not correlate with percent time spent below LLA in the subgroup of patients who did not achieve reperfusion (TICI 0, 1 or 2a), nor in those patients who did achieve recanalization (Panel D). * denotes statistical significance.

Blood pressure below the lower limit of autoregulation and infarct progression

In the subgroup of patients with baseline CT perfusion imaging, we calculated infarct progression by measuring infarct volume on CT or MRI at 36-48 hours and subtracting the core infarct on admission. In this subgroup, we observed a significant bivariate correlation between infarct progression and %time<LLA (Spearman's coefficient 0.31, *P*=0.016; Figure 25D).

Association between SBP above fixed thresholds with HT and functional outcome

Time spent above fixed SBP thresholds gradually decreased for increasing BP levels. On average patients spent 81.8±24.1% of their monitoring time above 120 mmHg compared to only 6.0±14.7% above 180 mmHg (Table 19). Using the tiered approach with SBP targets stratified by reperfusion status, patients spent on average 40.3%±35.4% and 17.2%±23.7% of the monitoring time above respective thresholds used in the DAWN and REVASCAT trials (Table 19). There was no significant association between time spent above any of the fixed SBP thresholds and HT, sICH or functional outcome (Tables 22-24).

Table 22. Association of percent time spent above SBP thresholds with outcome

Likelihood of a shift towards worse outcome on discharge mRS						
Variables	*OR*	*95% CI*	*p Value*	*aOR*	*95% CI*	*p Value*
%time SBP>140, per 10-percent	1.1	1.0-1.2	0.084	1.1	1.0-1.2	0.213
%time SBP>160, per 10-percent	1.1	1.0-1.3	0.148	1.1	0.9-1.3	0.272
%time SBP>180, per 10-percent	1.2	0.9-1.5	0.268	1.2	0.9-1.6	0.162

%time SBP>DAWN threshold	1.0	0.9-1.1	0.988	0.9	0.9-1.2	0.699
%time SBP> REVASCAT threshold	1.0	0.9-1.2	0.709	1.0	0.9-1.2	0.776
%time MAP within LA, per 10-percent	0.78	0.66-0.92	0.005	0.82	0.69-0.98	0.027
%time MAP<LLA, per 10-percent	1.3	0.97-1.60	0.082	1.13	0.88-1.46	0.34
Likelihood of a shift towards worse outcome on 90-day mRS						
Variables	*OR*	*95% CI*	*p Value*	*aOR*	*95% CI*	*p Value*
%time SBP>140, per 10-percent	1.2	1.1-1.4	0.003	1.2	1.0-1.3	0.053
%time SBP>160, per 10-percent	1.2	1.0-1.4	0.050	1.1	0.9-1.3	0.239
%time SBP>180, per 10-percent	1.0	0.74-1.4	0.929	0.9	0.6-1.2	0.498
%time SBP>DAWN threshold	1.1	1.0-1.2	0.311	1.0	0.9-1.2	0.549
%time SBP> REVASCAT threshold	1.1	0.9-1.3	0.395	1.0	0.8-1.2	0.856
%time MAP within LA, per 10-percent	0.77	0.63-0.92	0.005	0.78	0.64-0.95	0.014
%time MAP<LLA, per 10-percent	1.2	0.95-1.60	0.11	1.16	0.89-1.53	0.275

Table 22. Association of percent time spent above SBP thresholds of 120, 140, 160, and 180 mmHg with functional outcome at discharge and 90-days. The DAWN, and REVASCAT trials stratified blood pressure management by recanalization status. In DAWN, systolic blood pressure was maintained below 140 mmHg in patients who achieved successful recanalization (TICI 2b or 3). In REVASCAT, systolic blood pressure was maintained below 160 mmHg in patients with successful recanalization. In both trials, systolic blood pressure was maintained below 185 mmHg in patients with

unsuccessful recanalization (TICI 0, 1, or 2a). aOR, adjusted odd ratio (adjusted for age, admission NIHSS, ASPECT score, and TICI score); OR, odds ratio; SBP, systolic blood pressure; mRS, modified Rankin scale; CI, confidence interval; DAWN, DWI or CTP Assessment with Clinical Mismatch in the Triage of Wake-Up and Late Presenting Strokes Undergoing Neurointervention with Trevo; REVASCAT, Randomized Trial of Revascularization with Solitaire FR Device versus Best Medical Therapy in the Treatment of Acute Stroke Due to Anterior Circulation Large Vessel Occlusion Presenting within Eight Hours of Symptom Onset.

Table 23. Comparison of percent time spent above SBP thresholds in patients with and without hemorrhagic transformation

	No HT	*HT*	*p Value*
%time SBP>120 mmHg	92.9 (75.0-99.2)	90.2 (74.0-99.0)	0.967
%time SBP>140 mmHg	64.0 (18.6-83.9)	57.8 (33.0-86.8)	0.525
%time SBP>160 mmHg	12.4 (1.3-33.2)	15.8 (3.2-46.3)	0.478
%time SBP>180 mmHg	0.62 (0.18-4.1)	0.86 (0.35-5.3)	0.255
%time SBP>DAWN threshold	26.3 (3.0-75.3)	41.7 (5.0-77.1)	0.293
%time SBP>REVASCAT threshold	5.8 (0.42-22.7)	9.3 (1.1-26.2)	0.257

Table 23. Mann Whitney-U comparisons of percent time spent above SBP thresholds in patients with and without hemorrhagic transformation. HT, hemorrhagic transformation; SBP, systolic blood pressure. Data summarized by median and interquartile range.

Table 24. Comparison of percent time spent above SBP thresholds in patients with and without symptomatic intracerebral hemorrhage

	No sICH	*sICH*	*p Value*
%time SBP>120 mmHg	93.1 (75.1-99.3)	79.1 (67.2-84.7)	0.037†
%time SBP>140 mmHg	64.4 (28.0-86.0)	37.1 (8.5-54.7)	0.079
%time SBP>160 mmHg	15.8 (2.1-45.4)	5.4 (1.7-18.3)	0.178
%time SBP>180 mmHg	0.74 (0.16-5.7)	0.68 (0.44-1.4)	0.734
%time SBP>DAWN threshold	35.2 (3.4-78.1)	20.4 (1.3-54.7)	0.269
%time SBP>REVASCAT threshold	7.6 (0.77-26.6)	3.5 (0.34-18.3)	0.391

Table 24. Mann Whitney-U comparisons of percent time spent above SBP thresholds in patients with and without hemorrhagic transformation or

symptomatic intracerebral hemorrhage. sICH, symptomatic intracerebral hemorrhage; SBP, systolic blood pressure. Data summarized by median and interquartile range. † While this p-value dips below 0.05, the significant difference to which it pertains does not negate our primary hypothesis. In other words, the p-value demonstrates that patients with sICH spent significantly *less* time above 120 mmHg compared to patients without sICH. The Mann-Whitney U comparison does not assess directionality, but it is clear that exceeding this fixed SBP threshold does not correlate with sICH as a secondary outcome.

E. Discussion

In this study of 90 patients with LVO stroke undergoing thrombectomy, we showed that continuous estimation of optimal blood pressure and limits of cerebral autoregulation is feasible. We further demonstrated that exceeding individual and flexible thresholds of autoregulation is associated with hemorrhagic transformation and overall worse functional outcome, even after adjusting for important prognostic covariates in stroke. Every 10% increase in time spent above ULA was associated with a 1.9-fold increase in the odds of shifting towards a worse outcome on the mRS at 90 days. We did not find this association when applying fixed blood pressure thresholds, even when stratifying by reperfusion status.

To date, there are no randomized controlled trials of optimal blood pressure management after EVT, and data to guide treatment approaches are limited. The majority of patients enrolled in recent thrombectomy trials also received intravenous tPA and were managed according to current guidelines with blood pressure below 180/105 mmHg for 24 hours. [207, 209, 210, 213, 229] However, recanalization rates with EVT are much higher compared to intravenous thrombolysis alone, and it remains unclear if the same BP targets apply. While a higher BP may be acceptable or even beneficial in patients with incomplete

reperfusion by promoting perfusion to ischemic territories, it could lead to relative hyperperfusion with consequent cerebral edema and hemorrhage in those patients with complete reperfusion. This phenomenon is well described in chronic ischemia after carotid revascularization (via endarterectomy or stenting) but may also occur in acute stroke. [230-232] Indeed, Hashimoto *et al*. presented a case of cerebral hyperperfusion syndrome in 77-year-old patient with acute internal carotid and middle cerebral artery occlusions. Due to the patient's neurologic deterioration, the authors suggest that it is important to routinely monitor regional oxygen saturation with NIRS, perform single-photo emission CT to evaluate cerebral blood flow, and maintain antihypertensive therapy to prevent hyperperfusion after revascularization. It is also possible that this complication is more prevalent than the handful of published and available case reports might suggest. [232]

Several thrombectomy trials, therefore, used a tiered approach with lower BP targets if successful reperfusion was achieved. [208, 211, 212, 232] However, we did not find a correlation between BP above these limits and any of our radiographic or clinical outcomes. (A minor exception in Table 24 is that patients with sICH spent significantly less time above 120 mmHg. Because patients with sICH spent *less* time above this threshold, the p-value of 0.037 does not argue in favor of using a fixed systolic threshold, as the directionality of this association does not align with the physiologic assumption that higher pressures underlie HT and sICH.) Still, optimal BP ranges after EVT are likely influenced by numerous factors; stratifying by reperfusion status alone may be insufficient. For example, chronic hypertension and flow-limiting extracranial carotid disease can shift a patient's autoregulatory curve towards higher pressures, and aggressively lowering BP

after successful EVT in such a patient may result in cerebral hypoperfusion and infarct expansion. [233, 234] In contrast, optimal BP may shift towards lower targets among patients without a history of hypertension or pre-existing large-vessel disease.

Our data also suggests that limits of autoregulation are not static, but rather change over time; thus, maintaining the same BP target throughout the acute phase of ischemic stroke may lead to frequent episodes of hypo- and hyperperfusion. Figure 24 shows an example of a patient whose BP remained below the guideline-recommended target but frequently exceeded personalized autoregulatory limits. In addition, the patient's BP was above the lower BP threshold of 140 mmHg for almost the entire monitoring period. However, BP lowering in this particular patient may lead to a decrease below the LLA with consequent risk of ischemia. While there appears to be general trend towards worse outcome with increasing time above SBP thresholds of 140 mmHg and 160 mmHg, the effect sizes were much smaller when compared to the personalized, autoregulation-based approach. Moreover, they became non-significant when adjusting for covariates. These findings suggest that selecting a single BP target for all patients may not sufficiently account for patient-specific factors affecting cerebral perfusion. Therefore, taking into consideration individual patients' hemodynamic physiology and maintaining BP within autoregulatory targets may be a better strategy compared to the classical approach of maintaining SBP below fixed, pre-determined values.

To explore possible mechanisms underlying the association of BP outside autoregulatory limits and poor outcome, we evaluated several short-term imaging endpoints that have

strong associations with outcome after stroke. Time spent above the ULA, but not any of the fixed SBP thresholds, was associated with higher rates of HT. This finding is supported by the construct that above the ULA, cerebral vasculature acts as a pressure-passive system, in which increases in cerebral blood flow are not counteracted by vasoconstriction, resulting in periods of hyperperfusion. Furthermore, higher cerebral blood flow after reperfusion therapy, measured with arterial spin labeling MRI, has been shown to increase risk of HT. [235] In addition, several retrospective studies reported an association between elevated BP after thrombectomy and HT, [224, 236] although others did not find this association. [223] Differences in autoregulatory function may be one explanation for conflicting results. In our study, elevated BP relative to each patient's personalized ULA was associated with increased risk of sICH and neurologic worsening, rather than absolute increased BP alone. This hypothesis is succinctly summarized in the illustration below (Figure 26).

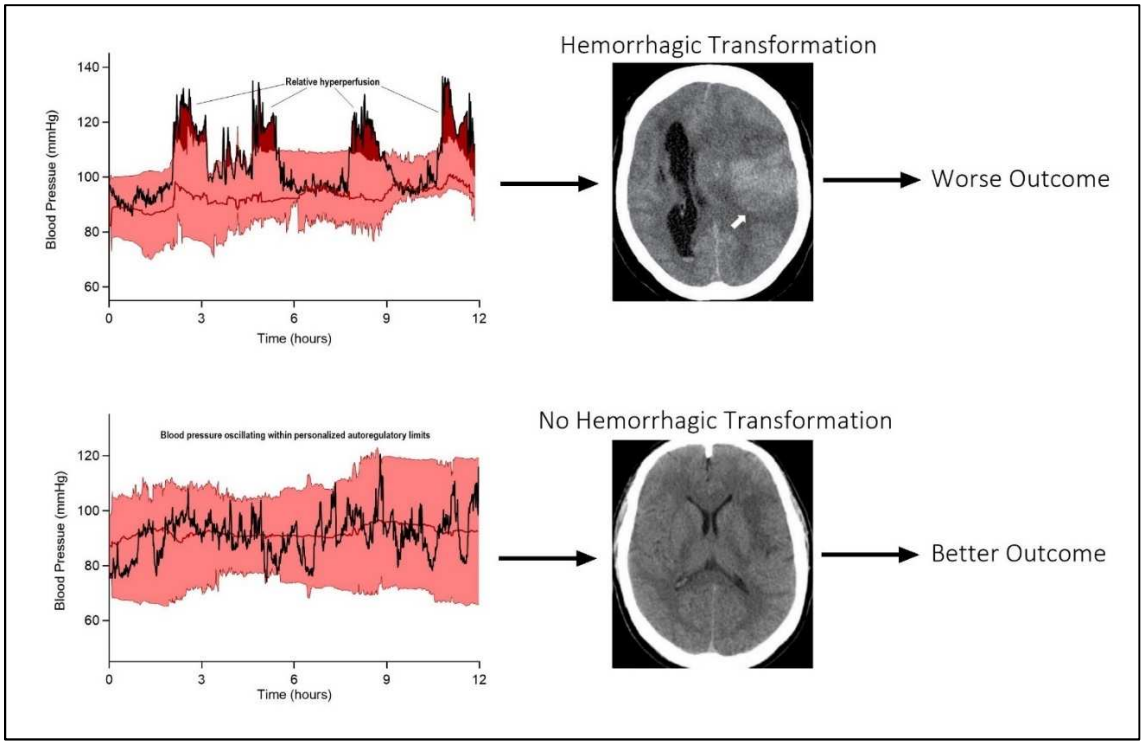

Figure 26. Relative hyperperfusion above the ULA may predispose patients to hemorrhagic transformation and worse outcomes. In contrast, patients who oscillate within their personalized limits of autoregulation may be protected from secondary brain injury after stroke.

BP management below the LLA was associated with greater infarct progression, suggesting that the sustenance of the ischemic brain tissue may be improved by maintaining cerebral perfusion above the LLA. In addition to subtotal reperfusion and autoregulatory impairment, microcirculatory dysfunction and distal embolization are possible mechanisms that also may increase vulnerability to relative hypoperfusion. [237, 238]

Limitations

This study has several important limitations. First, the sample size was modest, and while the study was significant for its primary outcome, we were not able to adjust for all predictors of poor outcome. The addition of short-term radiographic endpoints and a plausible biological mechanism help mitigate this limitation. Second, 12 patients enrolled

toward the beginning of our study were excluded from analysis due to insufficient recording time or poor signal quality. Technical challenges faced at the beginning of the study have since been overcome. Third, 3-month outcomes were available for only 86.7% (78/90) of patients. However, both groups (patients with and without 3-month outcomes) were comparable in terms of baseline characteristics (Table 25). Furthermore, a sensitivity analysis imputing 3-month outcomes using the last-observation-carried-forward approach resulted in similar associations and effect sizes between BP targets and outcome (Table 26). Finally, information produced from this study is descriptive and correlational; causation cannot be inferred. Conclusions about whether an autoregulation-guided therapy protocol will improve patient physiology or outcome are not possible at this stage.

Table 25. Comparison between patients with and without 3-month longitudinal outcome measures (90-day mRS)

Variable	*Patients with 90-day mRS (n=78)*	*Patients without 90-day mRS (n=12)*	*p Value*
Age, mean ± SD	72.2 (16.1)	67.5 (17.6)	0.348
Sex, F (%)	37 (47.4)	5 (41.7)	0.709
Admission NIHSS, mean ± SD	14.2 (5.8)	11.7 (4.3)	0.134
Admission ASPECTS, mean ± SD	8.8 (1.5)	8.4 (2.3)	0.974
Admission MAP, mean ± SD	107.4 (17.1)	106.8 (19.2)	0.967
Admission Glucose, mean ± SD	140.2 (72.4)	118.3 (24.2)	0.188
Affected Side, n (%)			
Left	38 (48.7)	7 (58.3)	0.535
Right	40 (51.3)	5 (41.7)	
Medical History, n (%)			
Hypertension	54 (69.2)	11 (91.7)	0.167
Coronary Artery Disease	11 (14.1)	0 (0.0)	0.348
Myocardial Infarction	5 (6.4)	1 (8.3)	0.587
Congestive Heart Failure	9 (11.5)	1 (8.3)	1.000
Atrial Fibrillation	43 (55.1)	4 (33.3)	0.218
Hyperlipidemia	32 (41.0)	4 (33.3)	0.756
Diabetes Mellitus (I & II)	17 (21.8)	3 (25.0)	0.725

Ischemic Stroke Cancer Thyroid Disease Current Smoker Past Smoker	15 (19.2) 11 (14.1) 8 (10.3) 14 (17.9) 16 (20.5)	2 (16.7) 3 (25.0) 1 (8.3) 5 (41.7) 3 (25.0)	1.000 0.390 1.000 0.061 0.712
Mean monitoring time (hours), mean ± SD	28.4 (18.7)	25.1 (16.6)	0.749
Percent time MAP within limits of autoregulation, mean ± SD	66.6 (22.6)	60.3 (25.4)	0.433
Percent time MAP above the upper limit of autoregulation, mean ± SD	15.6 (11.9)	22.8 (20.0)	0.226
Percent time MAP below the lower limit of autoregulation, mean ± SD	18.1 (15.7)	17.0 (11.0)	0.803
Mean MAP (mmHg), mean ± SD	93.1 (12.0)	97.6 (12.9)	0.141
Mean upper limit of autoregulation (mmHg), mean ± SD	104.4 (11.6)	107.2 (11.2)	0.302
Mean lower limit of autoregulation (mmHg), mean ± SD	83.2 (11.7)	87.2 (14.1)	0.302
Mean MAP_{OPT} (mmHg), mean ± SD	93.1 (11.8)	95.0 (13.6)	0.522
Treated with tPA, n (%)	33 (42.3)	5 (41.7)	0.967
Time to reperfusion (minutes), mean ± SD	582.4 (420.4)	532.6 (321.1)	0.834
Successful recanalization, n (%)	59 (75.6)	8 (66.7)	0.494
TICI Score, n (%) 0 1 2a 2b 3	 14 (17.9) 2 (2.6) 4 (5.1) 35 (44.9) 23 (29.5)	 1 (8.3) 1 (8.3) 2 (16.7) 6 (50.0) 2 (16.7)	 0.359
Hemorrhagic transformation, n (%) HT I HT II PH I PH II None	 14 (17.9) 9 (11.5) 6 (7.7) 5 (6.4) 44 (56.4)	 3 (25.0) 1 (8.3) 1 (8.3) 0 (0.0) 7 (58.3)	 0.759
Symptomatic hemorrhagic transformation, n (%)	7 (9.0)	1 (8.3)	1.000

Cerebral edema, n (%)	9 (11.5)	1 (8.3)	1.000
Final infarct volume (mL), mean ± SD	82.1 (86.6)	79.4 (72.9)	0.747
Infarct progression (mL), mean ± SD	80.2 (83.0)	71.9 (80.5)	0.722

Table 25. Univariate comparison between patients with longitudinal 3-month mRS outcomes and the subgroup of those patients who were lost to follow-up. Significant differences were determined using independent student's T-tests and chi-squared analysis for normally distributed data, while Mann-Whitney U tests were used for non-parametric variables. Fisher's exact test was employed for cross tables containing fewer than five patients.

Table 26. Last-observation-carried-forward sensitivity analysis						
Likelihood of a shift towards worse outcome on 90-day mRS						
Variables	*OR*	*95% CI*	*p Value*	*aOR*	*95% CI*	*p Value*
%time MAP>ULA, per 10-percent	1.7	1.2-2.3	0.002	1.7	1.2-2.3	0.002
%time MAP within LA, per 10-percent	0.8	0.6-0.9	0.002	0.8	0.7-0.9	0.004
%time MAP<LLA, per 10-percent	1.3	0.9-1.6	0.064	1.2	0.9-1.6	0.154

Table 26. Last-observation-carried-forward sensitivity analysis of outcomes at 90-days. aOR, adjusted odd ratio (adjusted for age, admission NIHSS, ASPECT score, and TICI score); OR, odds ratio; MAP, mean arterial pressure; mRS, modified Rankin scale; ULA, upper limit of autoregulation; LA, limits of autoregulation; LLA, lower limit of autoregulation; CI, confidence interval.

Conclusion of the ischemic stroke neuromonitoring study

Continuous estimation of limits of autoregulation after EVT is feasible and provides a BP range for individual patients tailored to their own physiology. Exceeding LA, but not fixed SBP thresholds, was associated with HT as well as overall poor functional outcome. This

information is particularly important in the evolving landscape of endovascular treatment approaches, in which more patients will require early management in neurological intensive care units. Further research is needed to test autoregulation-based treatment strategies – namely, a multicenter randomized controlled trial comparing our personalized autoregulatory approach to the guideline-recommended practice of maintaining SBP below fixed thresholds.

PART IV

A. Concluding remarks and future studies

Continuous neuromonitoring of cerebral autoregulation can be harnessed for bedside individualization of blood pressure care in critically ill patients. The past two decades have ushered in numerous reports on the clinical import of autoregulation and optimal cerebral perfusion pressure monitoring. Although these studies wield considerable disparities in methodology, patient population, and sample size, the vast majority demonstrate that dysfunctional cerebral autoregulation plays a key role in secondary brain injury after neurologic disease. As discussed throughout this thesis, this concept holds true for patients suffering from subarachnoid hemorrhage and ischemic stroke. Complications like DCI and HT are potentially devastating turning points during a given patient's hospitalization, and so any approach to predict and prevent them should be prioritized and rigorously evaluated in a randomized fashion. In Part II, our study on subarachnoid hemorrhage shows that deviation from individualized limits of autoregulation strongly associates with poor functional outcome at discharge and 90 days after the initial bleed. The study further demonstrates collinearity between invasive (ICP) and non-invasive (NIRS) measures of autoregulation. In Part III, our study on ischemic stroke shows that exceeding the upper limit of autoregulation correlates with worse functional outcome as well as worsening grades of HT. The study further compares our personalized approach to currently recommended fixed systolic thresholds and argues for future research in prospective, multicenter, and randomized trials. On the whole, these two studies regarding subarachnoid hemorrhage and ischemic stroke set the stage for such interventional trials.

In fact, we are currently planning a pilot trial to test the feasibility of an intervention protocol targeting a dynamic MAP_{OPT}. We will test the hypothesis that blood pressure adjustments during periods of dysautoregulation can restore autoregulatory function by shifting patients to a more favorable position on the autoregulatory curve (Figure 27A). Under the null hypothesis, the treatment would lower blood pressure but also the limits of autoregulation, shifting the autoregulatory curve to the left. As a result, MAP would never return to within limits of autoregulation (Figure 27B). Under the alternative hypothesis, blood pressure would return to within limits of autoregulation (Figure 27C).

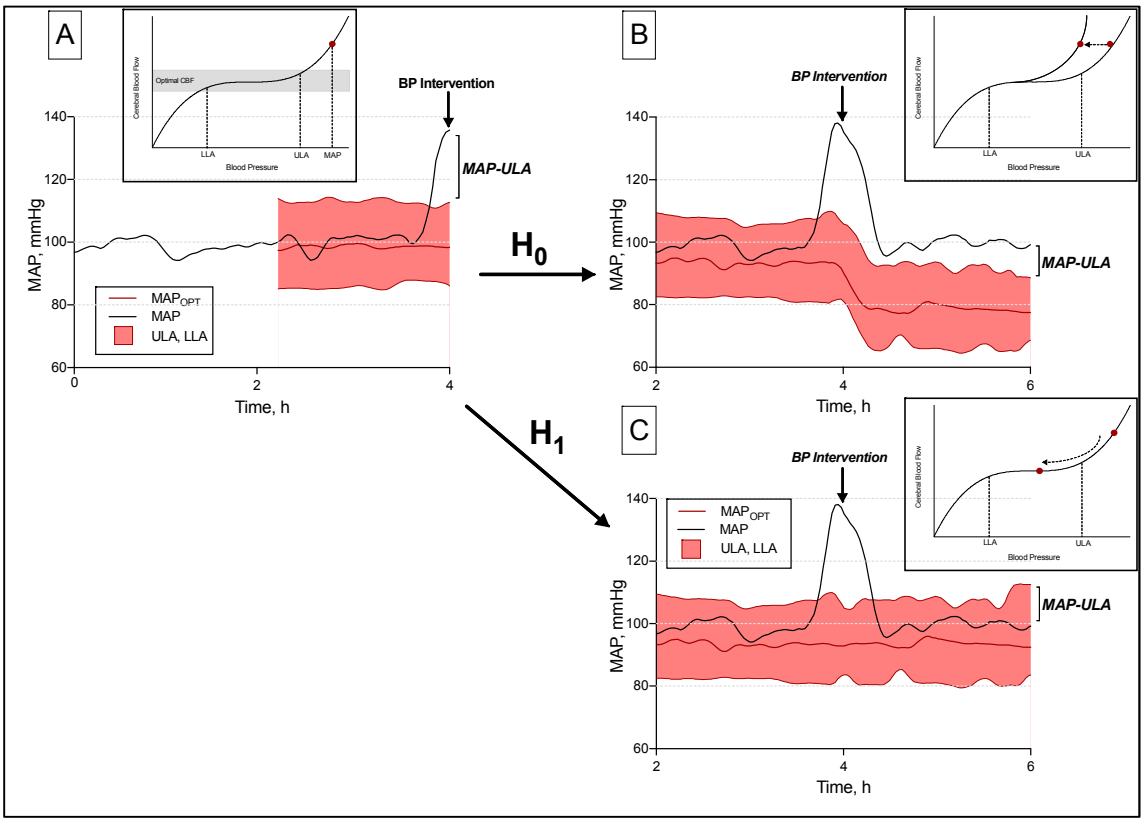

Figure 27. Possible effects of blood pressure intervention on autoregulatory function.

In this future study, patients with LVO ischemic stroke will receive personalized blood pressure recommendations every 6 hours to maintain MAP within personalized limits of autoregulation during the first 24 hours after LVO stroke. During the first 2 hours after enrollment, patients will be managed according to American Heart Association guidelines with BP <180/105 mmHg, bridging the time for ICM+ software to provide the first flexible MAP target. MAP_{OPT} will be assessed every 6 hours by the treating clinicians. An automated alert will ask the treating clinicians to review and set the new individual and flexible MAP target. If no MAP_{OPT} can be set for any variety of reasons (e.g., non-parabolic curve generation), the default clinical target (BP <180/105) will be used. To minimize risk of harm, MAP <60 or MAP >120 mmHg will not be targeted (predefined safety ranges). The treatment strategy to support arterial blood pressure will include blood pressure augmentation using intravenous fluids and/or vasopressors as a second-line approach, as well as active pharmacological lowering of blood pressure with antihypertensive medication (e.g., labetalol or metoprolol).

Although it may be possible to target the optimal blood pressure range in real-time, we will use regular intervals for data review, during which new blood pressure targets will be selected based on data from the prior 6 hours of monitoring. Blood pressure targets selected this way closely resemble a person's real-time autoregulatory limits (Figure 28). In addition, this approach adds an extra layer of safety, as treating clinicians would periodically review the data, such that they could always decide not to follow the MAP_{OPT} algorithm in light of clinical expertise and concerns regarding patient safety.

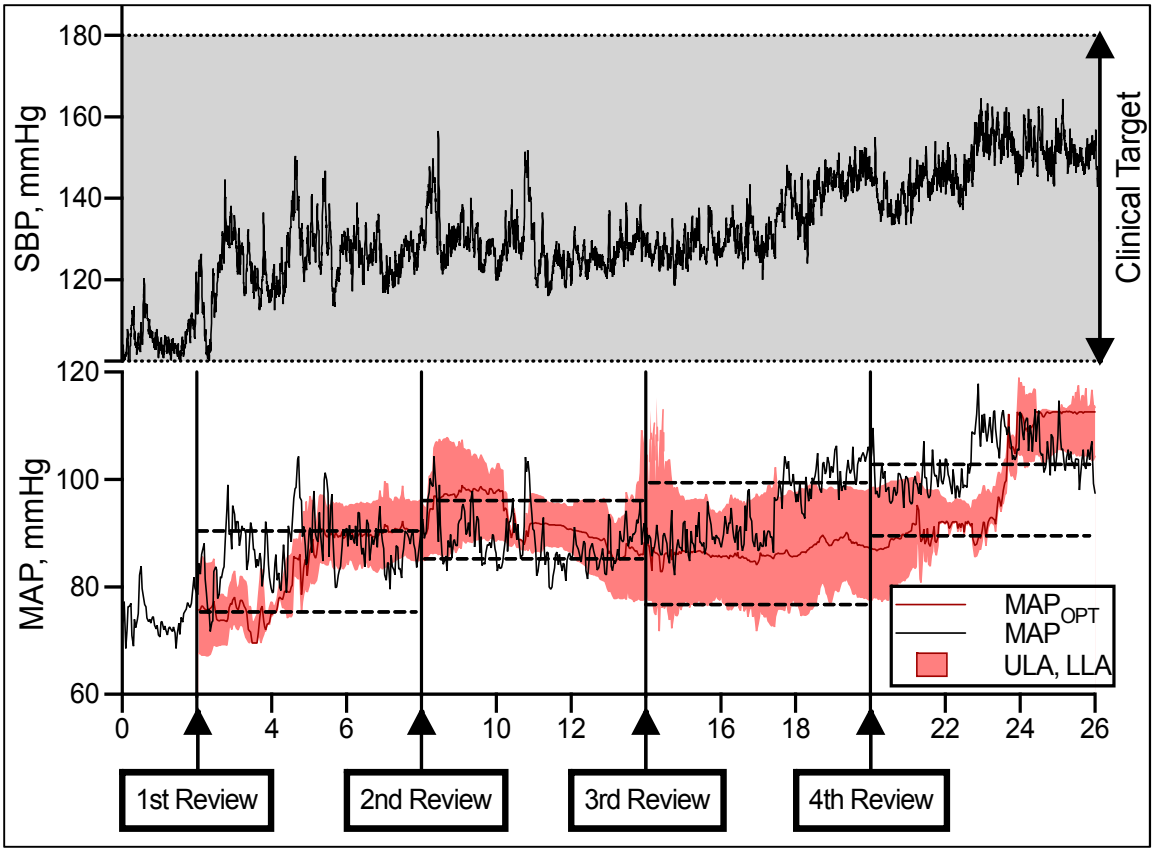

Figure 28. Clinical review of limits of autoregulation in a future interventional study.

Lastly, future studies may approach the patient from a broader physiologic perspective, as several hemodynamic parameters influence cerebral blood flow (not merely blood pressure). In fact, since mean arterial pressure is dependent on cardiac function, optimization of cardiac output might be an alternative, or perhaps adjunctive, approach in the effort to optimize cerebral perfusion pressure. It has been shown that cerebral perfusion depends on cardiac output in ischemic dysregulated brain territories. [239] Noting that 13-28% of stroke patients sustain cardiac contractility impairment, another study found that cerebral blood flow was significantly higher in patients with preserved left ventricular contractility. [240] A more recent study by Fuhrer *et al*. assessed cerebral perfusion in 10

patients with acute large hemispheric strokes, alongside their mean arterial pressures and cardiac indices. [241] The latter hemodynamic parameter strongly correlated with cerebral perfusion, whereas correlation with blood pressure was not observed. Despite limitations (particularly the sample size), the authors go so far as to propose a paradigm shift – namely, their results might challenge the current state of using blood pressure as the main clinical roadmap in the intensive care of patients with cerebral ischemia. Rather, they advocate for a cardiac output-guided hemodynamic strategy. This strategy is supported by basic physiology. After all, mean arterial pressure is the product of cardiac output and systemic vascular resistance, and cardiac output depends on other factors like preload, contractility, and heart rate. Blood pressure is just the afterload. To increase cardiac output, these parameters can be augmented with intravenous fluids or catecholamine administration, all in accordance with the Frank-Starling curve. Because the correlation between blood pressure and cardiac output is volume state dependent, the focus on blood pressure to improve brain oxygen delivery and perfusion may hold true only in the setting of isovolemia. With these basic principles in mind, the same team at the University of Freiburg has launched a multicenter randomized trial, entitled Optimizing Cardiac Out-Put to Increase Cerebral Penumbral Perfusion in Large Middle Cerebral Artery Ischemic Lesion (OPTIMAL Study). [242] The two arms seek to enroll 150 patients each and compare functional outcome at 3 and 6 months. The trial is in part based upon optimization of cardiac output in patients with severe subarachnoid hemorrhage. In those studies, increasing cardiac output, while keeping mean arterial pressure constant, led to higher cerebral blood flow readings, diminished rates of delayed cerebral ischemia, and improved functional outcomes. [243, 244] As we await the results of the OPTIMAL trial in stroke

patients, it is important to note that future surveillance and optimization of cardiac output may become an integral facet of acute stroke care. Regardless of a possible paradigm shift towards cardiac output, the ultimate goal of all of these trials will be to prevent penumbral injury, improve collateral flow, and maximize perfusion and sustenance to impaired brain tissue.

This is all to say that the heart-brain axis is highly complex, with many moving parts and puzzle pieces, and so the future will likely favor real-time, multimodal hemodynamic and neuromonitoring of critically ill patients. Nevertheless, our autoregulatory avenue appears extremely promising and is illuminated with the lampposts of many provocative studies, including those presented herein. We hope this path will intersect and merge with other branches of cardiovascular neurology, as a synergistic effort will likely lead to the best possible outcomes.

To conclude and summarize the results of this thesis, our group effectively demonstrated that individualized blood pressure targeting represents a highly feasible approach in the neuroscience intensive care unit. Using cerebral autoregulation monitoring, we were able to define and trend personalized pressure thresholds in real-time, across two different disease states. The primary outcome of both the subarachnoid hemorrhage and ischemic stroke studies pertained to the impact of deviation from those thresholds on radiographic and functional outcomes. In the subarachnoid hemorrhage study (Part II), deviating from autoregulatory limits strongly associated with functional outcome, and invasive and non-invasive measures of autoregulation demonstrated collinearity. In the ischemic stroke study

(Part III), exceeding the upper limit of autoregulation – but not any of the fixed systolic thresholds – correlated with functional outcome and hemorrhagic transformation. At this exciting juncture, many future directions are possible, but the local stage is set for an interventional trial at Yale-New Haven Hospital, in which our team will titrate pressures according to our autoregulation-guided algorithm in patients with ischemic stroke.

References

1. Lassen, N.A., *Cerebral blood flow and oxygen consumption in man.* Physiol Rev, 1959. **39**(2): p. 183-238.
2. Mokri, B., *The Monro-Kellie hypothesis: applications in CSF volume depletion.* Neurology, 2001. **56**(12): p. 1746-8.
3. Roy, C.S. and C.S. Sherrington, *On the Regulation of the Blood-supply of the Brain.* J Physiol, 1890. **11**(1-2): p. 85-158 17.
4. Bayliss, W.M., *On the local reactions of the arterial wall to changes of internal pressure.* J Physiol, 1902. **28**(3): p. 220-31.
5. Fog, M., *The Relationship between the Blood Pressure and the Tonic Regulation of the Pial Arteries.* J Neurol Psychiatry, 1938. **1**(3): p. 187-97.
6. Castro, P., E. Azevedo, and F. Sorond, *Cerebral Autoregulation in Stroke.* Curr Atheroscler Rep, 2018. **20**(8): p. 37.
7. Forbes, H.S., *The cerebral circulation I Observation and measurement or pial vessels.* Archives of Neurology and Psychiatry, 1928. **19**(5): p. 751-761.
8. Forbes, H.S. and H.G. Wolff, *Cerebral circulation III The vasomotor control of cerebral vessels.* Archives of Neurology and Psychiatry, 1928. **19**(6): p. 1057-1086.
9. Klein, S.P., et al., *Autoregulation assessment by direct visualisation of pial arterial blood flow in the piglet brain.* Sci Rep, 2019. **9**(1): p. 13333.
10. Paulson, O.B., S. Strandgaard, and L. Edvinsson, *Cerebral autoregulation.* Cerebrovasc Brain Metab Rev, 1990. **2**(2): p. 161-92.
11. Budohoski, K.P., et al., *Clinical relevance of cerebral autoregulation following subarachnoid haemorrhage.* Nat Rev Neurol, 2013. **9**(3): p. 152-63.
12. Rivera-Lara, L., et al., *Cerebral Autoregulation-oriented Therapy at the Bedside: A Comprehensive Review.* Anesthesiology, 2017. **126**(6): p. 1187-1199.
13. Petersen, N.H., et al., *Association of Personalized Blood Pressure Targets With Hemorrhagic Transformation and Functional Outcome After Endovascular Stroke Therapy.* JAMA Neurol, 2019.
14. Silverman, A., et al., *Deviation From Personalized Blood Pressure Targets Is Associated With Worse Outcome After Subarachnoid Hemorrhage.* Stroke, 2019. **50**(10): p. 2729-2737.
15. Wang, A., S. Ortega-Gutierrez, and N.H. Petersen, *Autoregulation in the Neuro ICU.* Curr Treat Options Neurol, 2018. **20**(6): p. 20.
16. Aries, M.J., et al., *Continuous determination of optimal cerebral perfusion pressure in traumatic brain injury.* Crit Care Med, 2012. **40**(8): p. 2456-63.
17. Diedler, J., et al., *Optimal cerebral perfusion pressure in patients with intracerebral hemorrhage: an observational case series.* Crit Care, 2014. **18**(2): p. R51.
18. Budohoski, K.P., et al., *Monitoring Cerebral Autoregulation After Subarachnoid Hemorrhage.* Acta Neurochir Suppl, 2016. **122**: p. 199-203.
19. Hori, D., et al., *Hypotension After Cardiac Operations Based on Autoregulation Monitoring Leads to Brain Cellular Injury.* Ann Thorac Surg, 2015. **100**(2): p. 487-93.

20. Lee, J.K., et al., *Cerebrovascular blood pressure autoregulation monitoring and postoperative transient ischemic attack in pediatric moyamoya vasculopathy.* Paediatr Anaesth, 2018. **28**(2): p. 94-102.
21. Burton, V.J., et al., *A pilot cohort study of cerebral autoregulation and 2-year neurodevelopmental outcomes in neonates with hypoxic-ischemic encephalopathy who received therapeutic hypothermia.* BMC Neurol, 2015. **15**: p. 209.
22. Lee, J.K., et al., *Optimizing Cerebral Autoregulation May Decrease Neonatal Regional Hypoxic-Ischemic Brain Injury.* Dev Neurosci, 2017. **39**(1-4): p. 248-256.
23. Brain Trauma, F., et al., *Guidelines for the management of severe traumatic brain injury. IX. Cerebral perfusion thresholds.* J Neurotrauma, 2007. **24 Suppl 1**: p. S59-64.
24. Hemphill, J.C., 3rd, et al., *Guidelines for the Management of Spontaneous Intracerebral Hemorrhage: A Guideline for Healthcare Professionals From the American Heart Association/American Stroke Association.* Stroke, 2015. **46**(7): p. 2032-60.
25. Connolly, E.S., Jr., et al., *Guidelines for the management of aneurysmal subarachnoid hemorrhage: a guideline for healthcare professionals from the American Heart Association/american Stroke Association.* Stroke, 2012. **43**(6): p. 1711-37.
26. Porto, G.B., et al., *Blood Pressure Guideline Adherence in Patients with Ischemic and Hemorrhagic Stroke in the Neurointensive Care Unit Setting.* Neurocrit Care, 2015. **23**(3): p. 313-20.
27. Cecconi, M., et al., *Consensus on circulatory shock and hemodynamic monitoring. Task force of the European Society of Intensive Care Medicine.* Intensive Care Med, 2014. **40**(12): p. 1795-815.
28. Beqiri, E., et al., *Feasibility of individualised severe traumatic brain injury management using an automated assessment of optimal cerebral perfusion pressure: the COGiTATE phase II study protocol.* BMJ Open, 2019. **9**(9): p. e030727.
29. Petersen, N.H., S. Kodali, and K.N. Sheth, *Towards Individualized Blood Pressure Management After Stroke.* Am J Hypertens, 2019. **32**(3): p. 242-244.
30. Xiong, L., et al., *Impaired cerebral autoregulation: measurement and application to stroke.* J Neurol Neurosurg Psychiatry, 2017. **88**(6): p. 520-531.
31. Faraci, F.M. and D.D. Heistad, *Regulation of large cerebral arteries and cerebral microvascular pressure.* Circ Res, 1990. **66**(1): p. 8-17.
32. Liu, J., et al., *Cerebral autoregulation of blood velocity and volumetric flow during steady-state changes in arterial pressure.* Hypertension, 2013. **62**(5): p. 973-9.
33. Ibrahim, J., et al., *Sex-specific differences in cerebral arterial myogenic tone in hypertensive and normotensive rats.* Am J Physiol Heart Circ Physiol, 2006. **290**(3): p. H1081-9.
34. Osol, G. and W. Halpern, *Myogenic properties of cerebral blood vessels from normotensive and hypertensive rats.* Am J Physiol, 1985. **249**(5 Pt 2): p. H914-21.

35. Halpern, W., G. Osol, and G.S. Coy, *Mechanical behavior of pressurized in vitro prearteriolar vessels determined with a video system.* Ann Biomed Eng, 1984. **12**(5): p. 463-79.
36. Knot, H.J. and M.T. Nelson, *Regulation of arterial diameter and wall [Ca2+] in cerebral arteries of rat by membrane potential and intravascular pressure.* J Physiol, 1998. **508 (Pt 1)**: p. 199-209.
37. Chrissobolis, S. and C.G. Sobey, *Evidence that Rho-kinase activity contributes to cerebral vascular tone in vivo and is enhanced during chronic hypertension: comparison with protein kinase C.* Circ Res, 2001. **88**(8): p. 774-9.
38. Laher, I., et al., *Protein kinase C potentiates stretch-induced cerebral artery tone by increasing intracellular sensitivity to Ca2+.* Biochem Biophys Res Commun, 1989. **165**(1): p. 312-8.
39. Berg, R.M., *Myogenic and metabolic feedback in cerebral autoregulation: Putative involvement of arachidonic acid-dependent pathways.* Med Hypotheses, 2016. **92**: p. 12-7.
40. Ampuero, I., et al., *On the diagnosis of CADASIL.* J Alzheimers Dis, 2009. **17**(4): p. 787-94.
41. Chabriat, H., et al., *Cadasil.* Lancet Neurol, 2009. **8**(7): p. 643-53.
42. Dziewulska, D., *Mysteries of CADASIL - the contribution of neuropathology to understanding of the disease.* Folia Neuropathol, 2009. **47**(1): p. 1-10.
43. Formichi, P., et al., *Apoptosis in CADASIL: an in vitro study of lymphocytes and fibroblasts from a cohort of Italian patients.* J Cell Physiol, 2009. **219**(2): p. 494-502.
44. Lacombe, P., et al., *Impaired cerebral vasoreactivity in a transgenic mouse model of cerebral autosomal dominant arteriopathy with subcortical infarcts and leukoencephalopathy arteriopathy.* Stroke, 2005. **36**(5): p. 1053-8.
45. Joutel, A., et al., *Cerebrovascular dysfunction and microcirculation rarefaction precede white matter lesions in a mouse genetic model of cerebral ischemic small vessel disease.* J Clin Invest, 2010. **120**(2): p. 433-45.
46. Toth, P., et al., *Isolated human and rat cerebral arteries constrict to increases in flow: role of 20-HETE and TP receptors.* J Cereb Blood Flow Metab, 2011. **31**(10): p. 2096-105.
47. Hamel, E., *Perivascular nerves and the regulation of cerebrovascular tone.* J Appl Physiol (1985), 2006. **100**(3): p. 1059-64.
48. Cauli, B., et al., *Cortical GABA interneurons in neurovascular coupling: relays for subcortical vasoactive pathways.* J Neurosci, 2004. **24**(41): p. 8940-9.
49. Hall, C.N., et al., *Interpreting BOLD: towards a dialogue between cognitive and cellular neuroscience.* Philos Trans R Soc Lond B Biol Sci, 2016. **371**(1705).
50. Sheffield, J.M. and D.M. Barch, *Cognition and resting-state functional connectivity in schizophrenia.* Neurosci Biobehav Rev, 2016. **61**: p. 108-20.
51. Lake, E.M., P. Bazzigaluppi, and B. Stefanovic, *Functional magnetic resonance imaging in chronic ischaemic stroke.* Philos Trans R Soc Lond B Biol Sci, 2016. **371**(1705).
52. Iadecola, C., *Neurovascular regulation in the normal brain and in Alzheimer's disease.* Nat Rev Neurosci, 2004. **5**(5): p. 347-60.

53. Lincoln, J., *Innervation of cerebral arteries by nerves containing 5-hydroxytryptamine and noradrenaline.* Pharmacol Ther, 1995. **68**(3): p. 473-501.
54. Cipolla, M.J., R. Li, and L. Vitullo, *Perivascular innervation of penetrating brain parenchymal arterioles.* J Cardiovasc Pharmacol, 2004. **44**(1): p. 1-8.
55. Teotonio, R., et al., *Posterior reversible encephalopathy syndrome: the importance of early diagnosis.* BMJ Case Rep, 2012. **2012**.
56. Faraci, F.M., W.G. Mayhan, and D.D. Heistad, *Segmental vascular responses to acute hypertension in cerebrum and brain stem.* Am J Physiol, 1987. **252**(4 Pt 2): p. H738-42.
57. Tetsuka, S. and T. Ogawa, *Posterior reversible encephalopathy syndrome: A review with emphasis on neuroimaging characteristics.* J Neurol Sci, 2019. **404**: p. 72-79.
58. Hoiland, R.L., J.A. Fisher, and P.N. Ainslie, *Regulation of the Cerebral Circulation by Arterial Carbon Dioxide.* Compr Physiol, 2019. **9**(3): p. 1101-1154.
59. Yoshihara, M., K. Bandoh, and A. Marmarou, *Cerebrovascular carbon dioxide reactivity assessed by intracranial pressure dynamics in severely head injured patients.* J Neurosurg, 1995. **82**(3): p. 386-93.
60. Paulson, O.B., J. Olesen, and M.S. Christensen, *Restoration of autoregulation of cerebral blood flow by hypocapnia.* Neurology, 1972. **22**(3): p. 286-93.
61. Czosnyka, M., et al., *Cerebrovascular time constant: dependence on cerebral perfusion pressure and end-tidal carbon dioxide concentration.* Neurol Res, 2012. **34**(1): p. 17-24.
62. Harris, A.D., et al., *Cerebral blood flow response to acute hypoxic hypoxia.* NMR Biomed, 2013. **26**(12): p. 1844-52.
63. Tallroth, G., E. Ryding, and C.D. Agardh, *Regional cerebral blood flow in normal man during insulin-induced hypoglycemia and in the recovery period following glucose infusion.* Metabolism, 1992. **41**(7): p. 717-21.
64. Golding, E.M., et al., *Endothelium-derived hyperpolarizing factor in the brain: a new regulator of cerebral blood flow?* Stroke, 2002. **33**(3): p. 661-3.
65. Endres, M. and U. Laufs, *Effects of statins on endothelium and signaling mechanisms.* Stroke, 2004. **35**(11 Suppl 1): p. 2708-11.
66. Czosnyka, M., et al., *Monitoring of cerebrovascular autoregulation: facts, myths, and missing links.* Neurocrit Care, 2009. **10**(3): p. 373-86.
67. Steiner, L.A., et al., *Assessment of cerebrovascular autoregulation in head-injured patients: a validation study.* Stroke, 2003. **34**(10): p. 2404-9.
68. Aaslid, R., et al., *Cerebral autoregulation dynamics in humans.* Stroke, 1989. **20**(1): p. 45-52.
69. Giller, C.A., *A bedside test for cerebral autoregulation using transcranial Doppler ultrasound.* Acta Neurochir (Wien), 1991. **108**(1-2): p. 7-14.
70. Soehle, M., et al., *Continuous assessment of cerebral autoregulation in subarachnoid hemorrhage.* Anesth Analg, 2004. **98**(4): p. 1133-9, table of contents.
71. Mahony, P.J., et al., *Assessment of the thigh cuff technique for measurement of dynamic cerebral autoregulation.* Stroke, 2000. **31**(2): p. 476-80.

72. Panerai, R.B., *Assessment of cerebral pressure autoregulation in humans--a review of measurement methods.* Physiol Meas, 1998. **19**(3): p. 305-38.
73. Tiecks, F.P., et al., *Comparison of static and dynamic cerebral autoregulation measurements.* Stroke, 1995. **26**(6): p. 1014-9.
74. Menzel, M., et al., *Brain tissue oxygen monitoring for assessment of autoregulation: preliminary results suggest a new hypothesis.* J Neurosurg Anesthesiol, 2003. **15**(1): p. 33-41.
75. Czosnyka, M., et al., *Continuous assessment of the cerebral vasomotor reactivity in head injury.* Neurosurgery, 1997. **41**(1): p. 11-7; discussion 17-9.
76. Zweifel, C., et al., *Noninvasive monitoring of cerebrovascular reactivity with near infrared spectroscopy in head-injured patients.* J Neurotrauma, 2010. **27**(11): p. 1951-8.
77. Jobsis, F.F., *Noninvasive, infrared monitoring of cerebral and myocardial oxygen sufficiency and circulatory parameters.* Science, 1977. **198**(4323): p. 1264-7.
78. Matcher, S.J., et al., *Performance comparison of several published tissue near-infrared spectroscopy algorithms.* Anal Biochem, 1995. **227**(1): p. 54-68.
79. Zweifel, C., et al., *Continuous assessment of cerebral autoregulation with near-infrared spectroscopy in adults after subarachnoid hemorrhage.* Stroke, 2010. **41**(9): p. 1963-8.
80. Yoshitani, K., et al., *Effects of hemoglobin concentration, skull thickness, and the area of the cerebrospinal fluid layer on near-infrared spectroscopy measurements.* Anesthesiology, 2007. **106**(3): p. 458-62.
81. Rolfe, P., *In vivo near-infrared spectroscopy.* Annu Rev Biomed Eng, 2000. **2**: p. 715-54.
82. Steppan, J. and C.W. Hogue, Jr., *Cerebral and tissue oximetry.* Best Pract Res Clin Anaesthesiol, 2014. **28**(4): p. 429-39.
83. Wintermark, M., et al., *Comparative overview of brain perfusion imaging techniques.* J Neuroradiol, 2005. **32**(5): p. 294-314.
84. Arshi, B., W.J. Mack, and B. Emanuel, *Invasive and noninvasive multimodal bedside monitoring in subarachnoid hemorrhage: a review of techniques and available data.* Neurol Res Int, 2013. **2013**: p. 987934.
85. Sandsmark, D.K., et al., *Multimodal monitoring in subarachnoid hemorrhage.* Stroke, 2012. **43**(5): p. 1440-5.
86. Petersen, N.H., et al., *Dynamic cerebral autoregulation is transiently impaired for one week after large-vessel acute ischemic stroke.* Cerebrovasc Dis, 2015. **39**(2): p. 144-50.
87. Claassen, J.A., et al., *Transfer function analysis of dynamic cerebral autoregulation: A white paper from the International Cerebral Autoregulation Research Network.* J Cereb Blood Flow Metab, 2016. **36**(4): p. 665-80.
88. Czosnyka, M., et al., *Monitoring of cerebral autoregulation in head-injured patients.* Stroke, 1996. **27**(10): p. 1829-34.
89. Budohoski, K.P., et al., *Cerebral autoregulation after subarachnoid hemorrhage: comparison of three methods.* J Cereb Blood Flow Metab, 2013. **33**(3): p. 449-56.
90. Sorrentino, E., et al., *Critical thresholds for cerebrovascular reactivity after traumatic brain injury.* Neurocrit Care, 2012. **16**(2): p. 258-66.

91. Donnelly, J., et al., *Individualizing Thresholds of Cerebral Perfusion Pressure Using Estimated Limits of Autoregulation.* Crit Care Med, 2017. **45**(9): p. 1464-1471.
92. Steiner, L.A., et al., *Near-infrared spectroscopy can monitor dynamic cerebral autoregulation in adults.* Neurocrit Care, 2009. **10**(1): p. 122-8.
93. Moerman, A.T., et al., *Assessment of Cerebral Autoregulation Patterns with Near-infrared Spectroscopy during Pharmacological-induced Pressure Changes.* Anesthesiology, 2015. **123**(2): p. 327-35.
94. Blaine Easley, R., et al., *Continuous cerebrovascular reactivity monitoring and autoregulation monitoring identify similar lower limits of autoregulation in patients undergoing cardiopulmonary bypass.* Neurol Res, 2013. **35**(4): p. 344-54.
95. Lee, J.K., et al., *Cerebrovascular reactivity measured by near-infrared spectroscopy.* Stroke, 2009. **40**(5): p. 1820-6.
96. Novak, V., et al., *Multimodal pressure-flow method to assess dynamics of cerebral autoregulation in stroke and hypertension.* Biomed Eng Online, 2004. **3**(1): p. 39.
97. Tian, F., et al., *Wavelet coherence analysis of dynamic cerebral autoregulation in neonatal hypoxic-ischemic encephalopathy.* Neuroimage Clin, 2016. **11**: p. 124-132.
98. Tan, C.O., *Defining the characteristic relationship between arterial pressure and cerebral flow.* J Appl Physiol (1985), 2012. **113**(8): p. 1194-200.
99. Santos, G.A., et al., *Pathophysiologic differences in cerebral autoregulation after subarachnoid hemorrhage.* Neurology, 2016. **86**(21): p. 1950-6.
100. Reinhard, M., et al., *Cerebral dysautoregulation and the risk of ischemic events in occlusive carotid artery disease.* J Neurol, 2008. **255**(8): p. 1182-9.
101. Lang, E.W., et al., *Noninvasive cerebrovascular autoregulation assessment in traumatic brain injury: validation and utility.* J Neurotrauma, 2003. **20**(1): p. 69-75.
102. Ono, M., et al., *Validation of a stand-alone near-infrared spectroscopy system for monitoring cerebral autoregulation during cardiac surgery.* Anesth Analg, 2013. **116**(1): p. 198-204.
103. Lavinio, A., et al., *Noninvasive evaluation of dynamic cerebrovascular autoregulation using Finapres plethysmograph and transcranial Doppler.* Stroke, 2007. **38**(2): p. 402-4.
104. Czosnyka, M., et al., *An assessment of dynamic autoregulation from spontaneous fluctuations of cerebral blood flow velocity: a comparison of two models, index of autoregulation and mean flow index.* Anesth Analg, 2008. **106**(1): p. 234-9, table of contents.
105. Highton, D., et al., *Monitoring cerebral autoregulation after brain injury: multimodal assessment of cerebral slow-wave oscillations using near-infrared spectroscopy.* Anesth Analg, 2015. **121**(1): p. 198-205.
106. Budohoski, K.P., et al., *The relationship between cerebral blood flow autoregulation and cerebrovascular pressure reactivity after traumatic brain injury.* Neurosurgery, 2012. **71**(3): p. 652-60; discussion 660-1.

107. Lang, E.W., et al., *Short pressure reactivity index versus long pressure reactivity index in the management of traumatic brain injury.* J Neurosurg, 2015. **122**(3): p. 588-94.
108. Santos, E., et al., *Low-frequency sampling for PRx calculation does not reduce prognostication and produces similar CPPopt in intracerebral haemorrhage patients.* Acta Neurochir (Wien), 2011. **153**(11): p. 2189-95.
109. Barth, M., et al., *Correlation of clinical outcome with pressure-, oxygen-, and flow-related indices of cerebrovascular reactivity in patients following aneurysmal SAH.* Neurocrit Care, 2010. **12**(2): p. 234-43.
110. Steiner, L.A., et al., *Continuous monitoring of cerebrovascular pressure reactivity allows determination of optimal cerebral perfusion pressure in patients with traumatic brain injury.* Crit Care Med, 2002. **30**(4): p. 733-8.
111. Depreitere, B., et al., *Pressure autoregulation monitoring and cerebral perfusion pressure target recommendation in patients with severe traumatic brain injury based on minute-by-minute monitoring data.* J Neurosurg, 2014. **120**(6): p. 1451-7.
112. Weersink, C.S., et al., *Clinical and Physiological Events That Contribute to the Success Rate of Finding "Optimal" Cerebral Perfusion Pressure in Severe Brain Trauma Patients.* Crit Care Med, 2015. **43**(9): p. 1952-63.
113. Lewis, P.M., et al., *Cerebrovascular Pressure Reactivity in Children With Traumatic Brain Injury.* Pediatr Crit Care Med, 2015. **16**(8): p. 739-49.
114. Dias, C., et al., *Optimal Cerebral Perfusion Pressure Management at Bedside: A Single-Center Pilot Study.* Neurocrit Care, 2015. **23**(1): p. 92-102.
115. Jaeger, M., et al., *Effects of cerebrovascular pressure reactivity-guided optimization of cerebral perfusion pressure on brain tissue oxygenation after traumatic brain injury.* Crit Care Med, 2010. **38**(5): p. 1343-7.
116. Petkus, V., et al., *Optimal cerebral perfusion pressure-targeted treatment for severe traumatic brain injury.* J Neurotrauma, 2019.
117. Bijlenga, P., et al., *"Optimal cerebral perfusion pressure" in poor grade patients after subarachnoid hemorrhage.* Neurocrit Care, 2010. **13**(1): p. 17-23.
118. Hori, D., et al., *Cerebral Autoregulation Monitoring with Ultrasound-Tagged Near-Infrared Spectroscopy in Cardiac Surgery Patients.* Anesth Analg, 2015. **121**(5): p. 1187-93.
119. Hori, D., et al., *Optimal blood pressure during cardiopulmonary bypass defined by cerebral autoregulation monitoring.* J Thorac Cardiovasc Surg, 2017. **154**(5): p. 1590-1598 e2.
120. Lee, J.K., et al., *Cerebrovascular autoregulation in pediatric moyamoya disease.* Paediatr Anaesth, 2013. **23**(6): p. 547-56.
121. Rivera-Lara, L., et al., *Optimizing Mean Arterial Pressure in Acutely Comatose Patients Using Cerebral Autoregulation Multimodal Monitoring With Near-Infrared Spectroscopy.* Crit Care Med, 2019. **47**(10): p. 1409-1415.
122. Macdonald, R.L. and T.A. Schweizer, *Spontaneous subarachnoid haemorrhage.* Lancet, 2017. **389**(10069): p. 655-666.
123. Feigin, V.L., et al., *Worldwide stroke incidence and early case fatality reported in 56 population-based studies: a systematic review.* Lancet Neurol, 2009. **8**(4): p. 355-69.

124. Johnston, S.C., S. Selvin, and D.R. Gress, *The burden, trends, and demographics of mortality from subarachnoid hemorrhage.* Neurology, 1998. **50**(5): p. 1413-8.
125. de Rooij, N.K., et al., *Incidence of subarachnoid haemorrhage: a systematic review with emphasis on region, age, gender and time trends.* J Neurol Neurosurg Psychiatry, 2007. **78**(12): p. 1365-72.
126. Andreasen, T.H., et al., *Modifiable risk factors for aneurysmal subarachnoid hemorrhage.* Stroke, 2013. **44**(12): p. 3607-12.
127. Feigin, V.L., et al., *Risk factors for subarachnoid hemorrhage: an updated systematic review of epidemiological studies.* Stroke, 2005. **36**(12): p. 2773-80.
128. Lawton, M.T. and G.E. Vates, *Subarachnoid Hemorrhage.* N Engl J Med, 2017. **377**(3): p. 257-266.
129. Ruigrok, Y.M., E. Buskens, and G.J. Rinkel, *Attributable risk of common and rare determinants of subarachnoid hemorrhage.* Stroke, 2001. **32**(5): p. 1173-5.
130. Kurki, M.I., et al., *High risk population isolate reveals low frequency variants predisposing to intracranial aneurysms.* PLoS Genet, 2014. **10**(1): p. e1004134.
131. Xu, H., et al., *mRNA Expression Profiles from Whole Blood Associated with Vasospasm in Patients with Subarachnoid Hemorrhage.* Neurocrit Care, 2019.
132. Macdonald, R.L., *Delayed neurological deterioration after subarachnoid haemorrhage.* Nat Rev Neurol, 2014. **10**(1): p. 44-58.
133. Rosengart, A.J., et al., *Prognostic factors for outcome in patients with aneurysmal subarachnoid hemorrhage.* Stroke, 2007. **38**(8): p. 2315-21.
134. Frontera, J.A., et al., *Defining vasospasm after subarachnoid hemorrhage: what is the most clinically relevant definition?* Stroke, 2009. **40**(6): p. 1963-8.
135. Dreier, J.P., *The role of spreading depression, spreading depolarization and spreading ischemia in neurological disease.* Nat Med, 2011. **17**(4): p. 439-47.
136. Ostergaard, L., et al., *The role of the microcirculation in delayed cerebral ischemia and chronic degenerative changes after subarachnoid hemorrhage.* J Cereb Blood Flow Metab, 2013. **33**(12): p. 1825-37.
137. Diringer, M.N., et al., *Critical care management of patients following aneurysmal subarachnoid hemorrhage: recommendations from the Neurocritical Care Society's Multidisciplinary Consensus Conference.* Neurocrit Care, 2011. **15**(2): p. 211-40.
138. Gress, D.R. and H. Participants in the International Multi-Disciplinary Consensus Conference on the Critical Care Management of Subarachnoid, *Monitoring of volume status after subarachnoid hemorrhage.* Neurocrit Care, 2011. **15**(2): p. 270-4.
139. Karimy, J.K., et al., *Inflammation-dependent cerebrospinal fluid hypersecretion by the choroid plexus epithelium in posthemorrhagic hydrocephalus.* Nat Med, 2017. **23**(8): p. 997-1003.
140. Ecker, A. and P.A. Riemenschneider, *Arteriographic demonstration of spasm of the intracranial arteries, with special reference to saccular arterial aneurysms.* J Neurosurg, 1951. **8**(6): p. 660-7.
141. Harders, A.G. and J.M. Gilsbach, *Time course of blood velocity changes related to vasospasm in the circle of Willis measured by transcranial Doppler ultrasound.* J Neurosurg, 1987. **66**(5): p. 718-28.

142. Macdonald, R.L., et al., *Clazosentan, an endothelin receptor antagonist, in patients with aneurysmal subarachnoid haemorrhage undergoing surgical clipping: a randomised, double-blind, placebo-controlled phase 3 trial (CONSCIOUS-2).* Lancet Neurol, 2011. **10**(7): p. 618-25.
143. Macdonald, R.L., *Clazosentan: an endothelin receptor antagonist for treatment of vasospasm after subarachnoid hemorrhage.* Expert Opin Investig Drugs, 2008. **17**(11): p. 1761-7.
144. Rasmussen, G., et al., *Cerebral blood flow autoregulation in experimental subarachnoid haemorrhage in rat.* Acta Neurochir (Wien), 1992. **119**(1-4): p. 128-33.
145. Harper, A.M., et al., *The effect of experimental spasm on the CO2 response of cerebral bloodflow in primates.* Neuroradiology, 1972. **3**(3): p. 134-6.
146. Harper, A.M. and H.I. Glass, *Effect of alterations in the arterial carbon dioxide tension on the blood flow through the cerebral cortex at normal and low arterial blood pressures.* J Neurol Neurosurg Psychiatry, 1965. **28**(5): p. 449-52.
147. Fitch, W., et al., *Autoregulation of cerebral blood flow during controlled hypotension in baboons.* J Neurol Neurosurg Psychiatry, 1976. **39**(10): p. 1014-22.
148. Voldby, B., E.M. Enevoldsen, and F.T. Jensen, *Cerebrovascular reactivity in patients with ruptured intracranial aneurysms.* J Neurosurg, 1985. **62**(1): p. 59-67.
149. Budohoski, K.P., M. Czosnyka, and P.J. Kirkpatrick, *The Role of Monitoring Cerebral Autoregulation After Subarachnoid Hemorrhage.* Neurosurgery, 2015. **62 Suppl 1**: p. 180-4.
150. Rasulo, F.A., et al., *Are optimal cerebral perfusion pressure and cerebrovascular autoregulation related to long-term outcome in patients with aneurysmal subarachnoid hemorrhage?* J Neurosurg Anesthesiol, 2012. **24**(1): p. 3-8.
151. Lam, J.M., et al., *Predicting delayed ischemic deficits after aneurysmal subarachnoid hemorrhage using a transient hyperemic response test of cerebral autoregulation.* Neurosurgery, 2000. **47**(4): p. 819-25; discussions 825-6.
152. Ratsep, T. and T. Asser, *Cerebral hemodynamic impairment after aneurysmal subarachnoid hemorrhage as evaluated using transcranial doppler ultrasonography: relationship to delayed cerebral ischemia and clinical outcome.* J Neurosurg, 2001. **95**(3): p. 393-401.
153. Lang, E.W., R.R. Diehl, and H.M. Mehdorn, *Cerebral autoregulation testing after aneurysmal subarachnoid hemorrhage: the phase relationship between arterial blood pressure and cerebral blood flow velocity.* Crit Care Med, 2001. **29**(1): p. 158-63.
154. Tseng, M.Y., et al., *Effects of acute treatment with pravastatin on cerebral vasospasm, autoregulation, and delayed ischemic deficits after aneurysmal subarachnoid hemorrhage: a phase II randomized placebo-controlled trial.* Stroke, 2005. **36**(8): p. 1627-32.
155. Tseng, M.Y., et al., *Effects of acute treatment with statins on cerebral autoregulation in patients after aneurysmal subarachnoid hemorrhage.* Neurosurg Focus, 2006. **21**(3): p. E10.

156. Tseng, M.Y., et al., *Effects of acute pravastatin treatment on intensity of rescue therapy, length of inpatient stay, and 6-month outcome in patients after aneurysmal subarachnoid hemorrhage.* Stroke, 2007. **38**(5): p. 1545-50.
157. Jaeger, M., et al., *Clinical Significance of Impaired Cerebrovascular Autoregulation After Severe Aneurysmal Subarachnoid Hemorrhage.* Stroke, 2012.
158. Jaeger, M., et al., *Continuous monitoring of cerebrovascular autoregulation after subarachnoid hemorrhage by brain tissue oxygen pressure reactivity and its relation to delayed cerebral infarction.* Stroke, 2007. **38**(3): p. 981-6.
159. Christ, M., et al., *Continuous cerebral autoregulation monitoring by improved cross-correlation analysis: comparison with the cuff deflation test.* Intensive Care Med, 2007. **33**(2): p. 246-54.
160. Tseng, M.Y., et al., *Enhancement of cerebral blood flow using systemic hypertonic saline therapy improves outcome in patients with poor-grade spontaneous subarachnoid hemorrhage.* J Neurosurg, 2007. **107**(2): p. 274-82.
161. Tseng, M.Y., et al., *Acute systemic erythropoietin therapy to reduce delayed ischemic deficits following aneurysmal subarachnoid hemorrhage: a Phase II randomized, double-blind, placebo-controlled trial. Clinical article.* J Neurosurg, 2009. **111**(1): p. 171-80.
162. Rasulo, F.A., et al., *Are Optimal Cerebral Perfusion Pressure and Cerebrovascular Autoregulation Related to Long-term Outcome in Patients With Aneurysmal Subarachnoid Hemorrhage?* J Neurosurg Anesthesiol, 2011.
163. Budohoski, K.P., et al., *Impairment of cerebral autoregulation predicts delayed cerebral ischemia after subarachnoid hemorrhage: a prospective observational study.* Stroke, 2012. **43**(12): p. 3230-7.
164. Budohoski, K.P., et al., *Cerebral autoregulation after subarachnoid hemorrhage: comparison of three methods.* J Cereb Blood Flow Metab, 2012.
165. Budohoski, K.P., et al., *Bilateral failure of cerebral autoregulation is related to unfavorable outcome after subarachnoid hemorrhage.* Neurocrit Care, 2015. **22**(1): p. 65-73.
166. Steinmeier, R., et al., *Slow rhythmic oscillations of blood pressure, intracranial pressure, microcirculation, and cerebral oxygenation. Dynamic interrelation and time course in humans.* Stroke, 1996. **27**(12): p. 2236-43.
167. Soehle, M., M. Jaeger, and J. Meixensberger, *Online assessment of brain tissue oxygen autoregulation in traumatic brain injury and subarachnoid hemorrhage.* Neurol Res, 2003. **25**(4): p. 411-7.
168. Hecht, N., et al., *Modified flow- and oxygen-related autoregulation indices for continuous monitoring of cerebral autoregulation.* J Neurosci Methods, 2011. **201**(2): p. 399-403.
169. Johnson, U., et al., *Bedside Xenon-CT Shows Lower CBF in SAH Patients with Impaired CBF Pressure Autoregulation as Defined by Pressure Reactivity Index (PRx).* Neurocrit Care, 2016. **25**(1): p. 47-55.
170. Calviere, L., et al., *Prediction of Delayed Cerebral Ischemia After Subarachnoid Hemorrhage Using Cerebral Blood Flow Velocities and Cerebral Autoregulation Assessment.* Neurocrit Care, 2015. **23**(2): p. 253-8.

171. Sugimoto, K., et al., *Continuous Monitoring of Spreading Depolarization and Cerebrovascular Autoregulation after Aneurysmal Subarachnoid Hemorrhage.* J Stroke Cerebrovasc Dis, 2016. **25**(10): p. e171-7.
172. Liu, G., et al., *Monitoring of the Effect of Cerebral Autoregulation on Delayed Cerebral Ischemia in Patients with Aneurysmal Subarachnoid Hemorrhage.* World Neurosurg, 2018. **118**: p. e269-e275.
173. Al-Jehani, H., et al., *Early abnormal transient hyperemic response test can predict delayed ischemic neurologic deficit in subarachnoid hemorrhage.* Crit Ultrasound J, 2018. **10**(1): p. 1.
174. Otite, F., et al., *Impaired cerebral autoregulation is associated with vasospasm and delayed cerebral ischemia in subarachnoid hemorrhage.* Stroke, 2014. **45**(3): p. 677-82.
175. Ortega-Gutierrez, S., et al., *Changes on Dynamic Cerebral Autoregulation Are Associated with Delayed Cerebral Ischemia in Patients with Aneurysmal Subarachnoid Hemorrhage.* Acta Neurochir Suppl, 2020. **127**: p. 149-153.
176. Rynkowski, C.B., et al., *Early Transcranial Doppler Evaluation of Cerebral Autoregulation Independently Predicts Functional Outcome After Aneurysmal Subarachnoid Hemorrhage.* Neurocrit Care, 2019. **31**(2): p. 253-262.
177. Gaasch, M., et al., *Cerebral Autoregulation in the Prediction of Delayed Cerebral Ischemia and Clinical Outcome in Poor-Grade Aneurysmal Subarachnoid Hemorrhage Patients.* Crit Care Med, 2018. **46**(5): p. 774-780.
178. Jaeger, M., et al., *Clinical significance of impaired cerebrovascular autoregulation after severe aneurysmal subarachnoid hemorrhage.* Stroke, 2012. **43**(8): p. 2097-101.
179. Al-Rawi, P.G., P. Smielewski, and P.J. Kirkpatrick, *Evaluation of a near-infrared spectrometer (NIRO 300) for the detection of intracranial oxygenation changes in the adult head.* Stroke, 2001. **32**(11): p. 2492-500.
180. Lee, S.B., et al., *Artifact removal from neurophysiological signals: impact on intracranial and arterial pressure monitoring in traumatic brain injury.* J Neurosurg, 2019: p. 1-9.
181. Aries, M.J., et al., *Observation of Autoregulation Indices During Ventricular CSF Drainage After Aneurysmal Subarachnoid Hemorrhage: A Pilot Study.* Neurocrit Care, 2015. **23**(3): p. 347-54.
182. Klein, S.P., et al., *Comparison of Intracranial Pressure and Pressure Reactivity Index Obtained Through Pressure Measurements in the Ventricle and in the Parenchyma During and Outside Cerebrospinal Fluid Drainage Episodes in a Manipulation-Free Patient Setting.* Acta Neurochir Suppl, 2018. **126**: p. 287-290.
183. Czosnyka, M., et al., *Contribution of mathematical modelling to the interpretation of bedside tests of cerebrovascular autoregulation.* J Neurol Neurosurg Psychiatry, 1997. **63**(6): p. 721-31.
184. Saver, J.L., *Novel end point analytic techniques and interpreting shifts across the entire range of outcome scales in acute stroke trials.* Stroke, 2007. **38**(11): p. 3055-62.
185. Rivera-Lara, L., et al., *Predictors of Outcome With Cerebral Autoregulation Monitoring: A Systematic Review and Meta-Analysis.* Crit Care Med, 2017. **45**(4): p. 695-704.

186. Kramer, A.H., et al., *Continuous Assessment of "Optimal" Cerebral Perfusion Pressure in Traumatic Brain Injury: A Cohort Study of Feasibility, Reliability, and Relation to Outcome.* Neurocrit Care, 2019. **30**(1): p. 51-61.
187. Donnelly, J., et al., *Regulation of the cerebral circulation: bedside assessment and clinical implications.* Crit Care, 2016. **20**(1): p. 129.
188. Nornes, H. and P. Wikeby, *Cerebral arterial blood flow and aneurysm surgery. Part 1: local arterial flow dynamics.* J Neurosurg, 1977. **47**(6): p. 810-8.
189. Nornes, H., H.B. Knutzen, and P. Wikeby, *Cerebral arterial blood flow and aneurysm surgery. Part 2: Induced hypotension and autoregulatory capacity.* J Neurosurg, 1977. **47**(6): p. 819-27.
190. Eide, P.K., et al., *Pressure-derived versus pressure wave amplitude-derived indices of cerebrovascular pressure reactivity in relation to early clinical state and 12-month outcome following aneurysmal subarachnoid hemorrhage.* J Neurosurg, 2012. **116**(5): p. 961-71.
191. Yu, Z., et al., *Predictive Value of Cerebral Autoregulation Impairment for Delayed Cerebral Ischemia in Aneurysmal Subarachnoid Hemorrhage: A Meta-Analysis.* World Neurosurg, 2019. **126**: p. e853-e859.
192. Krishnamurthi, R.V., et al., *Global and regional burden of first-ever ischaemic and haemorrhagic stroke during 1990-2010: findings from the Global Burden of Disease Study 2010.* Lancet Glob Health, 2013. **1**(5): p. e259-81.
193. Benjamin, E.J., et al., *Heart Disease and Stroke Statistics-2017 Update: A Report From the American Heart Association.* Circulation, 2017. **135**(10): p. e146-e603.
194. Collaborators, G.B.D.L.R.o.S., et al., *Global, Regional, and Country-Specific Lifetime Risks of Stroke, 1990 and 2016.* N Engl J Med, 2018. **379**(25): p. 2429-2437.
195. Lozano, R., et al., *Global and regional mortality from 235 causes of death for 20 age groups in 1990 and 2010: a systematic analysis for the Global Burden of Disease Study 2010.* Lancet, 2012. **380**(9859): p. 2095-128.
196. Casper, M.L., et al., *The shifting stroke belt. Changes in the geographic pattern of stroke mortality in the United States, 1962 to 1988.* Stroke, 1995. **26**(5): p. 755-60.
197. Rich, D.Q., J.M. Gaziano, and T. Kurth, *Geographic patterns in overall and specific cardiovascular disease incidence in apparently healthy men in the United States.* Stroke, 2007. **38**(8): p. 2221-7.
198. Glymour, M.M., A. Kosheleva, and B. Boden-Albala, *Birth and adult residence in the Stroke Belt independently predict stroke mortality.* Neurology, 2009. **73**(22): p. 1858-65.
199. Adams, H.P., Jr., et al., *Classification of subtype of acute ischemic stroke. Definitions for use in a multicenter clinical trial. TOAST. Trial of Org 10172 in Acute Stroke Treatment.* Stroke, 1993. **24**(1): p. 35-41.
200. Smith, W.S., et al., *Significance of large vessel intracranial occlusion causing acute ischemic stroke and TIA.* Stroke, 2009. **40**(12): p. 3834-40.
201. Lima, F.O., et al., *Prognosis of untreated strokes due to anterior circulation proximal intracranial arterial occlusions detected by use of computed tomography angiography.* JAMA Neurol, 2014. **71**(2): p. 151-7.

202. Rabinstein, A.A., *Treatment of Acute Ischemic Stroke.* Continuum (Minneap Minn), 2017. **23**(1, Cerebrovascular Disease): p. 62-81.
203. Wardlaw, J.M., G. del Zoppo, and T. Yamaguchi, *Thrombolysis for acute ischaemic stroke.* Cochrane Database Syst Rev, 2000(2): p. CD000213.
204. Hacke, W., et al., *Thrombolysis with alteplase 3 to 4.5 hours after acute ischemic stroke.* N Engl J Med, 2008. **359**(13): p. 1317-29.
205. Wahlgren, N., et al., *Thrombolysis with alteplase for acute ischaemic stroke in the Safe Implementation of Thrombolysis in Stroke-Monitoring Study (SITS-MOST): an observational study.* Lancet, 2007. **369**(9558): p. 275-82.
206. Goyal, M., et al., *Endovascular thrombectomy after large-vessel ischaemic stroke: a meta-analysis of individual patient data from five randomised trials.* Lancet, 2016. **387**(10029): p. 1723-31.
207. Berkhemer, O.A., et al., *A randomized trial of intraarterial treatment for acute ischemic stroke.* N Engl J Med, 2015. **372**(1): p. 11-20.
208. Goyal, M., et al., *Randomized assessment of rapid endovascular treatment of ischemic stroke.* N Engl J Med, 2015. **372**(11): p. 1019-30.
209. Saver, J.L., et al., *Stent-retriever thrombectomy after intravenous t-PA vs. t-PA alone in stroke.* N Engl J Med, 2015. **372**(24): p. 2285-95.
210. Campbell, B.C., et al., *Endovascular therapy for ischemic stroke with perfusion-imaging selection.* N Engl J Med, 2015. **372**(11): p. 1009-18.
211. Jovin, T.G., et al., *Thrombectomy within 8 hours after symptom onset in ischemic stroke.* N Engl J Med, 2015. **372**(24): p. 2296-306.
212. Nogueira, R.G., et al., *Thrombectomy 6 to 24 Hours after Stroke with a Mismatch between Deficit and Infarct.* N Engl J Med, 2018. **378**(1): p. 11-21.
213. Powers, W.J., et al., *2018 Guidelines for the Early Management of Patients With Acute Ischemic Stroke: A Guideline for Healthcare Professionals From the American Heart Association/American Stroke Association.* Stroke, 2018. **49**(3): p. e46-e110.
214. Jovin, T.G., et al., *Diffusion-weighted imaging or computerized tomography perfusion assessment with clinical mismatch in the triage of wake up and late presenting strokes undergoing neurointervention with Trevo (DAWN) trial methods.* Int J Stroke, 2017. **12**(6): p. 641-652.
215. Immink, R.V., et al., *Dynamic cerebral autoregulation in acute lacunar and middle cerebral artery territory ischemic stroke.* Stroke, 2005. **36**(12): p. 2595-600.
216. Guo, Z.N., et al., *Dynamic cerebral autoregulation is heterogeneous in different subtypes of acute ischemic stroke.* PLoS One, 2014. **9**(3): p. e93213.
217. Castro, P., et al., *Efficacy of Cerebral Autoregulation in Early Ischemic Stroke Predicts Smaller Infarcts and Better Outcome.* Front Neurol, 2017. **8**: p. 113.
218. Reinhard, M., et al., *Dynamic cerebral autoregulation associates with infarct size and outcome after ischemic stroke.* Acta Neurol Scand, 2012. **125**(3): p. 156-62.
219. Castro, P., et al., *Hemorrhagic transformation and cerebral edema in acute ischemic stroke: Link to cerebral autoregulation.* J Neurol Sci, 2017. **372**: p. 256-261.

220. Dohmen, C., et al., *Identification and clinical impact of impaired cerebrovascular autoregulation in patients with malignant middle cerebral artery infarction.* Stroke, 2007. **38**(1): p. 56-61.
221. Guo, Z.N., et al., *Characteristics of dynamic cerebral autoregulation in cerebral small vessel disease: Diffuse and sustained.* Sci Rep, 2015. **5**: p. 15269.
222. Xiong, L., et al., *Is Dynamic Cerebral Autoregulation Bilaterally Impaired after Unilateral Acute Ischemic Stroke?* J Stroke Cerebrovasc Dis, 2017. **26**(5): p. 1081-1087.
223. Goyal, N., et al., *Blood pressure levels post mechanical thrombectomy and outcomes in large vessel occlusion strokes.* Neurology, 2017. **89**(6): p. 540-547.
224. Mistry, E.A., et al., *Systolic Blood Pressure Within 24 Hours After Thrombectomy for Acute Ischemic Stroke Correlates With Outcome.* J Am Heart Assoc, 2017. **6**(5).
225. Kim, T.J., et al., *Blood pressure variability and hemorrhagic transformation in patients with successful recanalization after endovascular recanalization therapy: A retrospective observational study.* Ann Neurol, 2019. **85**(4): p. 574-581.
226. Mistry, E.A., S.A. Mayer, and P. Khatri, *Blood Pressure Management after Mechanical Thrombectomy for Acute Ischemic Stroke: A Survey of the StrokeNet Sites.* J Stroke Cerebrovasc Dis, 2018. **27**(9): p. 2474-2478.
227. Nogueira, R.G., et al., *Predictors and clinical relevance of hemorrhagic transformation after endovascular therapy for anterior circulation large vessel occlusion strokes: a multicenter retrospective analysis of 1122 patients.* J Neurointerv Surg, 2015. **7**(1): p. 16-21.
228. Fiorelli, M., et al., *Hemorrhagic transformation within 36 hours of a cerebral infarct: relationships with early clinical deterioration and 3-month outcome in the European Cooperative Acute Stroke Study I (ECASS I) cohort.* Stroke, 1999. **30**(11): p. 2280-4.
229. Albers, G.W., et al., *Thrombectomy for Stroke at 6 to 16 Hours with Selection by Perfusion Imaging.* N Engl J Med, 2018. **378**(8): p. 708-718.
230. van Mook, W.N., et al., *Cerebral hyperperfusion syndrome.* Lancet Neurol, 2005. **4**(12): p. 877-88.
231. Galyfos, G., A. Sianou, and K. Filis, *Cerebral hyperperfusion syndrome and intracranial hemorrhage after carotid endarterectomy or carotid stenting: A meta-analysis.* J Neurol Sci, 2017. **381**: p. 74-82.
232. Hashimoto, T., et al., *Cerebral Hyperperfusion Syndrome After Endovascular Reperfusion Therapy in a Patient with Acute Internal Carotid Artery and Middle Cerebral Artery Occlusions.* World Neurosurg, 2018. **110**: p. 145-151.
233. Marshall, R.S., et al., *Dissociation among hemodynamic measures in asymptomatic high grade carotid artery stenosis.* J Neurol Sci, 2016. **367**: p. 143-7.
234. Strandgaard, S., *Autoregulation of cerebral blood flow in hypertensive patients. The modifying influence of prolonged antihypertensive treatment on the tolerance to acute, drug-induced hypotension.* Circulation, 1976. **53**(4): p. 720-7.
235. Okazaki, S., et al., *Cerebral hyperperfusion on arterial spin labeling MRI after reperfusion therapy is related to hemorrhagic transformation.* J Cereb Blood Flow Metab, 2017. **37**(9): p. 3087-3090.

236. Butcher, K., et al., *Postthrombolysis blood pressure elevation is associated with hemorrhagic transformation.* Stroke, 2010. **41**(1): p. 72-7.
237. Mori, E., et al., *Inhibition of polymorphonuclear leukocyte adherence suppresses no-reflow after focal cerebral ischemia in baboons.* Stroke, 1992. **23**(5): p. 712-8.
238. Ames, A., 3rd, et al., *Cerebral ischemia. II. The no-reflow phenomenon.* Am J Pathol, 1968. **52**(2): p. 437-53.
239. Tranmer, B.I., et al., *Loss of cerebral regulation during cardiac output variations in focal cerebral ischemia.* J Neurosurg, 1992. **77**(2): p. 253-9.
240. Wira, C.R., 3rd, et al., *The impact of cardiac contractility on cerebral blood flow in ischemia.* West J Emerg Med, 2011. **12**(2): p. 227-32.
241. Fuhrer, H., M. Reinhard, and W.D. Niesen, *Paradigm Change? Cardiac Output Better Associates with Cerebral Perfusion than Blood Pressure in Ischemic Stroke.* Front Neurol, 2017. **8**: p. 706.
242. Fuhrer, H., et al., *Optimizing Cardiac Out-Put to Increase Cerebral Penumbral Perfusion in Large Middle Cerebral Artery Ischemic Lesion-OPTIMAL Study.* Front Neurol, 2017. **8**: p. 402.
243. Yoneda, H., et al., *Multicenter prospective cohort study on volume management after subarachnoid hemorrhage: hemodynamic changes according to severity of subarachnoid hemorrhage and cerebral vasospasm.* Stroke, 2013. **44**(8): p. 2155-61.
244. Mutoh, T., et al., *Early intensive versus minimally invasive approach to postoperative hemodynamic management after subarachnoid hemorrhage.* Stroke, 2014. **45**(5): p. 1280-4.